Mouse Models for the Study of Viral Hepatitis

(intra)cellular innate immunity

Martijn D.B. van de Garde

Colophon

The studies described in this thesis were performed at the Department of Gastroenterology and Hepatology, Erasmus University Medical Center, Rotterdam, The Netherlands.

Cover: Mouse identity numbers of all mice transplanted with human hepatocytes in these studies.

Printing of this thesis was financially supported by: Erasmus MC department of Gastroenterology and Hepatology and the Dutch Society for Hepatology (NVH)

Printed by: Printenbind.nl

Mouse Models for the Study of Viral Hepatitis

(intra)cellular innate immunity

Muis modellen voor het bestuderen van virale hepatitis

aangeboren (intra)cellulaire immuniteit

Proefschrift

ter verkrijging van de graad van doctor aan de
Erasmus Universiteit Rotterdam
op gezag van de
rector magnificus

Prof.dr. H.A.P. Pols

en volgens besluit van het College voor Promoties.
De openbare verdediging zal plaatsvinden op
woensdag 17 januari 2018 om 11:30 hrs

Martijn Daniëlla Bertha van de Garde

geboren te Gilze-Rijen

Erasmus University Rotterdam

Doctoral committee

Promotor:	Prof.dr. R.A. de Man
Inner Committee :	Prof.dr. T. Kuiken Prof.dr. W.H.M van der Poel Dr. P.J.M. Leenen
Copromotors:	Dr. T. Vanwolleghem Dr. P.A. Boonstra

Table of contents

Chapter 1

Introduction

Viral hepatitis

Chronic viral hepatitis, predominantly caused by the hepatitis B and C viruses (HBV and HCV, respectively) and recently described by genotype (gt) 3 Hepatitis E virus (HEV), is a global health burden affecting almost five percent of the world's population. Not all patients develop a chronic infection after exposure to these viruses. Chronicity rates for HBV are 95% in neonates, 30% in children below age of 6 years, and 5% in adults, whereas the chronicity rates for HCV are approximately 80% (1, 2). Patients at risk for developing chronic HEV infection are immunocompromised patients comprising mainly solid organ transplant (SOT) patients (3-5), and to lesser extent patients infected with the human immunodeficiency virus (HIV) (6, 7), patients on chemotherapy (8) and bone marrow transplant recipients (9, 10). In HEV gt3 infected SOT patients a chronicity rate up to 57% has been reported (11). In 50-70% of chronic hepatitis patients, liver fibrosis and cirrhosis ensues, which eventually may lead to hepatic failure and the requirement of a liver transplant (12-15).

Hepatitis B virus

HBV is an enveloped partially double-stranded DNA virus, belonging to the family of the Hepadnaviridae within the genus Orthohepadnavirus. The genome of HBV is 3.2kb and contains four major open reading frames (ORF) called C, P, S, and X. ORF C encodes the Hepatitis B core antigen (HBcAg) and hepatitis B early or pre-core antigen (HBeAg), P encodes the DNA polymerase, the hepatitis B surface antigen (HBsAg) is encoded by S, and the HBV X protein (HBX) by X (Figure 1A) (12, 16, 17). HBV infects specifically human hepatocytes via the sodium taurocholate cotransporting polypeptide receptor (18). Upon entry the nucleocapsid is released in the cytoplasm and is transported to the nucleus where it releases its viral DNA. In the nucleus the viral DNA forms a minichromosome, so called covalently closed circular DNA (cccDNA), encoding all viral proteins (19). Incomplete eradication of cccDNA leads to resurgence of newly produced viral particles. Besides infectious virions HBV infection also produces an excessive amount of virus-like particles (VLP) consisting of HBsAg aggregates. These HBsAg containing VLPs have shown to modulate host immune functions by impairment of frequency and function of dentritic cells and possible interference of Toll-Like Receptor (TLR) signaling (20).

Hepatitis C virus

HCV is an enveloped, positive-sense single-stranded RNA virus of the family Flaviviridae within the genus Hepacivirus. One single ORF encodes a polyprotein and is flanked by 5' and 3' non-coding regions (NCR), within the HCV 9.6kb genome. The NCRs are essential for translation and replication of the viral RNA. After translation the viral polyprotein is cleaved by host and viral proteases into 3 structural proteins (Core protein, C; envelop proteins, E1 and E2) and 7 non-structural proteins (NS1, NS2, NS3, NS4a, NS4b, NS5a, and NS5b) important for viral replication (Figure 1B) (21-23). HCV primarily infects human hepatocytes through clathrin-mediated endocytosis after interaction with CD81, scavenger receptor BI, Claudin-1 and Occludin (24). In the cell HCV virions are uncoated and the genomic RNA can undergo replication or translation of the polyprotein generating new viral particles (25).

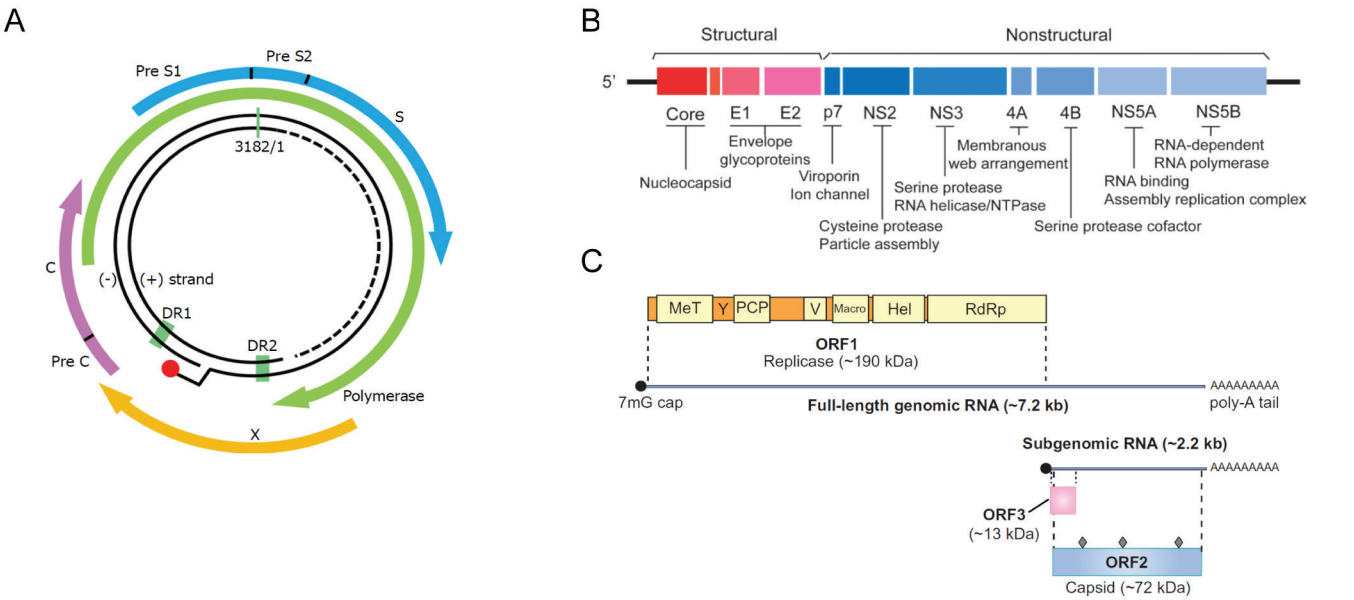

Figure 1. Genomic structure of hepatitis viruses. (A) The HBV DNA genome is a partially double-stranded relaxed circular DNA and is 3.2 kb long. The genome consists of four genes: C, core protein; P, polymerase; S, surface protein; X, x-protein, which partially overlap (adapted from Ohno M. et al WJG 2015 (17)). (B) The HCV RNA consists of a major open reading frame (ORF), encoding a single polyprotein, within the 9.6kb-long genome. Cleavage of the polyprotein gives rise to the structural (core, envelope proteins E1 and E2, and p7) and nonstructural (NS) viral proteins (NS2 through NS5B) (adapted from Boonstra A. et al. Hepatol 2009 (35)). (C) The 7.2kb-long positive-stranded RNA genome of HEV consist of three ORFs. ORF1 encodes a polyprotein consisting of methyltransferase (Met), Y, putative papain-like cysteine protease (PCP), variable (V), macro, RNA helicase (Hel, and RNA-dependent RNA polymerase (RdRp) domains. ORF2 encodes the capsid protein, and ORF3 overlaps with ORF2 and encodes a viroporin (adapted from Debing Y. et al. J Hepatol 2016 (36)).

Hepatitis E virus

For a long time viral infections with hepatitis E virus (HEV) were considered to be restricted to developing countries. However, recently European countries, including France, the United Kingdom and the Netherlands, have documented increasing numbers of endemic infections with gt3 HEV (26-28). HEV is a non-enveloped positive-sense single-stranded RNA virus, belonging to the family Hepeviridae within the genus Orthohepevirus. Seven different genotypes have been described so far, of which gt1 and gt3 are most prevalent in humans (29). The genome of HEV is approximately 7.2kb and contains three ORFs. ORF1 encodes several non-structural proteins including a methyltransferase, a y-domain, a papain-like cysteine protease, a helicase, and the RNA-dependent RNA polymerase. ORF2 encodes for structural proteins forming the viral capsid. ORF3 overlaps with ORF2 and encodes a viroporin essential for the release of infectious particles (Figure 1C) (30). The viral replication cycle of HEV is not completely understood. Non-specific molecules called heparin sulfate proteoglycans on the host cell facilitate virus attachment (31). However, subsequent entry into host cells is suggested to occur through unknown receptors (32). The genomic RNA is released into the cytosol after entry followed by translation of ORF1, including the RNA-dependent RNA polymerase, which synthesizes an intermediate, replicative negative-sense RNA strand (33). The negative-sense RNA strand serves as template for the production of new positive-sense viral genomes from which the ORF2 and ORF3 are translated, which eventually result in the packaging and release of new viral particles (34).

Treatment of chronic viral hepatitis

Despite the existence of a good vaccine against HBV, no curative treatment options are available at this moment and treatment of chronic HBV patients is therefore aimed at suppressing viral replication (37). Treatments available are either nucleoside (Lamivudine, Telbivudine, Entecavir) or nucleotide (Adefovir, and Tenofovir) analogues, which act as chain terminators for the viral DNA polymerase or reverse transcriptase, or pegylated-interferon-alpha (pegIFNα), which activates the host's anti-viral immune response (38). These current treatments fail to cure HBV as they have limited impact on the existing cccDNA reservoir in the nucleus of the infected cells. Current research is aiming to identify mechanisms which either eliminate or inactivate the HBV cccDNA (39, 40).

For years, treatment of chronic HCV patients consisted of pegIFNα plus ribavirin (RBV), which resulted in sustained virological response rates (SVR) 24 weeks after treatment stop in up to 42% of the HCV gt1, and 80% of the HCV gt2 and gt3 patients (41, 42). Low intrahepatic interferon-stimulated gene (ISG) expression levels were found to be predictive for SVR upon pegIFNα treatment in chronic HCV patients (43, 44). Currently, chronic HCV patients are treated with a new generation of direct acting antivirals targeting viral protease, polymerase and RNA binding assembly binding complex, which are able to suppress HCV replication and result in an SVR in over 90% of all the patients with minimal side effects in a shorter timeframe of 12 weeks (45, 46).

Antiviral treatment options for chronic HEV-infected immunocompromised patients are limited. Therefore, a dose reduction of immunosuppressive drugs in SOT patients is often tried as first intervention and has shown to result in HEV clearance in one third of the patients (3). The second treatment option available is RBV monotherapy, which is based on safety and efficacy treatment studies for chronic HCV infections, and leads to viral clearance in roughly 75% of chronic HEV patients. However, the optimal RBV treatment dosage and duration remain to be determined. The last option available is pegIFNα, which has been administered to a number of patients in doses comparable to HCV

treatment regimens with similar treatment success compared to RBV (47, 48). However, the use of pegIFNα in kidney and heart transplant recipients is not recommended, due to concerns for acute graft rejection.

Animal models for the study of viral hepatitis

Due to ethical constraints, studies of liver-residing leukocytes are limited in patients, although these cells are essential in determining the outcome of the infection. The restricted host range of the hepatitis viruses has hampered the development of suitable animal models. Available models for HBV and HCV comprise Chimpanzee, Treeshrews, transgenic mice, and infection of viral homologues in their natural host; such as woodchuck hepatitis virus in woodchucks, duck hepatitis B virus in ducks, and Tamarins infected with GB-virus A and B (49, 50). Possible models for HEV consist mainly of naturally occurring HEV or hepatitis E-like virus infection in pigs, rabbits, ferrets, rats, and birds. Despite their proven use in the study of viral hepatitis, immunopathogenesis studies in these models are limited. Furthermore, HEV infections in natural hosts rarely result in chronic infections. In order to study these viruses in a scalable small animal model, different immune-deficient and immune-competent mouse models have been suggested, namely the immun-deficient human-liver chimeric mouse model and immune-competent lymphocytic choriomeningitis virus (LCMV) infection model.

Immune-deficient mouse model

The development of human-liver chimeric mouse models was a big leap forward in the study of human hepatitis viruses (51-62). These mice have a hepatocyte-specific, albumin promotor-directed, overexpression of a urokinase plasminogen activator (uPA) transgene, which induces severe liver damage generating a nich for viable hepatocytes. The diseased liver could be replaced with viable non-transgenic donor mouse hepatocytes, showing increased survival of mice (51). Backcrossing the uPA-transgene into an immune-deficient background permitted the reconstruction of the transgenic liver with human hepatocytes, thereby generating human-liver chimeric mice. Successful engraftment and functionality of human hepatocytes was reflected by the production of human serum proteins including human albumin (52). Several groups used this idea to develop other models using the same principles, e.g. Fah–/–Rag2–/–Il2rg–/–, HSVtk-NOD/Shi-scid IL2Rgnull (NOG), and uPA-NOG mice (53-55).

Human-liver chimeric mouse models showed to be susceptible to HCV and HBV, with active replication reaching high titers in serum and liver (52, 56-58). Besides HBV mono-infection, these models

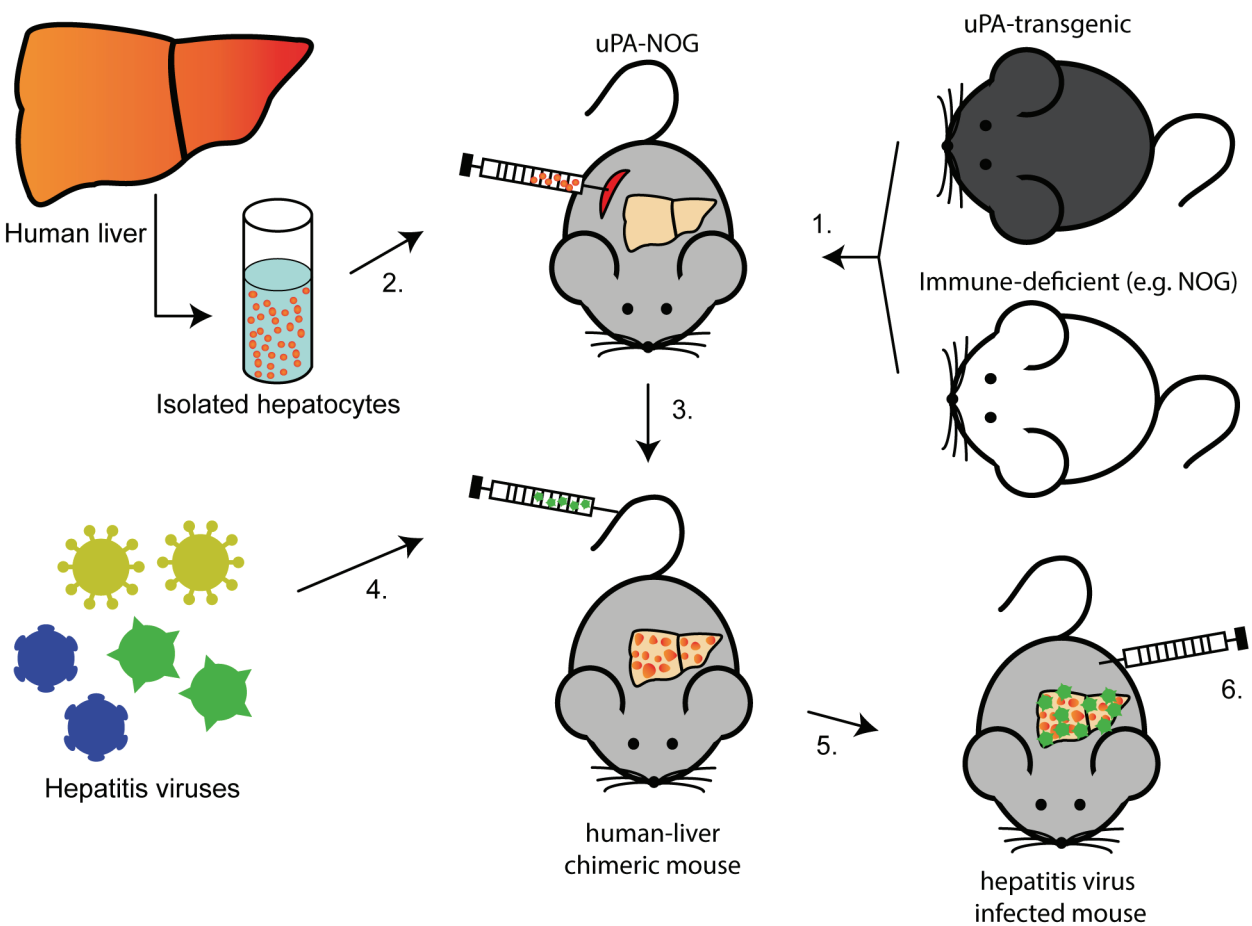

Figure 2. Schematic overview of the human-liver chimeric mouse model for the study of viral hepatitis. 1) uPA-transgenic mice were crossbred with immune-deficient (NOG) mice to generate uPA-NOG mice. uPA overexpression damages the liver generating space and need for viable hepatocytes. 2) Isolation and transplantation of human hepatocytes via intra-splenic injection. Transplanted hepatocytes migrate with the bloodflow towards the liver. 3) Expansion of engrafted human hepatocytes. 4) Inoculation of hepatitis viruses (infectivity studies). 5) Viral replication in chimeric mouse liver (infection kinetics and virus-host interaction studies). 6) Preclinical evaluation of antiviral drugs (Antiviral treatment and intervention studies).

also showed to support HBV coinfection with hepatitis D virus (HDV) (59). To date, infected humanized mice resemble closest a natural infection in human. Therefore, besides infection studies of human hepatotropic viruses, antiviral compounds, viral entry inhibitors and IFN-based therapies were tested to cure or prevent viral infection (60-62) (Figure 2).

The immune-deficient background of these mice prevents studies of the cellular and humoral immune responses. Nonetheless, this model is very useful to study the direct interaction of the virus with human hepatocytes. In addition, it has been shown that adoptive transfer of human immune cells in these mice is possible, and that these cells were able to prevent HCV infection in humanized mice (63). However, limitations in studying the immune cells in this model remain and illustrate the need for an immune-competent model to study chronic viral hepatitis.

Immune-competent animal model

As an alternative to study HCV- and HBV-induced immune responses in humans or chimpanzees, mice infected with the persistent variant of LCMV have been established to model virus-host interactions. Since the first descriptions of human chronic viral infections, LCMV-challenged mice have been used as model to study immunological events during persistent viral replication. Several significant research milestones have been achieved using the LCMV model. In 1974, the Major Histocompatibility Complex (MHC)-restricted action of cytotoxic T lymphocytes was discovered by Zinkernagel and Doherty, which resulted in the Nobel Prize in 1996 (64-66). Studying LCMV also contributed to our understanding of perforin-based T cell-mediated cell lysis and a key feature of the adaptive immune response, namely T cell memory (67-70). Furthermore, the concept and experimental evidence of immune dysfunction and immune exhaustion arise in part from LCMV studies (71-74). In addition, LCMV also contributed to the understanding of the innate immune system. Early cytotoxic cells (now known as NK cells) emerged 1 day after LCMV inoculation, killing infected and non-infected cells (75). All these achieved milestones illustrate the importance of this immune-competent model to study persistent viral infections.

Several strains of LCMV are known, of which Armstrong and Clone (Cl) 13 are generally used to study acute and chronic infections, respectively. The genomes of these strains only differ in five nucleotides, resulting in two amino acid changes in the viral polymerase and glycoprotein (76, 77). Interestingly, these changes result in completely distinct infection profiles. Infection of C57/BL6 mice with LCMV Armstrong is cleared within 8 days and is due to strong induction of LCMV-specific CD4+ and CD8+ T cells, thereby coined the “acute LCMV strain” (78, 79). In contrast, LCMV Cl13 infections persist in several organs with high viral titers weeks after inoculation, as a result of insufficient antigen presentation and thus preventing a strong T cell response (80, 81). Although LCMV Cl13 is genetically distant from HCV or HBV, the immunological landscape observed during chronic LCMV infection in mice mimics in many ways the immune alterations of the immune system upon persistent human viral infections. The ability of LCMV to infect hepatocytes, among other cells, underlines the relevance of this model for the study of virus induced hepatitis (82-84).

Innate immune response

Intracellular innate immune response

The host organism depends on a fast defense response in order to protect itself from potentially harmful viruses. Therefore, most cells contain so called pattern recognition receptors (PRR), which recognize foreign pathogen-associated molecular patterns (PAMP) (85). To protect against viruses, the cytosolic PRRs are most important and consist of TLR3, TLR7, TLR8, TLR9, retinoic acid-inducible gene (RIG)-I, melanoma-differentiation-associated gene 5 (MDA5), and the cyclic GMP-AMP Synthase (cGAS) - stimulator of Interferon Genes (STING) pathway. These PRRs bind viral nucleic acids such as CpG-DNA, 5’ppp-ssRNA, ssRNA, dsDNA, and dsRNA, which can be presented intracellularly upon infection of the host cell. Binding of PAMPs to PRRs can initiate various intracellular signaling cascades leading to the activation of transcription factors, including interferon-regulatory factors (IRF) and NF-κB. Subsequently, these transcription factors initiate the production of inflammatory cytokines and interferons (IFN) (86, 87). Hepatocytes infected with HBV revealed minimal or no intracellular immune response, whereas infection with HCV showed a strong induction of defense responses, indicated by increased transcription of ISGs (88, 89). Despite the activated innate immune response in HCV-infected cells, HCV is rarely cleared. Interestingly, viruses have developed various ways to counteract the innate immune signaling cascades or prevent sensing by the host cell’s response (90, 91). Therefore, in order to clear the viral infection a cellular innate immune response and the development of a good adaptive immune response are required.

Cellular innate immune response

Immune-mediated clearance of HBV, HCV, and HEV infection in patients is executed by multi epitope-specific adaptive CD4+ T, CD8+ T and B cell responses (92-94). The development of good T and B cell immune responses against hepatitis viruses are dependent and shaped by the early immunological events provided by innate immune cells in the liver (95, 96). In the LCMV model it has been demonstrated that NK cells direct a good adaptive immune response (97). In addition to NK cells, the liver innate immune cells comprise granulocytes, dendritic cells, monocytes and macrophages. The latter two have been suggested to play various roles in homeostasis and during inflammation, but are not well studied in the context of viral hepatitis.

Macrophages

Macrophages are, together with monocytes and dendritic cells, part of the mononuclear phagocyte system. Liver tissue macrophages, also known as Kupffer cells (KC), are derived from embryonic progenitors that seed developing tissues before birth and are the largest immune cel population in the liver. During life, these tissue macrophages can proliferate at low levels in the steady state (98). KCs are abundantly present in the liver sinusoids, are crucial players in maintaining tissue homeostasis, and form, together with sinusoidal endothelial cells, the first barrier for pathogens to enter the liver (99). KCs can respond to danger signals using a variety of PRRs, such as TLR, scavenger and antibody-receptors and, depending on the local environment, initiate an inflammatory response, or induce tolerogenic T cell responses (100, 101). Only a few studies have looked into the role of KC during LCMV infection in mice. One study showed rapid LCMV dissemination and enhanced viral replication in mice with chlodronate-depleted KCs or IFNα-receptor deficient KCs (102). Suggesting, a crucial role for KCs in controlling LCMV spread and replication.

Monocytes

Also part of the mononuclear phagocyte system are the monocytes, which are continuously generated in the bone marrow from hematopoietic stem cells (98). Monocytes survey the body for inflammatory foci and are therefore among the first innate immune cells to respond to infection. They are equipped with chemokine and adhesion receptors to mediate migration to the site of infection or inflammation, upon which they can further differentiate into tissue-like macrophages and dendritic cells (103). Depending on the nature of the inflammatory agent and organ system involved, monocytes can exert both a pro-inflammatory as well as an anti-inflammatory role. They have the ability to produce tumor necrosis factor (TNF) and inducible nitric oxide synthase (iNOS) (104-106), to carry microbial antigens to local lymph nodes (107), and to present antigens to T cells (108-110). Alternatively, monocytes may differentiate into anti-inflammatory macrophage-like cells (106) or suppress proliferation and production of cytokines by T cells (111), suggesting their role in maintaining homeostasis.

Scope of this thesis

Objectives of this thesis are: 1) to better understand the cellular innate immune responses in the liver during LCMV-induced chronic hepatitis, and 2) to establish the human-liver chimeric mouse as model for chronic HEV infections in order to study the intracellular innate immune mechanisms upon HEV infection.

Outline of this thesis

In chapters 2 and 3, we aim to unravel how the cellular innate immune system deals with chronic viral infection in the liver. This knowledge is crucial to develop new antiviral strategies aimed at eradicating chronic viral infection. We model the chronic virus-host interaction by inoculating mice with a LCMV Cl13. In chapter 2, we set out to characterize in depth the phenotype, function and gene expression profiles of liver monocytes and KCs during the early phases of chronic LCMV infection. In chapter 3, we fully characterize the immune-related gene transcriptome of sorted KCs and liver monocytes during chronic LCMV infection.

In chapters 4, 5, and 6, we investigat Europe's new hepatitis threat. No adequate in vivo model system exists to mimic this disease course, which hampers studies on HEV infectivity, transmission, and antiviral drug development. In chapter 4, we explore the use human-liver chimeric mice as model for chronic HEV. Chapter 5 describes the genomic adaptation of HEV to in vitro culture, and inter-patient clinical isolates. In chapter 6, we examine the intracellular innate immune responses in human hepatocytes upon infection with HEV in human-liver chimeric mice. In addition, HEV-infected human-liver chimeric mice are treated with the intracellular innate-immune activating drugs, pegIFNα. The results presented in this thesis are summarized and discussed in chapter 7.

Chapter 2

Published in: Journal of Virology, 2015, 89:480

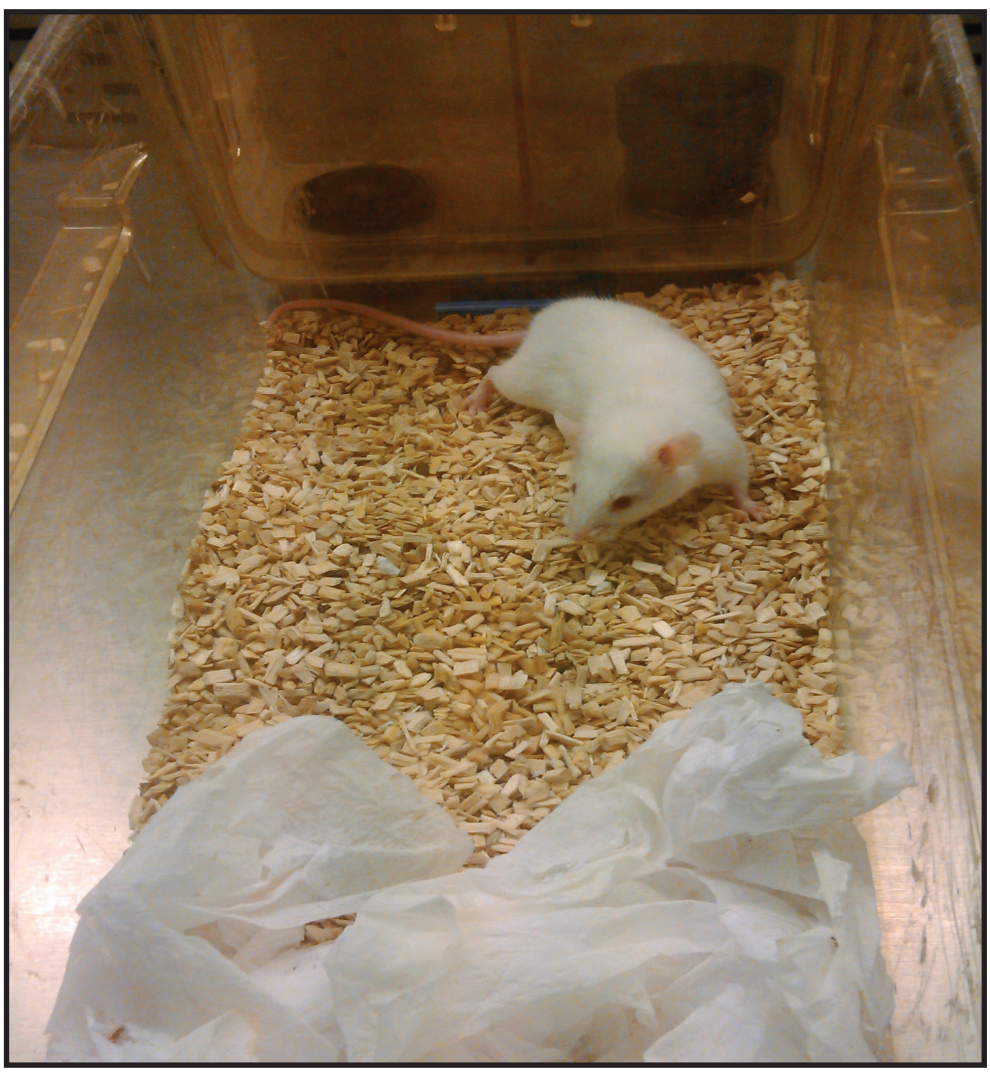

Mouse in an individual ventilated cage.

Recruited inflammatory monocytes adopt a Kupffer cell-like phenotype, but not function within 24 hours after virus-induced liver inflammation

Dowty Movita[1], Martijn D.B. van de Garde[1], Paula Biesta[1], Kim Kreefft[1], Bart Haagmans[2], Elina Zuniga[3], Florence Herschke[4], Sandra De Jonghe[4], Harry L.A. Janssen[1,5], Lucio Gama[6], Andre Boonstra[1,#], Thomas Vanwolleghem[1,#]

Abstract

Due to a scarcity of immunocompetent animal models for viral hepatitis, little is known about the early innate immune responses in the liver. In various hepatotoxic models both pro- and anti-inflammatory activities of recruited monocytes have been described. In this study, we compared the effect of liver inflammation induced by the TLR4 ligand LPS with that of a persistent virus, lymphocytic choriomeningitis virus (LCMV) Clone 13, on early innate intrahepatic immune responses in mice. LCMV infection induces a remarkable influx of inflammatory monocytes in the liver within 24 hours, accompanied by increased transcript levels of several pro-inflammatory cytokines and chemokines in whole liver. Importantly, while a single LPS injection results in similar recruitment of inflammatory monocytes to the liver, the functional properties of the infiltrating cells are dramatically different in response to LPS versus LCMV infection. In fact, intrahepatic inflammatory monocytes are skewed towards a secretory phenotype with impaired phagocytosis in LCMV-induced liver inflammation, but exhibit increased endocytic capacity after LPS challenge. In contrast, F4/80high-Kupffer cells retain their steady-state endocytic functions upon LCMV infection. Strikingly, the gene expression levels of inflammatory monocytes dramatically change upon LCMV exposure and resemble those of Kupffer cells. Since inflammatory monocytes outnumber Kupffer cells during the early phase of LCMV infection, inflammatory monocytes might be more important during the early phase of liver inflammation. Our findings are instrumental in understanding the early immunological events during virus-induced liver disease and point towards inflammatory monocytes as potential target cells for future treatment options in viral hepatitis.

[1]Department of Gastroenterology and Hepatology, [2]Viroscience, Erasmus University Medical Center, Rotterdam, The Netherlands, [3]Division of Biological Sciences, University of California San Diego, La Jolla, San Diego, California, [4]Janssen Infectious Disease and Drug Safety Sciences, Beerse, Belgium, [5]Liver Clinic, Toronto Western and General Hospital University Health Network Toronto, Toronto, Canada, [6]Department of Molecular and Comparative Pathobiology, The Johns Hopkins University School of Medicine, Baltimore, Maryland, USA, [#]these authors contributed equally to this work

Introduction

Chronic viral hepatitis, predominantly caused by the hepatitis B and C viruses (HBV and HCV, respectively), is a global health burden affecting almost three percent of the world's population. In 50-70% of patients, liver fibrosis ensues, of which a considerable proportion go on to develop cirrhosis, hepatic failure or hepatocellular carcinoma (12, 13). Although clearance of HBV and HCV infection is executed by multi epitope-specific adaptive CD4+ T, CD8+ T and B cell responses (92-95), these responses are dependent and shaped by the early immunological events provided by innate immune cells in the liver (95, 96). Immunological studies of HCV- or HBV-induced hepatitis have been impeded since these viruses only replicate in humans and non-human primates. Furthermore, immunocompetent small animal models for chronic viral hepatitis are not yet available (reviewed in (35, 112)). As an alternative to study HCV- and HBV-induced immune responses in humans or chimpanzees, mice infected with the persistent variant of lymphocytic choriomeningitis virus (LCMV) clone 13 (Cl13) has been proposed to model virus-host interactions during a chronic viral infection. Although LCMV Cl13 is genetically distant from HCV or HBV, the immunological landscape observed during chronic LCMV infection in mice mimics in many ways the immune alterations resulting from sustained stimulation of the immune system upon human persistent viral infections. In fact, numerous key findings observed in LCMV-induced immune regulation of adaptive immunity have later been confirmed in human studies, demonstrating the validity of this model system (reviewed in (113)). Although mice persistently infected with LCMV exhibit altered innate responses to subsequent toll like receptor (TLR) stimulations and secondary infections (114, 115), the overall and intrahepatic alterations of the innate immune system during early LCMV infections have been less studied.

Monocytes survey the body for inflammatory foci and are therefore among the first innate immune cells to respond to infection. They are equipped with chemokine and adhesion receptors to mediate migration to the site of infection or inflammation, upon which they can further differentiate into tissue macrophages and dendritic cells (103). Depending on the nature of the inflammatory agent and organ system involved, monocytes can exert both a pro-inflammatory as well as an anti-inflammatory role. They have the ability to produce TNF and iNOS (104-106), to carry microbial antigens to local lymph nodes (107), and to present antigens to T cells (108-110). Alternatively, monocytes may differentiate into anti-inflammatory macrophages (106) or suppress proliferation and production of cytokines by T cells (111), suggesting their role in maintaining homeostasis. In L. monocytogenes, M. tuberculosis and T. gondii mouse models for example, monocyte migration from bone marrow results in resistance to infection (105, 116-118). While in T. brucei and influenza virus models, monocyte recruitment impairs pathogen clearance and exacerbates immune-mediated pathology (104, 119, 120).

Upon recruitment to the liver, monocytes are referred to as inflammatory monocytes and identified as F4/80lowLy6C+CD11b+ cells (121-123). Similar to their systemic function, opposing roles during sterile toxin-induced liver inflammation have been identified. For example, in acetaminophen-induced hepatitis, hepatic inflammatory monocytes are endocytic and display an immunoregulatory phenotype (121), while in concanavalin A and CCl4 hepatitis, they promote Th1 cell proliferation and produce pro-inflammatory cytokines such as TNF and IL-6 (122-124). Due to the shortage of specific animal models, the role of these innate immune cells during virus-induced liver disease is less explored. Furthermore, before the recruitment of monocytes, Kupffer cells, together with dendritic cells, liver sinusoidal endothelial cells and stellate cells, are the first to encounter pathogens upon their passage through the liver sinusoids. Both Kupffer cells and inflammatory monocytes likely play a role in shaping the immune response, and thereby affect the outcome of a viral infection in the liver. We and others have previously shown that murine Kupffer cells can be unequivocally identified by the expression of F4/80, CD11b and CD68 and are predominantly phagocytic in a steady state condition (125, 126).

In the current study, we set out to characterize in depth the phenotype, function and gene expression profiles of liver monocytes and Kupffer cells during the early phases of chronic LCMV infection. We demonstrate a strong influx of inflammatory monocytes in the liver within 24 hours after LCMV inoculation. Using Nanostring gene expression analysis on highly purified Kupffer cells and inflammatory monocytes isolated from mouse liver, we demonstrated that under steady state conditions these cells are transcriptionally and functionally distinct. As a consequence of LCMV infection the expression profiles of both Kupffer cells and inflammatory monocytes are strongly altered. Strikingly, 24 hours after LCMV infection differences in gene expression levels of both cell types largely –but not completely- disappear, resulting in strong resemblance of Kupffer cells and inflammatory monocytes. These findings provide insight in the function of the cells involved in the early stages of virus-induced liver disease and present potential target cell types for the early control of viral hepatitis.

Materials and Methods

Mice, virus and antibodies

LCMV Cl13 was propagated in BHK21 cells and the titer was determined by plaque assay as previously described (76, 80). C57BL/6 mice aged 8-12 weeks old (Charles River, France) received LCMV Cl13 (2 x 106 PFU) i.v, 5 µg LPS (TLR4 ligand, S. Minnesota ultra-pure, Invivogen) i.p, or 200 µl PBS i.p. Animals were maintained in a BSL-III isolator according to Dutch national biosafety guidelines. Infection was confirmed by plaque assay on liver homogenate. All animal work was conducted according to relevant Dutch national guidelines. The study protocol was approved by the animal ethics committee of the Erasmus University Rotterdam. Antibodies used in flow cytometry: CD45 eFluor450 (30-F11), F4/80 APC or F4/80 FITC (BM8), CD11b PECy7 (M1/70), and TNF PerCPCy5.5 (MP6-XT22) from eBioscience, Ly6C APCCy7 (HK1.4) from Biolegend, MARCO FITC (ED31) from AbdSerotec, and Aqua Dead Cell Stain from Invitrogen. The VL4 cells, producing LCMV-nucleoprotein (LCMV-NP) monoclonal antibody, were a kind gift from Dr. M. Groettrup, University of Constance, Germany.

Isolation of total liver non-parenchymal cells

Liver was removed without perfusion, cut into small pieces, incubated in RPMI 1640 containing 30 µg/ml Liberase TM (Roche) and 20 µg/ml DNAse type I (Sigma) for 20 min, and passed through a 100 µm cell strainer. After centrifugation, cells were resuspended in PBS containing 1% FCS and 2.5 mM EDTA. Parenchymal cells were removed by low speed centrifugation at 50 g for 3 min and erythrocytes were lysed with 0.8% NH4Cl. The remaining non-parenchymal cells were resuspended in culture medium (RPMI 1640, 10% FCS, 10 mM HEPES, 2 mM L-glutamine,

100 U/ml / 100 µg/ml Pen/Strep, 50 µM β-mercaptoethanol) and used for further analysis.

Flow cytometry
Total liver non-parenchymal cells were stained with Aqua Dead Cell Stain, CD45 eFluor450, F4/80 APC, CD11b PECy7 and Ly6C APCCy7 (unless otherwise indicated), and fixed with 2% formaldehyde for 1 hour. F4/80high-Kupffer cells were identified as CD45+F4/80highCD11b+ and inflammatory monocytes as CD45+F4/80lowCD11bhighLy6Chigh using a FACSCanto-II flowcytometer and FACSDiva software (BD Biosciences).

RNA isolation of liver homogenates, generation of cDNA and real-time PCR
Liver was homogenized in RNAlater (Qiagen). RNA was extracted using Trizol (LifeTech) and a NucleoSpin RNAII kit (Bioké). cDNA was generated using the iScript cDNA Synthesis Kit (Bio-Rad Laboratories) according to the manufacturer's protocol. Quantitative PCR were performed using SYBR-green and MyIQ5 detection system (Bio-rad Laboratories). Sequences of primers are listed in Table 1. Expression of target genes was normalized to the expression of 18S or GAPDH using the formula 2-ΔCt, ΔCt=CtTLR-Ct18S or ΔCt=CtRNAX-CtGADPH.

RNA isolation of sorted cells and Nanostring
Kupffer cells and inflammatory cells were purified by cell sorting after initial enrichment using CD45 PE followed by anti-PE Microbeads (Milteny Biotec) selection. To obtain sufficient cells the organs of 6 mice were pooled. Following staining to identify Kupffer cells and inflammatory monocytes as described above, cells were fixed with 2% formaldehyde for 1 hour, and sorted on a FACS Aria SORP flow cytometer (BD Biosciences). Total RNA was isolated from these formaldehyde-fixed cells using reagents from the RNeasy FFPE kit (Qiagen) following manufacturers' protocols starting with adding 150 µl Buffer PKD. The nCounter® GX Mouse Immunology Kit (NanoString Technologies, Seattle, WA, USA) was used to measure the expression of 561 genes in our RNA samples.

Table 1. Gene-specific primers used in qPCR analysis

Gene ID	NCBI ID		Primer sequence
GAPDH	NM_008084.2	Forward	CGTCCCGTAGACAAAATGGT
		Reverse	TCTCCATGGTGGTGAAGACA
18S	NR_003278.3	Forward	GTAACCCGTTGAACCCCATT
		Reverse	CCATCCAATCGGTAGTAGCG
TNF	NM_013693.2	Forward	CAGGCGGTGCCTATGTCTC
		Reverse	CGATGACCCCGAAGTTCAGTAG
IL-10	NM_010548.2	Forward	CACAGGGGAGAAATCGATGACA
		Reverse	ATTTGAATTCCCTGGGTGAGAAG
IL-6	NM_031168.1	Forward	TGGTGACAACCACGGCCTTCC
		Reverse	AGCCTCCTGACTTGTGAAGTGGT
MCP-1	NM_011333.3	Forward	CAGGTCCCTGTCATGCTTCT
		Reverse	TCTGGACCCATTCCTTCTTG
RANTES	NM_013653.3	Forward	GCGGGTACCATGAAGATCTCTG
		Reverse	CACTTCTTCTCTGGGTTGGCAC
IFNα	NM_010504.2	Forward	AGGATTTTGGATTCCCCTTG
		Reverse	TATGTCCTCACAGCCAGCAG
IFNb	NM_010510.1	Forward	ATGAACAACAGGTGGATCCTCC
		Reverse	AGGAGCTCCTGACATTTCCGAA
IP-10	NM_021274.2	Forward	CCCCGGTGCTGCGATGGATG
		Reverse	AGCTGATGTGACCACGGCTGG

Following hybridization, transcripts were quantitated using the nCounter® Digital Analyzer. Samples were run by the Johns Hopkins Deep Sequencing & Microarray Core (127). To correct for background levels, the highest negative control value for each sample was subtracted from each count value of that sample. Following background subtraction, any negative count values were considered as 0. Values were normalized by the geometric mean of 13 housekeeping genes provided by the company panel.

Immunohistochemistry for F4/80
Liver was fixed in 4% formaldehyde, embedded in paraffin and cut into 5 µm sections. F4/80 antigen was retrieved using Proteinase K. Endogenous peroxidase was eliminated using 3% hydrogen peroxide. Liver sections were incubated with rat anti-F4/80 antibody (eBioscience) and rabbit anti-rat HRP (Dako). Upon addition of DAB, liver sections were counterstained with hematoxyline.

Intracellular detection of LCMV-nucleoprotein (LMCV-NP)
Intracellular LCMV-NP detection was performed as previously described (128). Total liver non-parenchymal cells were incubated with Aqua Dead Cell Stain, fixed with 2% formaldehyde for 1 hour, and permeabilized by 1% Triton X-100 (Sigma) for 20 minutes. Cells were further incubated with rat anti-LCMV NP antibody (VL4), goat anti-rat Alexa594 (Invitrogen) and blocking buffer (5% BSA and 10% rat serum). F4/80 FITC was used in the antibody cocktail. LCMV-NP positive F4/80high-Kupffer cells were identified.

Cytokine production by total liver non-parenchymal cells
Total liver non-parenchymal cells were cultured at 1x 106 cells/well in a 24-well plate (Costar) in 1 ml culture medium alone or in combination with PMA/ionomycin (50 and 500 ng/ml, respectively) for 5 hours. Brefeldin A (10 µg/ml, Sigma) was added after 1 hour. Next, cells were incubated with Aqua Dead Cell Stain, fixed with 2% formaldehyde for 1 hour, permeabilized with 0.5% saponin (Rectapur) and further stained with TNF PerCPCy5.5. TNF-positive F4/80high-Kupffer cells and the inflammatory monocytes were determined.

In vitro receptor-mediated endocytosis assay
One million total liver non-parenchymal cells were incubated for 45 min with dextran-FITC (10 µg/ml, 40,000 MW, Invitrogen) at 37°C or on ice. Dextran-positive F4/80high-Kupffer cells and inflammatory monocytes were determined.

ALT measurement
Serum ALT level was measured using an ELISA kit for Alanine Aminotransferase (Biotang USA) according to the manufacturer's protocol.

Data analysis and statistics
Differences between groups were calculated using one-way ANOVA (Kruskal-Wallis test, with Dunn's Multiple Comparison post-test) or two way ANOVA with Bonferroni post-test (GraphPad Prism version 5.01; GraphPad Software). Differences were considered significant when $P < 0.05$. Results are presented as the mean ± SEM, unless otherwise indicated.

Results

LCMV infection induces a rapid recruitment of inflammatory monocytes to the liver

Previous studies showed an accumulation of LCMV particles in the liver within minutes after an i.v challenge (102). In line with this, we observed a reproducible LCMV replication in the liver of mice inoculated 24 hours earlier, reaching average titers of 2.27 x 105 PFU/ gram liver. To examine the impact of viral replication versus sterile TLR ligand-induced challenge on the innate immune cell repertoire in the liver, we performed a flow cytometric analysis on total liver non-parenchymal cells obtained from LCMV-infected and LPS-treated mice. LPS was used as a model mimicking bacterial infection. F4/80high-Kupffer cells and inflammatory monocytes were identified as CD45+F4/80highCD11b+ and CD45+F4/80lowCD11bhighLy6Chigh cells, respectively (122, 125) (Figure 1A). After 24 hours, LCMV induced an almost 5-fold increase in the fraction of inflammatory monocytes similar to a single LPS injection (from 5.8% in healthy liver to 25.6% and 24.5% of total intrahepatic CD45+ cells in LPS- and LCMV- challenged livers,

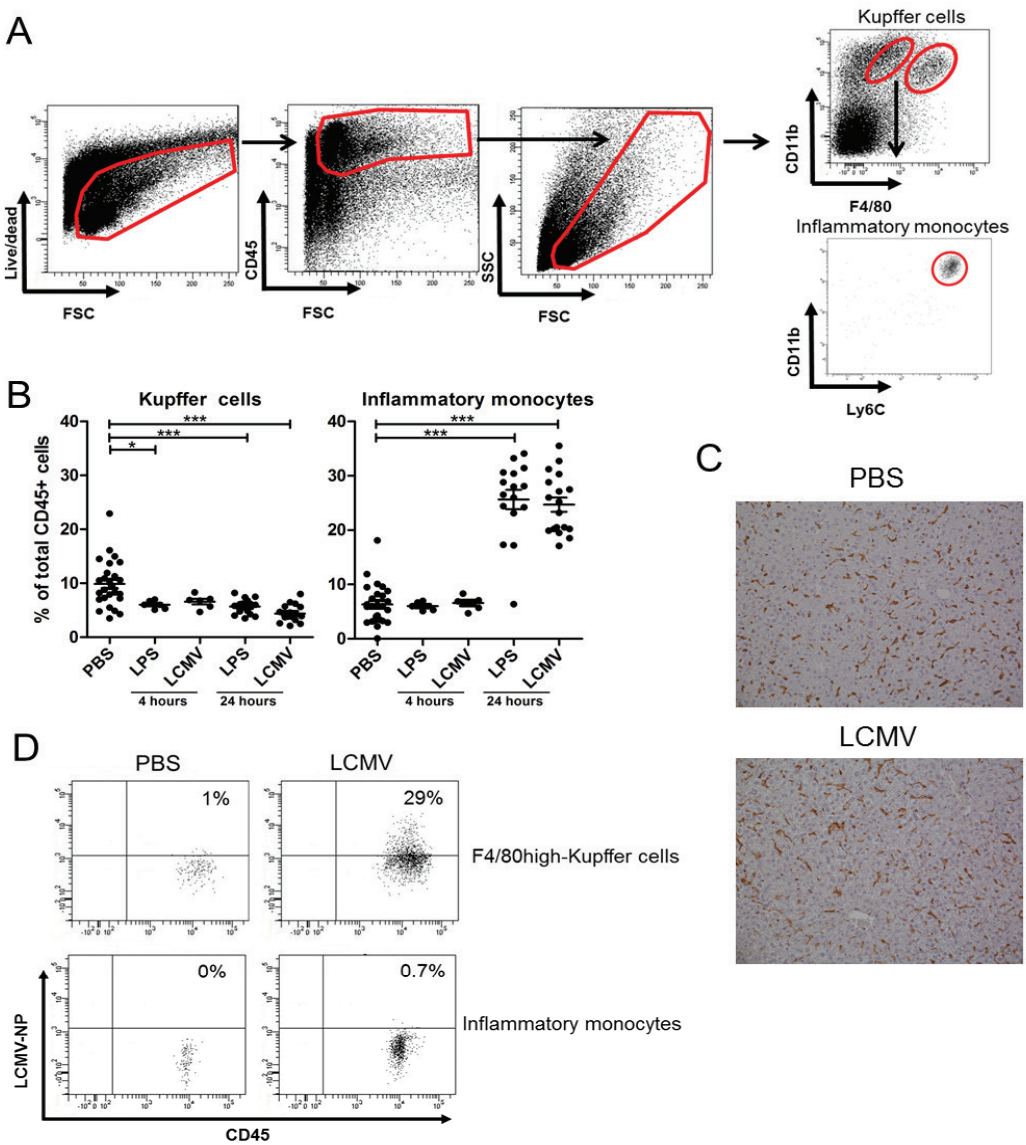

Figure 1. Infiltration of inflammatory monocytes characterizes the activation of the intrahepatic immune response upon challenge by LCMV as well as LPS. A) Representative dotplots showing flow cytometric identification of Kupffer cells and inflammatory monocytes in mouse liver. Total liver cells were determined using viability, CD45, and size and granularity gates. Inflammatory monocytes and F4/80high-Kupffer cells were identified as CD45+F4/80lowCD11bhighLy6Chigh and CD45+F4/80highCD11b+ cells, respectively. B) The frequencies of inflammatory monocytes and F4/80high-Kupffer cells in liver were determined as a percentage of total CD45+ cells at 24 hours post LCMV infection or LPS challenge or PBS control. The data were obtained from 4 separate experiments. Statistical analysis: one-way ANOVA (Kruskal-Wallis test with Dunn's Multiple Comparison post-test), ***p<0.001. Data shows the average ± SEM. C) Liver tissues from 6 PBS challenged or 6 infected mice (24h post infection) were subjected to F4/80 staining and evaluated by immunohistochemistry. In healthy liver, F4/80 positive cells appear as elongated cells with intense brown F4/80 staining, whereas upon LCMV infection, F4/80+ cells appear slightly larger in size with diffuse brown F4/80 staining in comparison to the F4/80+ cells in healthy liver. D) Representative dotplots (from n=8) of the frequency of LCMV-infected F4/80high-Kupffer cells and inflammatory monocytes as evidenced by intracellular LCMV-NP staining 24 hours post infection. Control staining without the addition of LCMV-NP antibody or anti-rat CD45 was used to set the threshold gate.

respectively; Figure 1B). Interestingly, monocyte recruitment was accompanied by a decrease in the frequency of F4/80high-Kupffer cells in the LPS-treated and LCMV-infected livers (from 10.4% in healthy to 5.7% and 4.4% of total intrahepatic CD45+ cells in LCMV-infected and LPS-treated livers, respectively).

To examine whether the reduction of intrahepatic CD45+F4/80highCD11b+ cells upon LCMV challenge corresponded to a genuine reduction in the frequency of Kupffer cells or a diminished surface expression of these markers, we performed an immunohistochemical analysis on 24-hour LCMV-infected and healthy livers (Figure 1C). Interestingly, in contrast to the flow cytometric quantification, there was no clear depletion of Kupffer cells upon LCMV infection. Instead, the morphology of F4/80+ cells, which predominantly consist of Kupffer cells, changed towards larger or swollen cells, with a less intense F4/80 staining (Figure 1C), suggesting a down-regulation of F4/80 expression in comparison to healthy liver. Importantly, no cleaved caspase-3+ cells could be identified in both healthy and 24-hour LCMV-infected livers, thereby excluding the presence of apoptotic parenchymal or non-parenchymal cells (data not shown). Kupffer cells, which retained their F4/80 expression and were still identifiable by flow cytometry, were further termed F4/80high-Kupffer cells.

Corroborating earlier data on infection of Kupffer cells (102), we observed that 29% of F4/80high-Kupffer cells were LCMV-NP+ within 24 hours after infection (Figure 1D). In addition, at this stage F4/80high-Kupffer cells were the predominant LCMV-NP+ cells in the liver (90%), while the remainder LCMV-NP+ cells were inflammatory monocytes (8%) and granulocytes (2%) (data not shown).

During early LCMV infection, F4/80high-Kupffer cells remain endocytic.

Previous data from our group and others have shown that Kupffer cells from healthy mice are specialized phagocytes with only marginal cytokine production ex-vivo under steady-state conditions (125), and that Kupffer cells are among the first to be infected with LCMV thereby limiting viral spread (77, 83, 102). We here studied in detail the endocytic ability of F4/80high-Kupffer cells and inflammatory monocytes during early LCMV infection. As shown in Figure 2A, the endocytic ability of F4/80high-Kupffer cells, as expressed by the fraction of dextran+F4/80high-Kupffer cells, was reduced in LCMV-infected compared to PBS-injected mice, but the majority of cells were able to perform endocytosis, which was similar to F4/80high-Kupffer cells from LPS-challenged mice. Inflammatory monocytes exhibited a weaker endocytic ability in control mice, which was completely lost upon LCMV infection, while LPS treatment increased it (14.8% vs 29.3% vs 1.5% dextran+ inflammatory monocytes, in healthy, LPS-treated and LCMV-infected livers, respectively; Figure 2A).

Next, we evaluated whether the endocytic function was reflected by the gene expression profile of the cells. F4/80high-Kupffer cells purified from unchallenged mice show higher expression levels of various complement genes (C1qa, C1qb, C2, C4a and C6) as compared to inflammatory monocytes, both isolated from unchallenged mice (Figure 1 and Supplementary Figure 1). Also, gene expression levels of F4/80, genes encoding various Fcγ receptors and Marco were more expressed by F4/80high-Kupffer cells than inflammatory monocytes, indicating a more pronounced activity of the "classical scavenger functions" of F4/80high-Kupffer cells under steady state conditions. As shown in Figure 2B, infection with LCMV or challenge with LPS upregulated the expression levels of Marco on F4/80high-Kupffer cells, while the expression of various genes encoding for complement remained high with the exception of C2 and C3, which were further upregulated. In LPS- or LCMV-challenged inflammatory monocytes the expression levels of the complement genes remained lower than observed in F4/80high-Kupffer cells: minimal upregulation of Marco, and complement genes, with the exception of C1qa and C1qb.

We then examined whether the observed differences in the

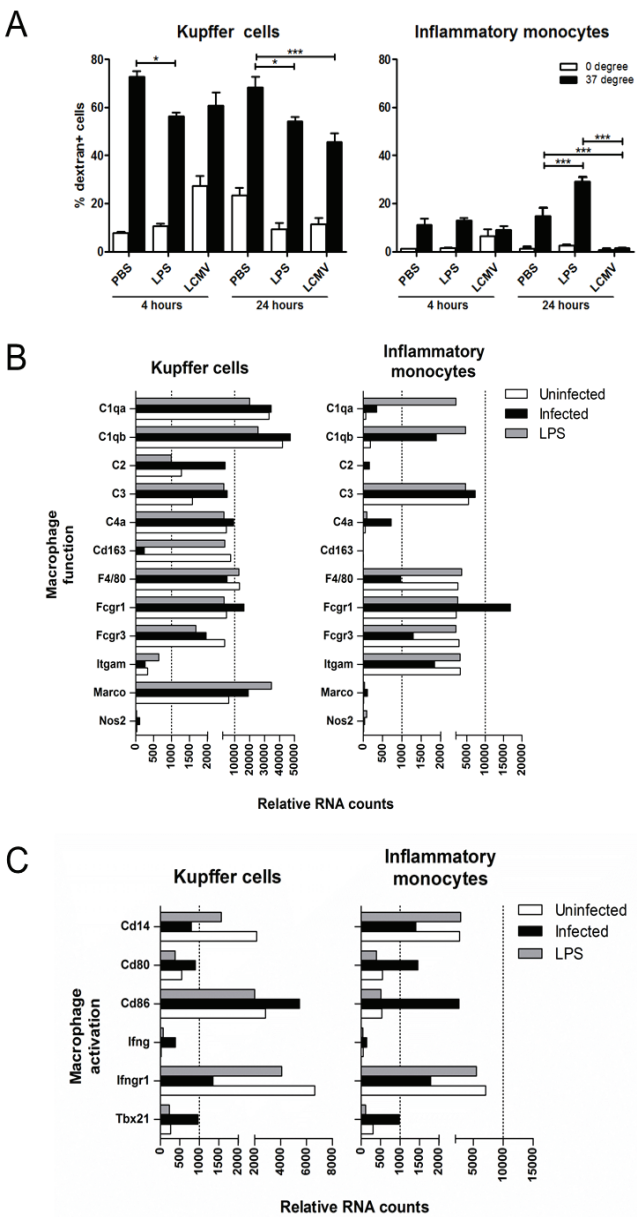

Figure 2. F4/80high-Kupffer cells retain a gene expression profile characteristic of phagocytic ability upon LCMV and LPS challenge, while this is only partially induced in inflammatory monocytes. Mice were infected with LCMV or challenged with LPS or PBS for 24 hours. A) Endocytosis was determined by flow cytometry by incubating total liver non-parenchymal cells with FITC-conjugated dextran at 0°C or 37°C for 45 minutes. Inflammatory monocytes and F4/80high-Kupffer cells were identified as CD45+F4/80lowCD11bhighLy6Chigh and CD45+F4/80highCD11b+ cells, respectively. Control staining without the addition of dextran was used to set the threshold gate. The assays were performed 2 times. Statistical analysis: two-way ANOVA with Bonferroni post-test, ***p<0.001. Data shows the average ± SEM. B) and C) Gene expression was determined by NanoString technology on total RNA isolated from formaldehyde-fixed, FACS sorted Inflammatory monocytes and F4/80high-Kupffer cells from LCMV infected or LPS challenged mice.

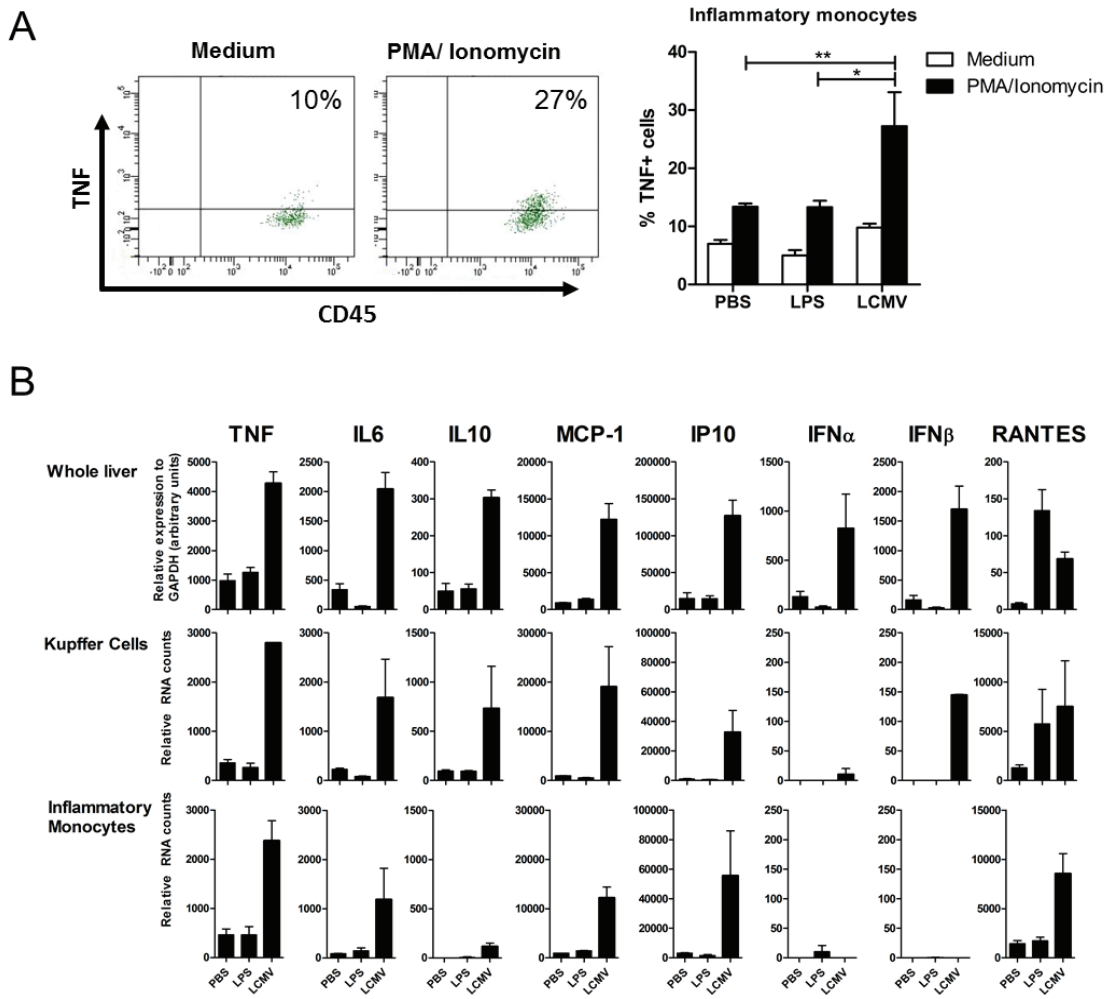

Figure 3. Both sorted Kupffer cells and inflammatory monocytes exhibit an active cytokine and chemokine transcriptional profile early after LCMV. Mice were infected with LCMV Cl13 or challenged with LPS or PBS (n=6-12 per group), and sacrificed 24 hours later. A) Total liver non-parenchymal cells were stimulated with medium or PMA/ionomycin for 5 hours. Flow cytometric analysis and graphic representation of the frequency of TNF-producing inflammatory monocytes (CD45+F4/80lowCD11bhighLy6Chigh cells) determined by intracellular cytokine staining. Control staining without the addition of TNF detecting antibody was used to set the threshold gate. Statistical analysis: 2-tailed t-test, *p<0.05, **p<0.01. B) Gene expression was determined in whole liver (n=4-6) by qPCR, and in RNA isolated from formaldehyde-fixed, FACS sorted inflammatory monocytes and F4/80high-Kupffer cells from infected or challenged mice by NanoString technology. The data shown are obtained from 2 independent experiments using 6 pooled livers. Data shows the average ± SEM.

endocytic response of F4/80high-Kupffer cells and inflammatory monocytes to LPS or LCMV were related to changes in the expression of genes associated with cell activation at 24 hours after challenge. As presented in Figure 2C, induction of mRNA expression of the activation markers CD80 and CD86 was observed for both F4/80high-Kupffer cells and inflammatory monocytes purified from the liver of LCMV-infected mice, whereas CD14 mRNA expression was down-regulated. The effects of in vivo exposure to LPS on the expression levels of these markers were minimal at 24 hours after challenge. In line with published data in Listeria monocytogenes as well as in vitro exposure of macrophages to IFNα (129, 130), we now show that both F4/80high-Kupffer cells and inflammatory monocytes isolated from LCMV infected mice exhibited down-regulation of the expression of IFNγR1, despite enhanced expression of IFNγ and Tbx21 mRNA.

Both sorted Kupffer cells and inflammatory monocytes exhibit an active cytokine and chemokine transcriptional profile early after LCMV infection

Next, we determined the ability of F4/80high-Kupffer cells and inflammatory monocytes to produce cytokines upon stimulation with PMA and ionomycin. As we published before, Kupffer cells produce low or undetectable cytokines (such as TNF and IL-12p40) following in vitro stimulation (125). We now show that F4/80high-Kupffer cells are weak producers even when isolated from mice challenged with LPS or LCMV (in all conditions on average less than 5% TNF+ cells). In contrast, here we demonstrate that inflammatory monocytes isolated from LCMV-infected mice produced higher levels of TNF compared to control mice after in vitro exposure to PMA and ionomycin. An increased ability to produce TNF by these cells was not seen after LPS treatment (Figure 3A, 13.4% vs 13.3% vs 27.5% TNF+ inflammatory monocytes in PBS-treated, LPS-treated and LCMV-infected livers, respectively, upon in vitro restimulation with PMA and ionomycin).

Next, we examined the hepatic gene expression levels in whole liver of pro- and anti-inflammatory cytokines, chemokines, interferons and interferon-inducible antiviral mediators in both experimental challenge conditions. Twenty-four hours after LCMV

inoculation, significant increases of intrahepatic mRNA levels of TNF, IL-6, IL-10, MCP-1, IP-10, IFNα, IFNβ and RANTES were noted by evaluation of the whole liver (Figure 3B). Distinct to the LCMV infection, LPS treatment primarily increased the mRNA levels of innate pro- and anti-inflammatory cytokines and chemokines at an earlier time point (i.e. 4 hours after injection, data not shown), which the exception of RANTES, which remained upregulated 24 hours post treatment. It is important to mention that this early LCMV-induced liver inflammation was not accompanied by a rise in serum transaminases or histological signs of liver damage (Supplementary Figure 2A and 2B). To determine the possible contribution of F4/80high-Kupffer cells and inflammatory monocytes as the source of the observed gene expression levels, we again determined the gene expression profile of cells isolated from mice challenged with LPS or LCMV. As shown in Figure 3B, overall, both F4/80high-Kupffer cells and inflammatory monocytes express mRNA for TNF, IL-6, IL-10, MCP-1, IP-10 and RANTES 24 hours after LCMV infection. In line with the findings in whole liver, challenge with LPS did not exhibit enhanced gene expression levels at 24h after challenge, except for RANTES mRNA in F4/80high-Kupffer cells. Interestingly, IFNβ mRNA was strongly induced in F4/80high-Kupffer cells from LCMV infected mice, but not in inflammatory monocytes, whereas IFNα was only weakly induced in both cell types.

Purified F4/80high-Kupffer cells as well as inflammatory monocytes induce an interferon response following early LCMV infection

The induction of IFNβ by F4/80high-Kupffer cells, but not inflammatory monocytes may indicate that these cell types possess distinct functions in the early events following LCMV infection. We therefore examined the expression of IFN-inducible genes in both cell types to determine to what extent inflammatory monocytes are triggered by IFN production derived from F4/80high-Kupffer cell-derived and other liver cells. As shown in Figure 4, both F4/80high-Kupffer cells and inflammatory monocytes strongly increase the expression of MxA mRNA early following LCMV infection. Similar findings were observed for Ifi35, Ifih1, Ifit2, various chemokines, as well as Irf1 and Irf7. In line with the expected induction of an IFN-dominated response, also the expression of Stat1, Stat2 and Stat3 mRNA was induced in both F4/80high-Kupffer cells and inflammatory monocytes, but not of Stat4, Stat5 and Stat6.

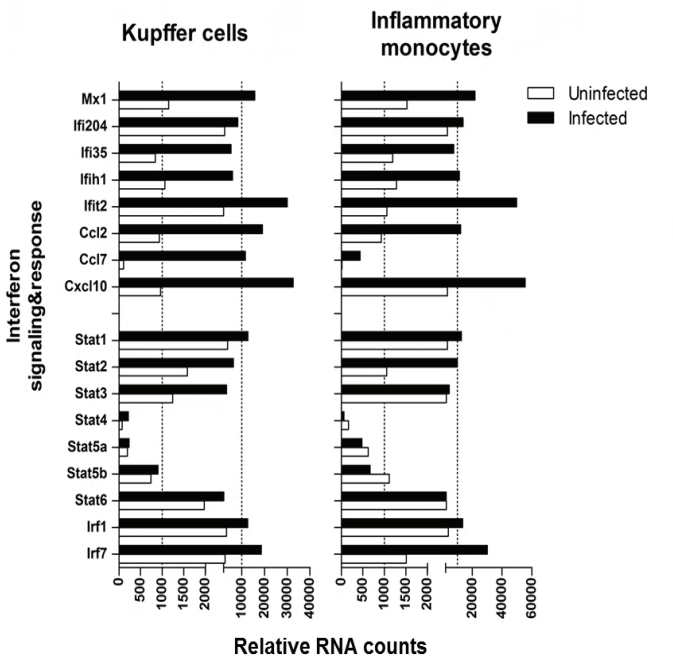

Figure 4. Both purified Kupffer cells and inflammatory monocytes are activated and induce an interferon response following early LCMV infection. Gene expression was determined in RNA isolated from formaldehyde-fixed, FACS sorted inflammatory monocytes and F4/80high-Kupffer cells from LCMV infected mice by NanoString technology. The data shown are obtained from 2 independent experiments using 6 pooled livers.

Discussion

Due to a lack of suitable animal models, our current understanding of early virus-host interactions in virus-induced liver disease is limited. In this study we make use of a short-term LCMV Cl13 infection in mice to examine phenotypical and functional changes in inflammatory monocytes and F4/80high-Kupffer cells, which are the first innate immune cells to encounter a viral pathogen in the liver. Here we show that LCMV induces a marked recruitment of infiltrating monocytes within 24 hours after infection. However, we observed that the major LCMV-NP+ population comprises F4/80high-Kupffer cells, which maintain their endocytic activity and present increased expression of several pro- and anti-inflammatory cytokines and chemokines after LCMV infection. On the other hand, inflammatory monocytes obtained from the liver of LCMV-infected mice exhibited weak endocytic activity, while the expression pattern of these inflammatory monocytes strongly resembled those of F4/80high-Kupffer cells early after LCMV infection. The observation that during early LCMV infection inflammatory monocytes outnumber the F4/80high-Kupffer cells indicates their important contribution to the early phase of LCMV-induced liver inflammation.

During early LCMV infection, we show that F4/80high-Kupffer cells become activated, take up LCMV-NP, and remain endocytic. The endocytic ability is in line with Lang et al, who demonstrated that active uptake of LCMV by Kupffer cells limits viral spread and immunopathology (102). Similar to the LCMV model, Kupffer cells represent the predominant cell population to eliminate adenovirus-5 from the liver (131). Previously, activated macrophages have been shown to reduce their F4/80 expression (132, 133). The immunohistological finding corroborates this flow cytometric down-regulation of F4/80 surface expression. Similar phenotypical changes in Kupffer cells have been observed after an adenovirus-5 infection in which cytoplasmic LysM expression was diminished as early as 20 minutes after infection, while membrane-associated MHC II expression was unaffected (131).

Despite the observation that ex vivo stimulations show minimal TNF production by F4/80high-Kupffer cells upon polyclonal stimulation, the gene expression profile of sorted F4/80high-Kupffer cells from LCMV-infected mice clearly show induction of pro- and anti-inflammatory cytokines and chemokines, including TNF, IL-6, IL-10 and others. The discrepancy between the results obtained from the in vitro and in vivo data need to be studied in detail, but may be due to the nature of the trigger used for restimulation of the cells in vitro. Detailed comparison of the gene expression levels of the cytokines and chemokines in whole liver versus the purified population strongly suggest that both F4/80high-Kupffer cells and inflammatory monocytes contribute, to a large extent, to the production of cytokines early during

LCMV infection. Importantly the mRNA expression levels of TNF, IL-6, MCP, IP-10, and RANTES are highly similar between both cell types, whereas IL-10 mRNA remains expressed at higher levels by F4/80high-Kupffer cells as compared to inflammatory monocytes. Despite the relatively high expression of IFNα mRNA in whole liver 24 hours after LCMV infection, low or undetectable levels are observed in F4/80high-Kupffer cells and inflammatory monocytes, indicating that other intrahepatic cells, such as plasmacytoid DC and hepatocytes are the source of this interferon. Another option is that both sorted cell types produce other IFNα subtypes then the IFNα1 and 2 detected by the Nanostring probes (NCBI ID codes NM_010502.2 and NM_010503.2 respectively). Furthermore, due to the known RNA fragmentation after formalin fixation, all tested qPCR primer sets yielded inconsistent results when tested on RNA from sorted F4/80high-Kupffer cells and inflammatory monocytes cells (data not shown) (127). IFNβ, on the other hand, was expressed by F4/80high-Kupffer cells, but not by inflammatory monocytes, which may be the direct result of triggering of IFNβ production upon LCMV infection and replication in F4/80high-Kupffer cells. Importantly, despite distinct and selective expression of type I IFN, both cell types have transcript levels for numerous ISG, encoding for chemokines as well as proteins that function to suppress viral replication, such as MxA. This might imply that Kupffer cell IFNβ-release is instrumental in activating the recruited inflammatory monocytes, which could therefore be an important therapeutic target.

Previous studies have shown the complexity of the functions of inflammatory monocytes found in different organs, during a bacterial, fungal, protozoal or viral infection (104-110). Although both LCMV infection and LPS treatment induce the recruitment of inflammatory monocytes to a similar extent, we show that the activity of LCMV-induced and LPS-induced inflammatory monocytes are functionally distinct. Similar to their role in colonic inflammation, LCMV-induced inflammatory monocytes are skewed towards a secretory function, as demonstrated by the increase in TNF production ability in comparison to liver monocytic cells from healthy mice and their gene expression profile, and completely lose their steady state endocytic ability (106). On the other hand, LPS-induced inflammatory monocytes do not increase their ability to produce or express cytokines or chemokines, but enhance their endocytosis potential. In mouse studies, TNF production by intrahepatic inflammatory monocytes has been associated with liver damage (123, 124). Similarly in patients with chronic inflammatory and fibrotic liver diseases, inflammatory monocyte-derived TNF, amongst other pro-inflammatory cytokines and chemokines, has been shown to be pro-fibrogenic (134). However, we did not find evidence of liver damage at this early stage after infection. In line with this, Karlmark et al have shown that the newly recruited inflammatory monocytes are not responsible for the early onset of CCl4-induced hepatitis (122). Alternatively, inflammatory monocyte-derived TNF might act as a positive feedback for further recruitment of inflammatory monocytes to the liver. Recently, the formation of intrahepatic myeloid cell aggregates that can stimulate local T cell proliferation (iMATE) has been attributed to monocyte-derived TNF (135). Our findings support the pro-inflammatory role of recruited monocytes in the setting of early virus-induced liver disease.

Our study substantiates the robustness of the liver as a filtering organ for viral pathogens. Early after LCMV infection a functional dichotomy is observed for inflammatory monocytes and F4/80high-Kupffer cells with respect to endocytosis, but their activation and cytokine gene expression profiles exhibit a strong resemblance. Especially inflammatory monocytes show a huge capacity for recruitment to the liver and plasticity dependent on the nature of the inflammatory signal, either viral or sterile. Although the relative contribution of inflammatory monocytes or F4/80high-Kupffer cells to the outcome of the infection needs to be investigated, our study points towards a crucial role for inflammatory monocytes in shaping the inflammatory environment in the liver early after infection.

Acknowledgement

We would like to thank Vincent Vaes, Judith van Agthoven and Dennis de Meulder from the Erasmus MC animal care facility for their assistance in performing biotechnical manipulations.

Chapter 3

Published in: PLoS One, 2016, 11:e0166094

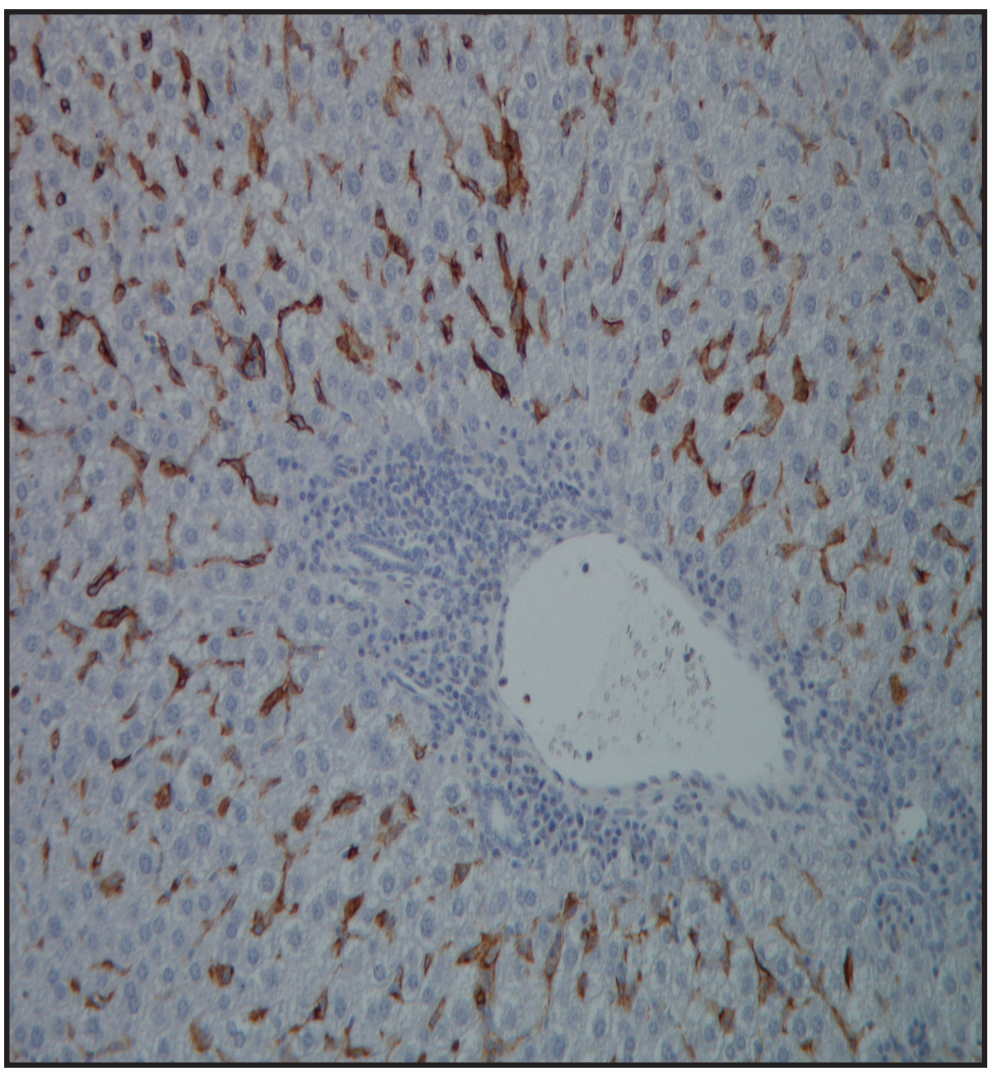

Mouse liver with Kupffer cells in brown (F4/80 staining) and infiltrating lymphocytes (small blue cells) after 22 days of LCMV infection.

Liver monocytes and Kupffer cells remain transcriptionally distinct during chronic viral infection

Martijn D.B. van de Garde[1], Dowty Movita[1], Marieke van der Heide[1], Florence Herschke[2], Sandra De Jonghe[2], Lucio Gama[3], Andre Boonstra[1,#], Thomas Vanwolleghem[1,#]

Abstract

Due to the scarcity of immunocompetent animal models for chronic viral hepatitis, little is known about the role of the innate intrahepatic immune system during viral replication in the liver. These insights are however fundamental for the understanding of the inappropriate adaptive immune responses during the chronic phase of the infection. We apply the Lymphocytic Choriomenigitis Virus (LCMV) clone 13 mouse model to examine chronic virus-host interactions of Kupffer cells (KC) and infiltrating monocytes (IM) in an infected liver. LCMV infection induced overt clinical hepatitis, with rise in ALT and serum cytokines, and increased intrahepatic F4/80 expression. Despite ongoing viral replication, whole liver transcriptome showed baseline expression levels of inflammatory cytokines, interferons, and interferon induced genes during the chronic infection phase. Transcriptome analyses of sorted KC and IMs using NanoString technology revealed two unique phenotypes with only minimal overlap. At the chronic viral infection phase, KC showed no increased transcription of activation markers Cd80 and Cd86, but an increased expression of genes related to antigen presentation, whereas monocytes were more activated and expressed higher levels of Tnf transcripts. Although both KCs and intrahepatic IM share the surface markers F4/80 and CD11b, their transcriptomes point towards distinctive roles during virus-induced chronic hepatitis.

[1]Department of Gastroenterology and Hepatology Erasmus University Medical Center, Rotterdam, The Netherlands, [2]Janssen-Pharmaceutica NV, Beerse, Belgium, [3]Department of Molecular and Comparative Pathobiology, The Johns Hopkins University School of Medicine, Baltimore, Maryland, USA, [#]These authors contributed equally to this work

Introduction

Detailed knowledge of intrahepatic immune responses is crucial for a better understanding of the processes underlying immunopathology. Chronic viral hepatitis induced by the Hepatitis B (HBV) and hepatitis C (HCV) virus affects almost 500 million people worldwide and leads to progressive liver fibrosis, decompensated cirrhosis, and hepatocellular carcinoma (136). Due to ethical constraints, studies of liver residing leukocytes are seldom performed in patients, although these cells are essential in determining the outcome of the infection. As alternative, the Lymphocytic Choriomeningitis Virus (LCMV) mouse model can be used. LCMV clone (Cl) 13 infection in mice is an established small animal model for immunological studies on persistent viral infection such as HIV, but also HBV and HCV (113). The ability of LCMV to infect hepatocytes, among other cells, underlines the relevance of this model for the study of virus induced hepatitis (77, 82-84, 137).

The largest innate immune cell population in the liver are the tissue-resident macrophages, also known as Kupffer cells (KC). KCs are abundantly present in the liver sinusoids, are crucial players in maintaining tissue homeostasis, and form together with sinusoidal endothelial cells the first barrier for pathogens to enter the liver (99). KCs can respond to danger signals using a variety of pathogen recognition receptors, such as Toll like, scavenger and antibody-receptors and, depending on the local environment, initiate an inflammatory response, or induce tolerogenic T-cell responses (100, 101). Previously, we described that liver inflammatory monocytes resembled KC but were functionally distinct after 24 hours of LCMV Cl13 infection in mice. Both cell types showed an activated phenotype with increased transcription of activation markers Cd80 and Cd86, and inflammatory cytokines Tnf and Il6 (137).

Monocytes patrol the body for inflammatory foci and are therefore among the first cells to respond to inflammation. They are quickly recruited in great numbers thereby shaping the immune environment (137, 138). These early monocytes are recruited in a CCL2/CCR2-dependent manner and are phenotyped in mice as F4/80+CD11b+CCR2hiLy6ChiCX3CR1low. They can exert pro-inflammatory and antimicrobial functions, such as secretion of inflammatory cytokines IL-6 and TNF (103, 137, 139). Previously, we showed that ex vivo HBsAg stimulation of blood monocytes revealed high cytokine induction (140). However, chronic HBV patient derived blood monocytes were not activated despite abundant viral proteins in their plasma (140). The role of liver monocytes and possible regulatory mechanisms controlling monocyte activation during chronic infection are still elusive.

KCs and monocytes are cells with high plasticity and can exert diverse functions depending on their environment. In mice, KCs have been shown to induce tolerogenic T-cells after phagocytosis of particle-bound antigens under homeostatic conditions, whereas monocytes showed no or minimal particle uptake. However, during early inflammatory conditions, monocytes were fit to counteract the tolerogenic KCs by taking up particles and producing TNF and inducible nitric oxide synthase (101). Experiments on Listeria monocytogenes infection revealed that monocytes replenish dead KCs in the liver and exert an inflammatory response, followed by a tissue-repair response to restore homeostasis (141). On the other hand, monocytes have also been described as regulatory cells that can suppress CD8+ T cell proliferation during LCMV Cl13 infection in mice (142).

We previously showed that CD14+ cells derived from chronic HBV patient livers displayed an activated phenotype and are able to interact directly with hepatitis B surface antigen (HBsAg) (143). In vitro, these CD14+ cells produce high amounts of tumor necrosis factor (TNF), interleukin (IL)-6, and CXCL8 after stimulation with HBsAg and can activate NK cells (143). As both IM and KC are CD14 positive, the precise roles of both cells during a chronic infection still need further elucidation. In the current paper we set out to fully characterize the immunology related gene transcription of sorted KCs and IM during chronic LCMV infection as a surrogate model for chronic viral hepatitis. We investigate whether these cells are distinct populations at the transcriptome level, and examine the role and activation status of both cells throughout chronic infection.

Materials and Methods

Study design, mice and virus

LCMV Cl13 was obtained as a kind gift from E. Zuniga, University of California in San Diego. LCMV Cl13 was propagated in BHK21 cells and the titer was determined by plaque assay as previously described (76, 80). Female C57BL/6 mice aged 4-6 weeks (Charles River, France) received 2 x 106 plaque forming units (PFU) LCMV Cl13 intravenously (i.v.). Mice were co-housed with a maximum of 4 mice per cage and were fed ad libitum. Animals were maintained in a Biosafety level-III isolator according to Dutch national biosafety guidelines. Body weight and the assessment of clinical symptoms were determined 2-3 times a week (Table 1). Blood was drawn from 6 mice at indicated time points to assess serum cytokines and liver enzymes. Mice were sacrificed in groups of 4-6 at indicated time point for whole liver qPCR, Immunohistochemistry, FACS analyses, and cell sorting (S1 Fig.). The study was approved by the animal ethics committee of the Erasmus University Rotterdam, and conducted according to relevant Dutch national guidelines.

Isolation of total liver non-parenchymal cells

Liver was removed without perfusion, cut into small pieces, and treated with 30 µg/ml Liberase TM (Roche) and 20 µg/ml DNAse type I (Sigma) for 30 min. Parenchymal cells were removed by low speed centrifugation at 50 g for 3 min and erythrocytes were lysed with 0.8% NH4Cl. The remaining non-parenchymal cells were resuspended in culture medium consisting of RPMI-1640 (Lonza) supplemented with 10% FCS (Sigma), 10 mM HEPES (Lonza), 2 mM L-glutamine (Lonza), 1% penicillin/streptomycin (Lonza) and used for further analysis.

Table 1. Clinical Scoring of LCMV infected mice

Clinical Score	Observation
CS 0	Normal behavior, active, no aberrant fur
CS 1	Pilo-erection AND/OR mild ruffled fur
CS 2	Mild hunched posture OR mild ruffled fur AND slightly less active
CS 3	Hunched posture AND ruffled fur AND less active
CS 4	Hunched posture AND ruffled fur AND inactive (very low or absent mobility)
CS 5	Death

Plaque Assay
Parts of infected livers were weighed, homogenized using ceramic beads, and centrifuged for 10 min at 450 g at 4°C. Supernatant was serially diluted in Dulbecco's modified Eagles Medium (DMEM, Lonza) supplemented with 10% FCS before inoculation onto overnight grown 90% confluent VeroE6 cells in 6 well plates (Corning). After 1 hour incubation, each 10^2 to 10^7 serial diluted inocula was removed and the cell layers were covered with a solution of 0.5% SeaKem®Agarose (Lonza) in Minimal essential Medium Eagle (EMEM, Lonza) supplemented with 10% FCS. The agarose layer was removed after 5 days incubation at 37°C, 5% CO2, and cells were stained with a crystal violet solution in 2% formaldehyde (Merck). The number of plaques at each dilution was counted and averaged to obtain the viral concentration of the sample in PFU/ml. Each sample was corrected for liver weight input and is expressed as PFU per gram liver.

Flow cytometry
Total liver non-parenchymal cells were stained with Aqua Dead Cell Stain from Invitrogen, and antibodies directed against CD45 eFluor450 (30-F11), F4/80 APC (BM8), CD11b PECy7 (M1/70) from eBioscience and Ly6C APCCy7 (HK1.4) from Biolegend (unless otherwise indicated), and fixed with 2% formaldehyde for 1 hour, after which cells were analyzed using a FACSCanto-II flow cytometer and FACSDiva software (BD Biosciences).

RNA isolation of liver homogenates, generation of cDNA and real-time PCR
Liver was homogenized in RNAlater (Qiagen). RNA was extracted using Trizol (LifeTech) and a NucleoSpin RNAII kit (Bioké). cDNA was generated using the iScript cDNA Synthesis Kit (Bio-Rad Laboratories) according to the manufacturer's protocol. Quantitative PCR were performed using SYBR-green and MyIQ5 detection system (Bio-rad Laboratories). Sequences of primers are listed in Table 2. Expression of target genes was normalized to the expression of GAPDH using the formula $2^{-\Delta Ct}$, $\Delta Ct = Ct_{RNAX} - Ct_{GADPH}$.

Table 2. Gene-specific primers used for whole liver RNA analyses

Taqman gene expression primers			
Gene ID	Primer ID*		
Ifng	Mm01168134_m1		
Gapdh	Mm99999915_g1		
SYBR green primers			
Gene ID	NCBI ID	Direction	Primer sequence 5' – 3'
Il6	NM_031168.1	F	TGGTGACAACCACGGCCTTCC
		R	AGCCTCCTGACTTGTGAAGTGGT
Tnf	NM_013693.2	F	CAGGCGGTGCCTATGTCTC
		R	CGATGACCCCGAAGTTCAGTAG
Ifnb	NM_010510.1	F	GCCTGGATGGTGGTCCGAGC
		R	ACTACCAGTCCCAGAGTCCGCC
Isg15	NM_015783.3	F	CAGGACGGTCTTACCCTTTCC
		R	AGGCTCGCTGCAGTTCTGTAC
Oas12	NM_011854.2	F	GGATGCCTGGGAGAGAATCG
		R	TCGCCTGCTCTTCGAAACTG
Gapdh	NM_008084,2	F	CGTCCCGTAGACAAAATGGT
		R	TCTCCATGGTGGTGAAGACA

*Primer/probe mixes from Life-technologies

RNA isolation of sorted cells and NanoString
KC and IM from 4-6 pooled livers were purified at day 0 (in duplicate), day 15, day 21, and day 41 post infection (p.i.), by cell sorting based on the expression of F4/80, CD11b and Ly6C, after initial enrichment using CD45 PE followed by anti-PE Microbeads (Milteny Biotec) selection. Following staining, cells were fixed with 2% formaldehyde for 1 hour, and sorted on a FACS Aria SORP flow cytometer (BD Biosciences). Total RNA was isolated from sorted cells using the RNeasy FFPE kit (Qiagen) following manufacturers' protocols starting with adding 150 µl Buffer PKD, to reverse any possible formaldehyde induced RNA modification. The nCounter GX Mouse Immunology Kit (NanoString Technologies, Seattle, WA, USA) was used to measure the expression of 561 genes in the RNA samples. Following hybridization, transcripts were quantitated using the nCounter Digital Analyzer. Samples were run by the Johns Hopkins Deep Sequencing & Microarray Core. To correct for background levels, the highest negative control value for each sample was subtracted from each count value of that sample. Following background subtraction, any negative count values were considered as 0. Values were normalized by the geometric mean of 13 housekeeping genes provided by the company panel.

Immunohistochemistry for F4/80
Liver was fixed in 4% formaldehyde, embedded in paraffin, and cut into 5 µm sections. F4/80 antigen was retrieved using Proteinase K (Sigma). Endogenous peroxidase was inactivated using 3% hydrogen peroxide (Dako). Liver sections were incubated with rat anti-F4/80 antibody (eBioscience) and rabbit anti-rat HRP (Dako). Upon addition of DAB, liver sections were counterstained with hematoxyline (Merck).

Cytokine measurement
Serum TNF, IL-10, IFNɣ and CXCL1 levels were measured using the MSD® MULTI-SPOT Assay System, Mouse Pro-Inflammatory 7-plex Ultra-Sensitive Kit (MesoScaleDiscovery, ref. K15012C-2), following the instruction manual. After an overnight incubation at 4°C, samples were measured in monoplicate undiluted and standard curve and blanks in duplicate. Electrochemiluminescence was read on a Sector Imager 6000 (MesoScaleDiscovery).

ALT measurement
Serum ALT levels were measured using an ELISA kit for Alanine Aminotransferase (Biotang) according to the manufacturer's protocol.

Data analysis and statistics
Differences between groups were calculated using one-way ANOVA with Dunn's Multiple Comparison post-test (GraphPad Prism version 5.01; GraphPad Software). Differences were considered significant when $P < 0.05$. Results are presented as the mean ± SEM, unless otherwise indicated. Principal component analyses was performed on whole log 2 transformed data set using Multi-experiment viewer (MeV) software version 4.9 and hierarchical clustering was executed using one minus pearson correlation in GENE-E software version 3.0.204 (Broad Institute, Inc). The statistical variance of all transcripts of 2 KC samples at day 0 were determined. The fold change of these values was calculated and used as cutoff to determine differentially expressed genes (1.27-fold for KC). The cutoff for differentially expressed genes in IM was determined similarly (1.15-fold for IM). Non-expressed genes were defined as <100 relative RNA counts and below four times the standard deviation in all samples.

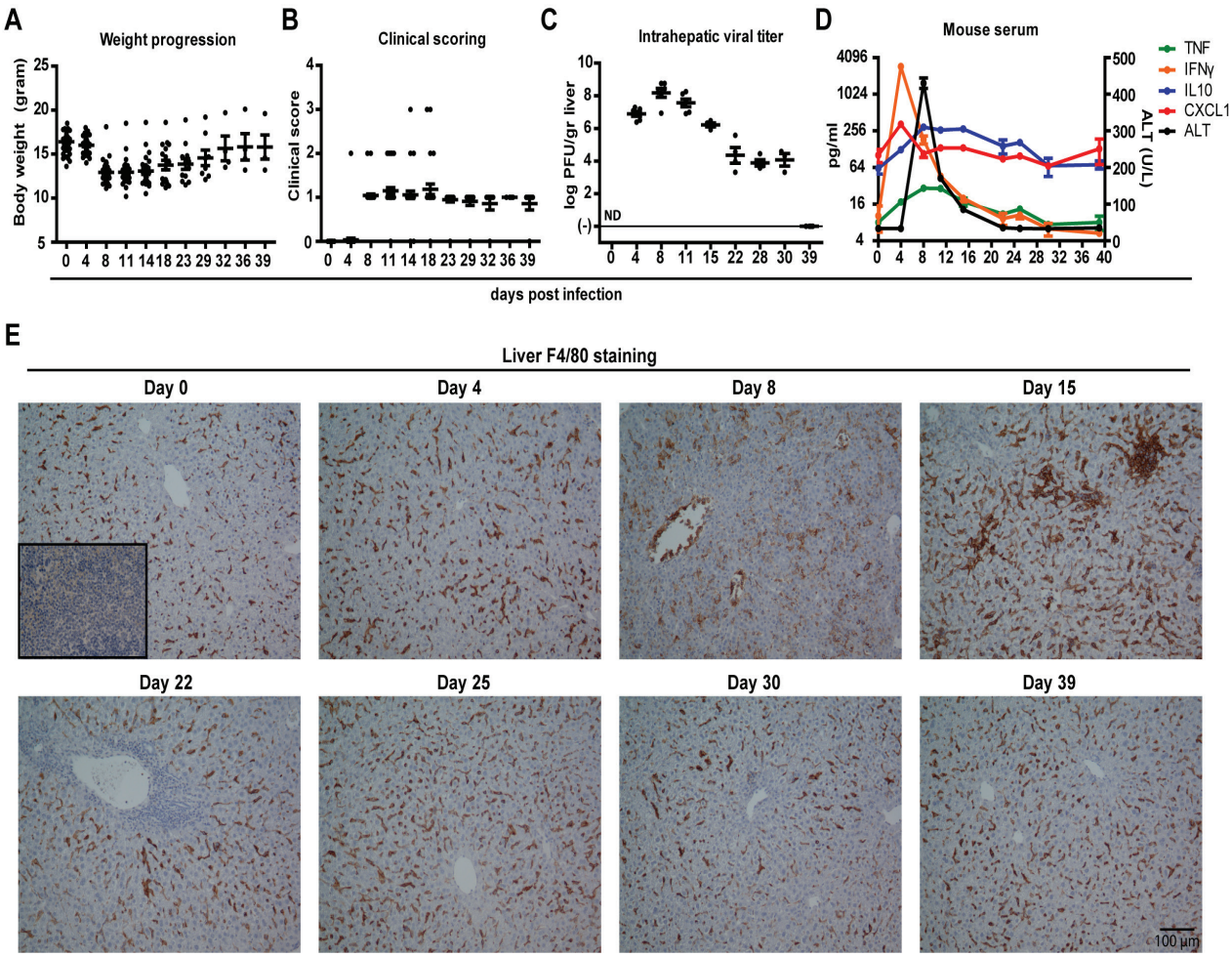

Figure 1. Evident LCMV-induced hepatitis with overt clinical symptoms, rise in serum cytokines and intensified F4/80+ cell staining. During the course of LCMV Cl13 infection mice were weighed (A) and clinically scored using predefined criteria (Table 1) (B). At regular intervals mice were sacrificed to determine the intrahepatic LCMV viral load (C). Serum was collected at different time points to measure ALT (D) and cytokines TNF, IFNγ, CXCL1, and IL10 (D) using a multiplex assay. X-axis shows days post infection (A-D). Error bars indicate mean ± SEM (A-D). ND, not determined (C). F4/80 IHC staining was performed at indicated time points to characterize the presence, morphology and localization of F4/80+ cells within the liver (E). Insert at day 0 shows non-primary control staining of mouse spleen (E). Scale bar indicates 100 µm (E).

Results

LCMV clone 13 infection induces evident hepatitis accompanied by changes in F4/80 expressing cells

Previously, we showed that LCMV Cl13 is able to infect the liver in addition to other organs (137). Infection with LCMV results in active intrahepatic replication, which can last up to 40 days (144). The progression of infection was accompanied by wasting (Fig. 1A, $p<0.001$ at peak of infection) and increased clinical scores based on set criteria (Table 1, and Fig. 1B, $p<0.001$ at peak of infection), which aggravated just after the peak of infection around day 14 p.i. and recovered towards viral clearance from the liver at day 39. At peak of infection, intrahepatic LCMV titers reached 8 log PFU/gr liver, which dropped to an average of 4 log PFU/gr liver from day 15 onwards (Fig. 1C). LCMV-specific T cell exhaustion is at highest level and sustained from day 15 p.i., which is therefore regarded as the onset of chronic infection in this model (145). Peak of intrahepatic LCMV replication was associated with evident rise of serum ALT, preceded by peak in IFNγ and CXCL1, and coincided with TNF and IL-10 levels (Fig. 1D).

To get insight in the kinetics, location, and morphology of F4/80+ myeloid cells during LCMV-induced hepatitis, immunohistochemistry was performed at several time points post infection. At the peak of intrahepatic LCMV replication F4/80+ cells changed their morphology into more elongated and swollen cells with decreased F4/80 intensity. During early chronic infection, cells were found in liver sinusoids with strong F4/80 intensity. Later on, liver F4/80 staining was comparable to non-infected livers (Fig. 1E). The changes in cell morphology and F4/80 intensity staining suggests that viral infection alters the phenotype and possibly the function of F4/80 positive cells.

No increased expression of cytokine and interferon in whole liver during LCMV-induced chronic hepatitis

We next examined the impact of LCMV-induced hepatitis on liver-specific innate immune responses. Increased levels of pro-inflammatory cytokine transcripts occurred before (Tnf), during (Ifng), or after (Il6) the peak of intrahepatic viral replication (Fig. 2A-C). Interestingly, these levels were not significantly different from baseline during the chronic phase of the infection. A similar intrahepatic expression pattern was seen in transcript levels of interferon (IFN)-beta and selected IFN stimulated genes (ISG,

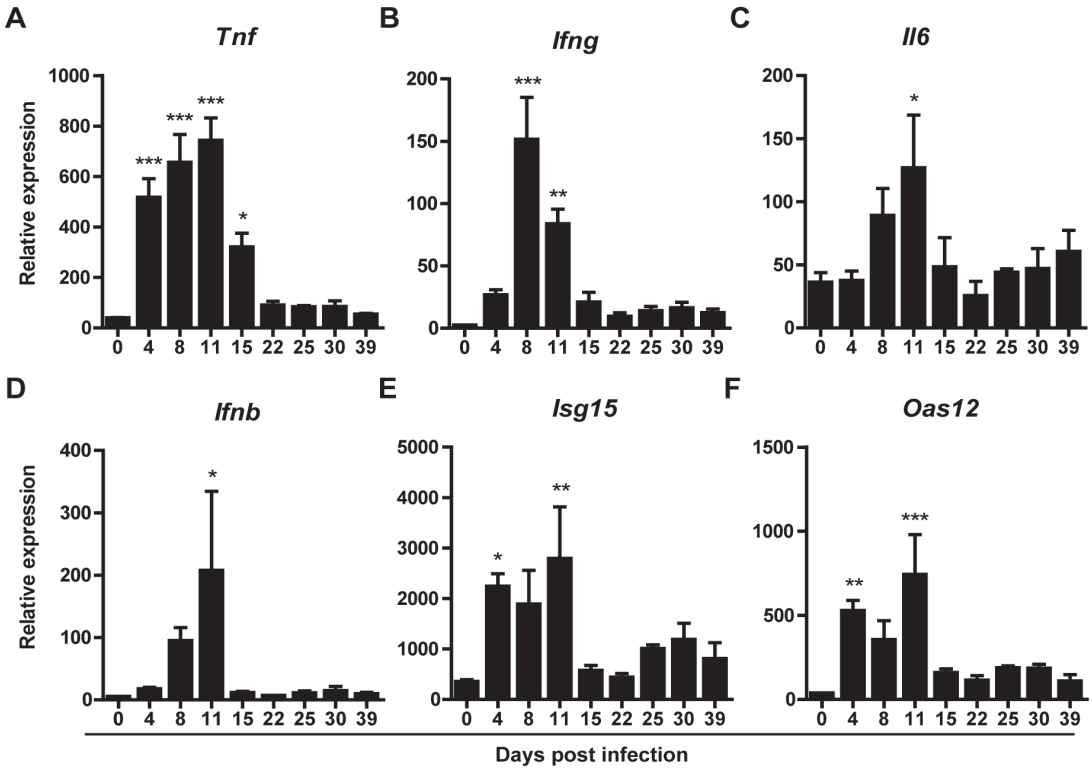

Figure 2. Hepatic cytokine and interferon transcript levels increase during the peak of LCMV replication but normalize thereafter. Whole liver RNA was isolated from LCMV infected mice at regular intervals and analyzed for transcription of inflammatory cytokines Tnf, (A) Ifng (B), Il6 (C), Ifnb (D) and interferon induced genes Isg15 (E) and Oas12 (F) using qPCR. Given values on y-axes are relative expression to GAPDH. X-axes shows days post infection. Error bars indicate mean ±SEM. Significance of each time point was assessed using one-way Anova with Dunnett's Multiple comparison test to day 0. *p<0.05, **p<0.01, ***p<0.001.

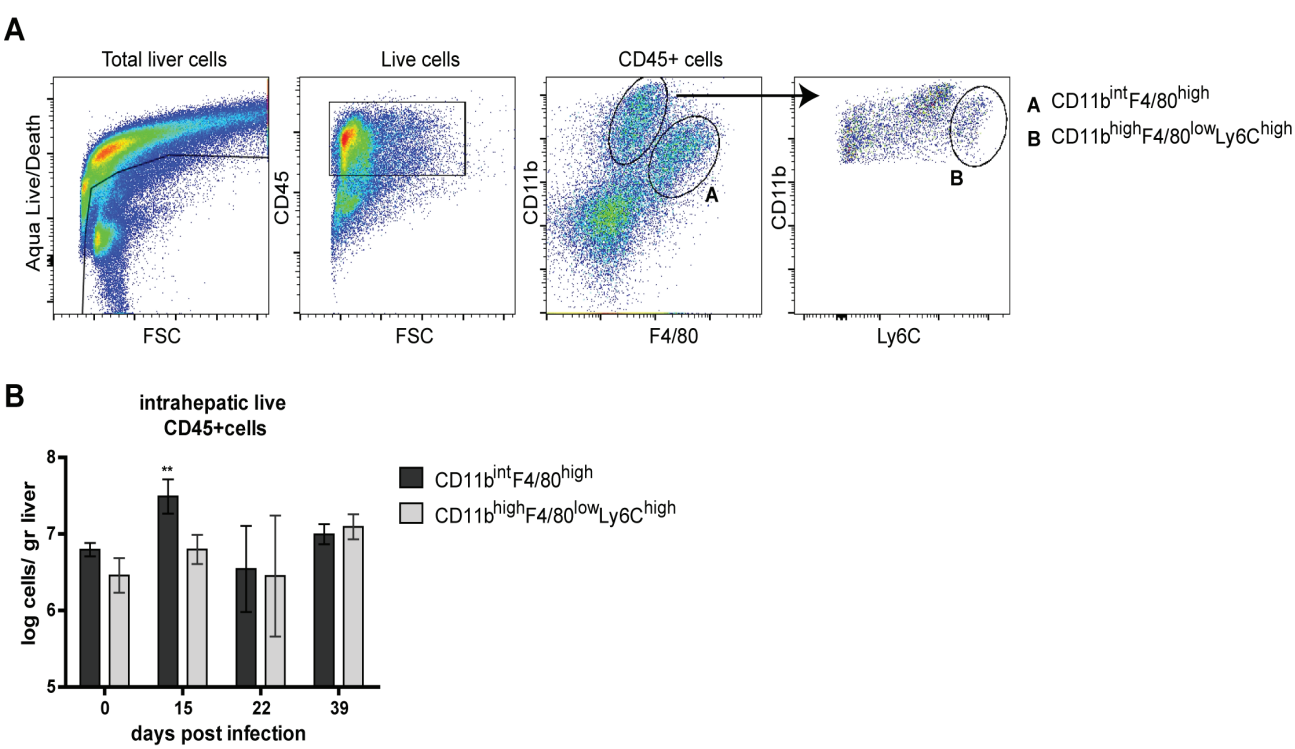

Figure 3. Kinetics of distinct F4/80+ cell populations from LCMV infected mouse livers. Mice were infected with LCMV Cl13 and were sacrificed at day 15, 22 or 39 p.i.. Distinct cell populations were determined using FACS analysis gating strategy of Live/CD45+F4/80highCD11bint and Live/CD45+F4/80lowCD11bhighLy6chigh (A). Arrow indicates follow-up gate for the selection of Live/CD45+F4/80lowCD11bhighLy6chigh (A). Quantification of F4/80highCD11bint (black bars) and F4/80lowCD11bhighLy6chigh (gray bars) cells as log cells per gram liver (B) isolated from mouse livers (n=4-6). Statistical significance was assessed using one-way Anova with Dunnett's Multiple comparison test to day 0. **p<0.01

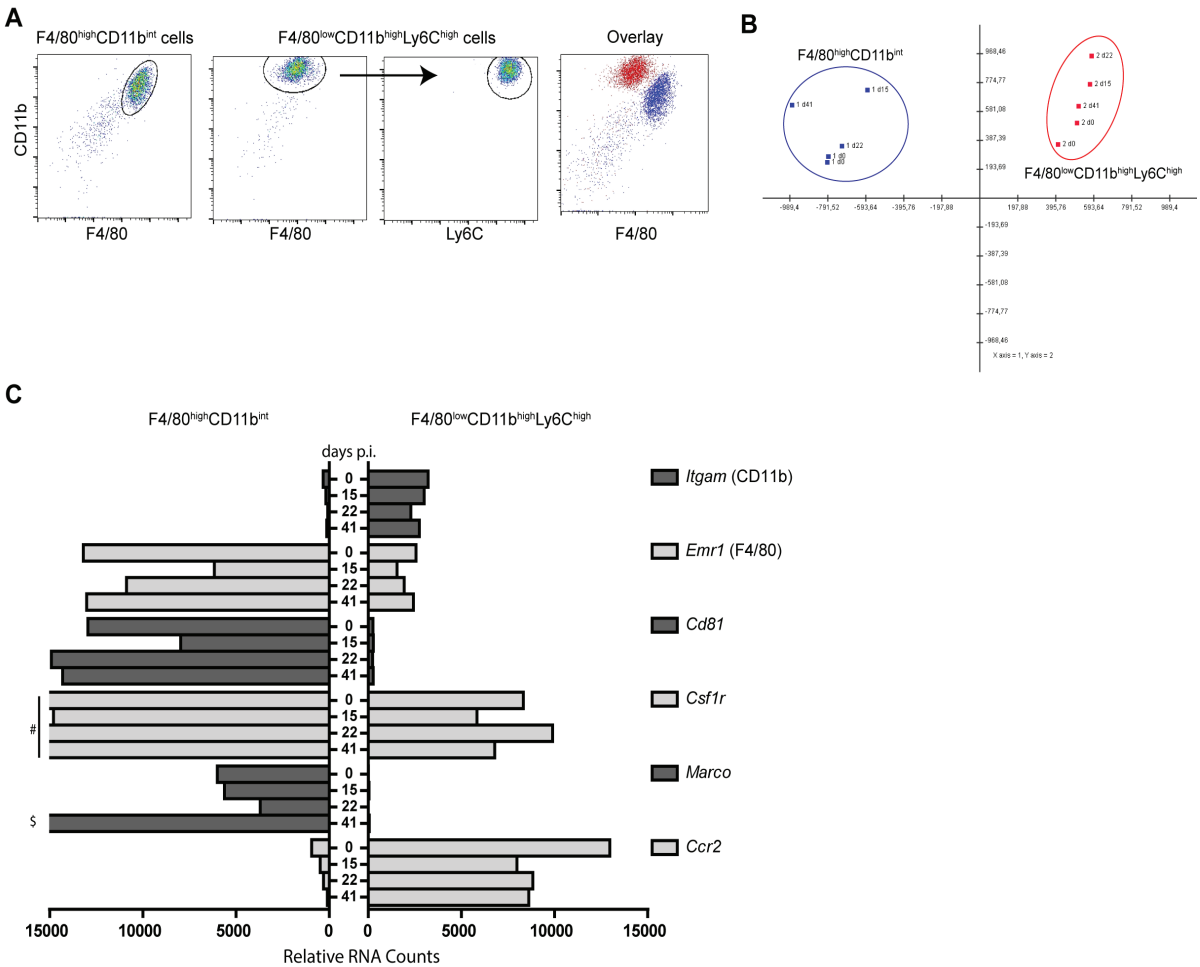

Figure 4. Transcriptomic changes during chronic LCMV-induced hepatitis in liver derived monocytes and Kupffer cells. Liver derived CD45+F4/80+CD11bint KC and CD45+F4/80intCD11bintLy6chigh IM were sorted and purity of sorted cells was assessed by FACS analyses and overlay graph (A). RNA was isolated from sorted cells at baseline (day 0) and after LCMV infection during the early chronic phase (day 15), chronic phase (day 22) and at time of viral clearance (day 41). Gene expression was measured using the nCounter GX Mouse Immunology Kit. Principal component 1 and 2 comprise 65% of the variance between samples (B). Transcription of myeloid cell defining markers for F4/80+CD11bint (Left) and F4/80intCD11bintLy6chigh (right) cells (C). Gene legend is indicated on the right side (C). Y-axis shows days post infection and X-axis indicates relative RNA counts (C). # 29297, 23963, 32090 relative RNA counts for Csf1r day 0, 22, and 41, respectively (C). $ 22720 relative RNA counts for Marco at day 41 (C).

Isg15 and Oas12) (Fig. 2D-F). Despite ongoing LCMV replication from day 15 onwards, gene expression of ISGs, interferons, and pro-inflammatory cytokines were not significantly different from baseline levels.

Kinetics of two distinct liver F4/80+ cell populations during chronic LCMV-induced hepatitis

Because F4/80 expressing cells showed clear histological changes despite normalized whole liver transcription for selected inflammatory signals, we analyzed the longitudinal changes of two distinct F4/80+ myeloid cell populations (CD45+F4/80highCD11bint and CD45+F4/80lowCD11bhighLy6chigh cells) by flow cytometry (Fig. 3A). Both cell subsets were observed at baseline and during different chronic phases of LCMV infection . Compared to non-infected mouse livers, CD45+F4/80highCD11bint cells increased significantly during the early chronic infection phase. In contrast, CD45+F4/80lowCD11bhighLy6chigh were not significantly altered during chronic LCMV infection (Fig. 3B). The increase in CD45+F4/80highCD11bint cells coincided with the more intense F4/80 staining in liver at day 15 p.i. (Fig. 1E). Irrespective of the phase of chronic LCMV infection both cell populations maintained their characteristic surface phenotype.

F4/80+ cell populations keep a distinct KC and IM phenotype throughout chronic infection

We previously described distinctive functions for KC (phagocytic) and IM (TNF production) (137). Plasticity is a well-known property of cells derived from the monocyte-macrophage lineage. Therefore we examined transcriptome profiles of F4/80highCD11bint and F4/80lowCD11bhighLy6chigh cells longitudinally. Cells were sorted from uninfected (day 0) and LCMV-infected mouse livers at the early chronic infection phase (day 15), during the chronic phase (day 22), and after clearance of LCMV from the liver (day 41). FACS analysis demonstrated highly pure non-overlapping cell populations (Fig. 4A, and S1 Fig.). Using the nCounter NanoString platform, transcripts of 547 immunology-related genes and 14 housekeeping genes were measured in sorted cells. Principal component analyses showed that 65% of the variance in gene expression could be explained using components 1 and 2, showing that both cells remained distinct on a transcriptome level throughout and after intrahepatic LCMV replication (Fig. 4B). The surface expression of the discriminating markers used

for FACS analyses of both populations, as shown in figure 3, were reflected in the cell's transcriptome. F4/80highCD11bint transcribed high amounts of Emr1 (F4/80) and low Itgam (CD11b) and vice versa for the F4/80lowCD11bhighLy6chigh cells (Fig. 4C and S3 Table). Furthermore, the F4/80highCD11bint cells showed higher expression of macrophage markers such as Marco, Cd81, and Csf1r. The F4/80lowCD11bhighLy6chigh cells expressed more Itgam and Ccr2 at all time points (Fig. 4C and S3 Table). These data unequivocally demonstrate that both F4/80+ cell populations remain distinctive during ongoing intrahepatic LCMV replication and confirm the KC and IM phenotypes of sorted cell populations.

Kupffer cells and Infiltrating monocytes display a distinct viral antigen associated gene regulation

Hierarchial clustering of sorted KC and IM from different time points showed that the transcriptomes at baseline and viral clearance cluster together for both cell types (Fig. 5A). This indicates that ongoing viral replication determines gene expression in both cells independently. We examined gene expression for up- and down-regulated patterns identical to the viral load pattern. Only 2 genes, Ccrl2 and Tnf, showed a similar expression pattern in both cells (Fig. 5 and S2 Fig.). Among other genes, KC upregulated the ISGs Ifi35 and Ifit2, and antigen presentation related genes H2-Ab1 and H2-Eb1, which positively correlated with the presence of virus in the liver (Fig. 5B). Inflammatory cytokine Il6 and activation marker Cd86 expression in KC negatively correlated to the presence of viral antigens in the liver (Fig. 5B). IM showed among others increased Ccl4 expression and decreased expression of Tlr8 and Tlr9 together with decreased inflammatory pathway molecules such as Myd88, Nfkb1, Irak1, Irak4. Furthermore, IM showed less transcription of several surface receptors including Ifnar2, Ifngr2, Il10ra, and Il10rb in the presence of viral antigens (Fig. 5C). These data indicates that each cell type distinctively respond to the presence of viral antigens during chronic infection.

IM and KC exhibit a distinctive activated transcriptional profile

The activation status of myeloid cells is often assessed by the expression of costimulatory molecules CD80 and CD86, and the

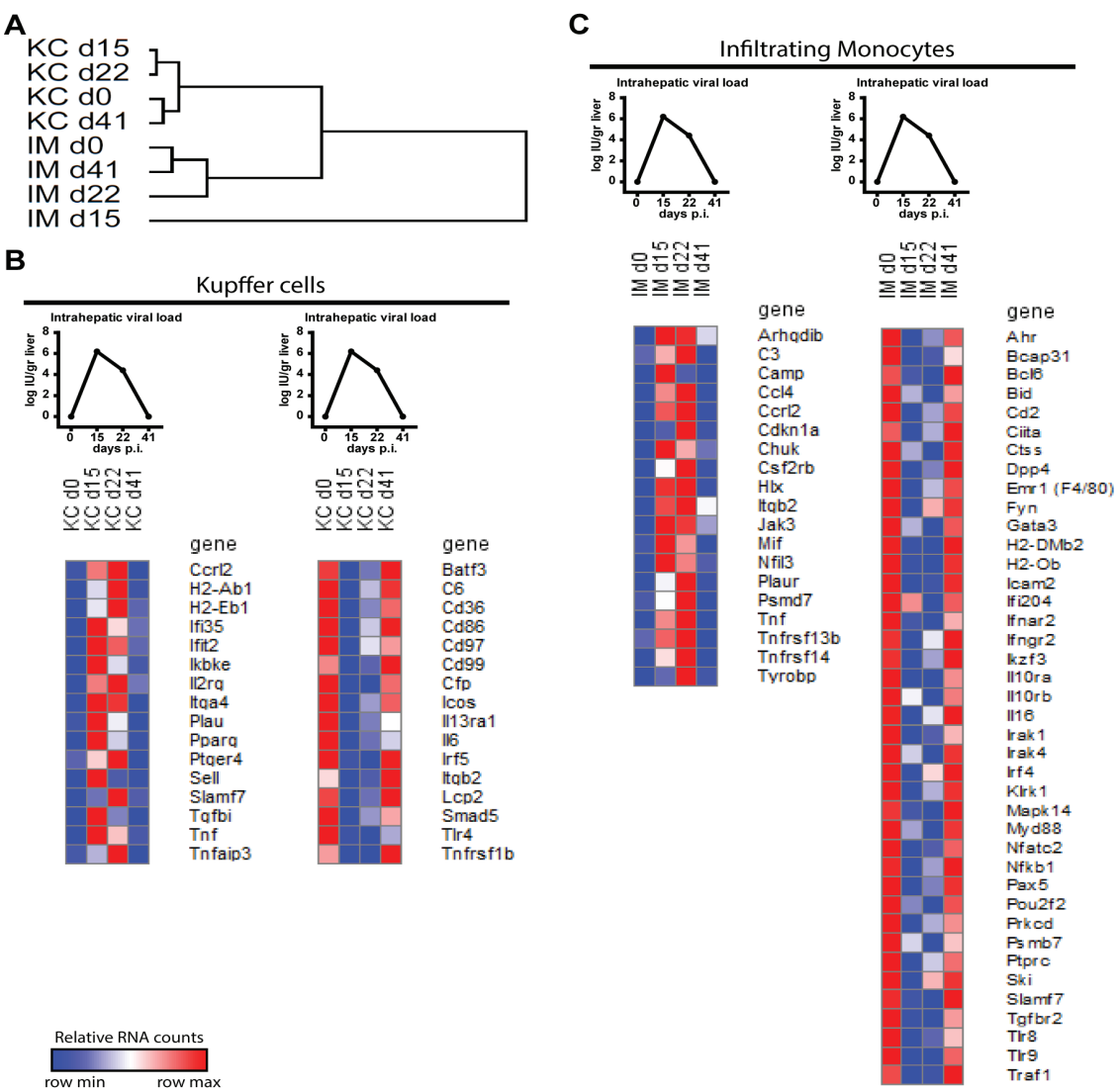

Figure 5. Kupffer cells and infiltrating monocytes exhibit a distinctive viral antigen associated gene expression. Hierarchical cluster of complete transcriptome of sorted KC and IM (A). Gene upregulation (left) and down regulation (right) associated with presence of viral antigens in the liver of KC (B) and IM (C). Viral antigen plots show simplified figure 1C (B, C). Dark red indicates row max value, dark blue indicates row min value (B, C).

production of cytokines and chemokines (99). Compared to IM, KC were less activated as indicated by a non-regulated expression of Cd80 and decreased expression of Cd86, while an increased expression of Cd80 at the early chronic phase and Cd86 during the whole chronic phases pointed towards more activated IM (Fig. 6A). Nevertheless, both cells transcribed more Tnf during chronic infection, albeit almost 2-fold higher in IM compared to KC (Fig. 6A). Overall, these data point to a differential activation status of KC and IM despite extraction from the same tissue and viral antigen rich environment.

KC, but not IM show a transcriptional specialization towards antigen presentation during chronic infection

Macrophages are able to present antigens (99). Here we observed that KC strongly upregulated several genes associated with antigen presentation with highest expression during the chronic phase at day 22 p.i.. In comparison, IM showed an overall much lower expression of most antigen presentation-related genes (Fig. 6B), indicating transcriptional differences between KC and IM and underlining the potential of KC to present antigens during chronic infection. IM showed exclusive expression (Camp, Trem1, IL1r2, Ltb4r1, and Mbp) and relative higher expression (Plaur, Spn, Tgfbi, S100a8, S100a9, and Sell) of a diverse set of immune-related genes, which comprised cytokines, membrane proteins and receptors, signal transduction molecules, compared to KC at baseline and during infection (S3 Table). However, this set of genes does not point to a specific pro- or anti-inflammatory signature for the sorted IM throughout infection.

KC and IM show an ambiguous antiviral response during chronic infection

During chronic infection KC showed an increased expression of Cxcl10, another marker for immune activation, whereas IM downregulated their Cxcl10 transcription (Fig. 6C). Cxcl10 is upregulated in response to interferons, however Ifna, Ifnb, and Ifng transcription was very low or absent in KC and IM at any time point during infection (S3 Table). Despite clear induction of Cxcl10 in KC and reduction in IM, other ISGs showed an irregular regulation (Fig. 6C), indicating an ambiguous antiviral response by KC and IM during chronic hepatitis.

Discussion

Our current understanding of liver specific immune cells during virus-induced liver disease has been hampered by the limited possibilities studying patient derived liver samples and the lack of suitable animal models. Here we use a surrogate model for human viral hepatitis, based on the infection of mice with LCMV Cl13. We show that LCMV Cl13 induced overt clinical hepatitis, with rise in serum cytokines during acute but not throughout the chronic phase. Similarly, acute HBV patients present high TNF and IFNγ in serum, whereas chronic HBV patients show normal levels of these

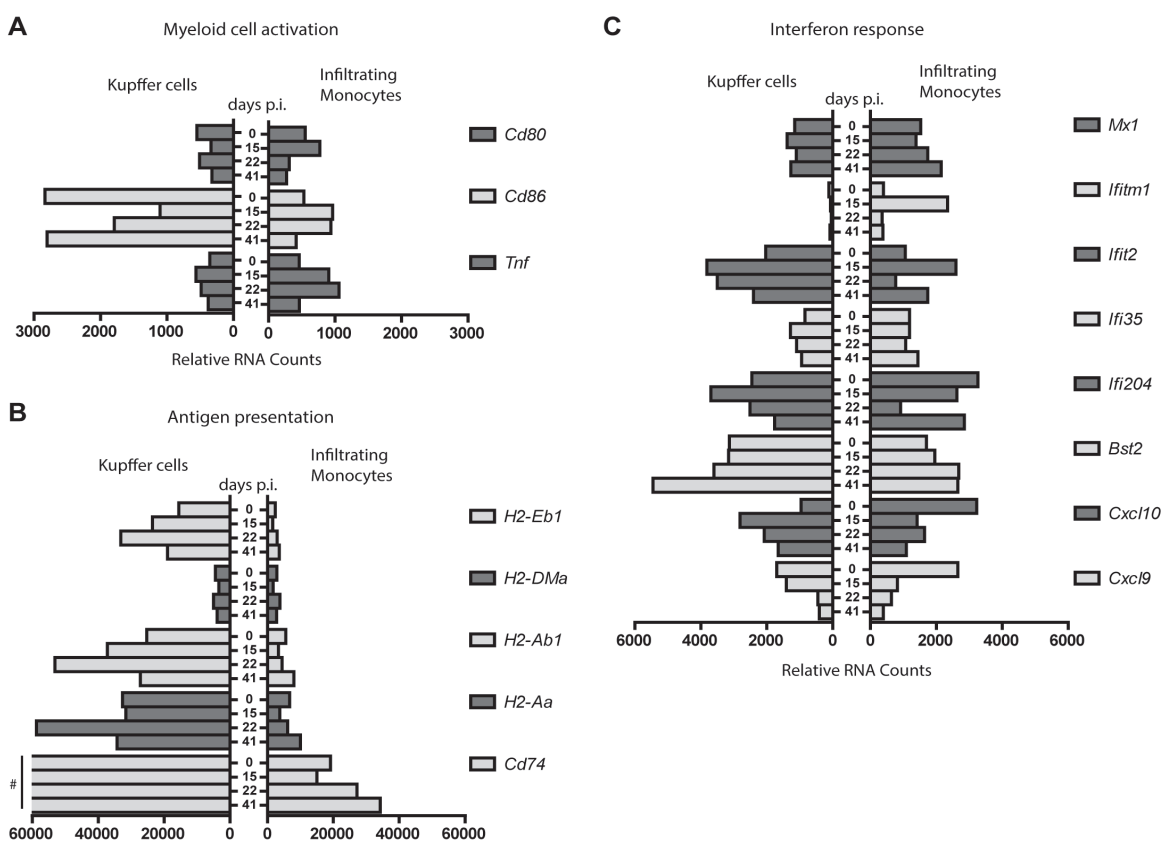

Figure 6. Kupffer cells and infiltrating monocytes display a distinct activation and functional transcriptomic profile. Gene expression profile of KC (left) and IM (right) related to myeloid cell activation (A), antigen presentation (B), and interferon response (C). Gene legend is indicated on the right side of each panel. Y-axis shows days post infection and X-axis indicates relative RNA counts. # 75413, 106998, 171430, 113981 relative RNA counts for Cd74 at day 0, 15, 22 and 41, respectively (B).

serum cytokines (146). The model was used to study liver resident and infiltrating myeloid cells during chronic viral hepatitis.

In order to sort cells from LCMV infected mice in a BSL-1 environment, cells required formaldehyde fixation, inherently leading to RNA strand breaks. Extracted RNA yield allowed only a limited number of qPCR reads, related to their fragmentation. For these materials, Nanostring hybridization has however been shown to yield reproducible gene expression data (147). To obtain sufficient RNA for gene expression analysis, livers were therefore pooled from 4-6 mice prior to cell isolation, staining, and flowcytometric sorting. Gene expression analysis of sample pools pick up large differences and flatten out biological variation of individual animals. Results are therefore more robust, have higher accuracy, but minor transcriptome changes might be missed (148).

We show by gene expression analyses of sorted KC and IM that these cells are distinct and maintain their respective phenotypes throughout the infection. Cell distinctive phenotypes were most evident by genes solely expressed (Marco and Trem1) by either cell type or genes regulated in opposite fashion (Cxcl10 and Cd86) throughout infection, suggesting either distinct regulatory mechanisms or that either cell type complements the other to maintain a balanced overall immune response.

During chronic infection, KC showed a less-activated phenotype. Conversely, IM were more activated, as shown by the upregulation of Cd80, Cd86, and Tnf, albeit lower when compared to acute LCMV clone13 infection as previously shown (137). Myeloid cells have been shown before to exert various functions ranging from maintaining homeostatic balance to initiating inflammation, regulating immune response, and tissue repair, depending on their milieu (149). Here, we found that KC have an increased expression of transcripts related to antigen presentation, suggesting that these cells are better equipped to present antigens and activate T cells during chronic infection.

Previously, we showed that after 24 hours of LCMV infection, KC were capable of expressing Ifng and Ifnb (137). Here we observed no transcription of IFNs in KC and IM during chronic infection, despite the local presence of viral antigens. However, KC showed increased transcription of Cxcl10. Increased CXCL10 levels in serum have been associated with immune activation and has been classically regarded as a marker of ISG responses in HCV infected hepatocytes (150-152). Moreover, evident ISG response in KC and not in hepatocytes have been shown to predict treatment outcome in chronic HCV patients, suggesting that KC are crucial players during chronic hepatitis (153).

We previously showed that intrahepatic CD14+ cells (comprising both KC and IM) from chronic HBV patients display an activated phenotype, based on higher expression of CD40 and CD80 (143). Moreover, these CD14+ cells had an increased HLA-ABC and HLA-DR transcription, which was also observed in KC isolated during chronic LCMV infection. In addition, upon encounter with HBV particles human liver non-parenchymal cells had an induced IL1b, IL6, CXCL8, and TNF transcription (154). Here, highly pure KC derived from LCMV infected livers also showed increased Tnf, but decreased Il1b and Il6 transcription. Furthermore, Tnf transcripts were much higher in sorted IM, indicating a balance of KC towards antigen presentation and less to pro-inflammatory cytokine production.

We showed that monocytes infiltrating the liver during LCMV-induced chronic hepatitis were activated and transcribed various genes including Tnf correlating with the presence of viral antigens. However, peripheral blood monocytes from chronic HBV patients remained unaffected by viral proteins and HBV DNA, although they can produce high amounts of IL-6 and TNF upon stimulation with HBsAg in vitro (140). In HBV patients, anti-inflammatory IL-10 in serum has been shown to be elevated and decreases cytokine production by monocytes (140, 155, 156), suggesting that regulatory mechanisms are in play during chronic viral hepatitis. We found elevated serum IL-10 levels during chronic LCMV infection and an exclusive transcription of Il10 in sorted KC and not IM suggesting a cell-specific regulation of immune responses (Fig. 1D and S3 Table). Based on the gene expression data presented here no clear functional specialization can as yet be ascribed to intrahepatic IM during virus induced hepatitis. Their function might be tightly regulated between a pro- or non-inflammatory state. Further insight will require a selective depletion of either KC or IM during or before LCMV, without disturbing the entire mononuclear phagocyte system (157).

In summary, we show that LCMV Cl13 induces evident chronic viral hepatitis with limited intrahepatic cytokine and interferon responses during the chronic infection. LCMV-induced hepatitis is characterized by morphological changes and increased intensity of the F4/80+ cell population, designated as IM and KC. KC and IM are distinct cell populations before, during, and after chronic infection, with important differences in activation status, antigen presentation, and gene expression profile correlating with the presence of viral antigens. Overall, these data suggest that intrahepatic monocytes and KC play distinctive roles during chronic virus-induced hepatitis.Acknowledgement

We would like to thank Elina Zuniga for sharing the LCMV strain, and Vincent Vaes, Judith van Agthoven and Dennis de Meulder from the Erasmus MC animal care facility for their assistance in performing biotechnical manipulations.

Acknowledgement

We would like to thank Elina Zuniga for sharing the LCMV strain, and Vincent Vaes, Judith van Agthoven and Dennis de Meulder from the Erasmus MC animal care facility for their assistance in performing biotechnical manipulations.

Supporting information

Supporting information is available online:
http://journals.plos.org/plosone/article?id=10.1371/journal.pone.0166094#sec023

S1 Figure. Schematic overview of experimental layout.
S2 Figure. Distinctive viral antigen associated gene expression.
S3 Table. Relative RNA counts of sorted Kupffer cells and infiltrating monocytes.

Chapter 4

Published in: Journal of Virology, 2016, 90:4394-4401

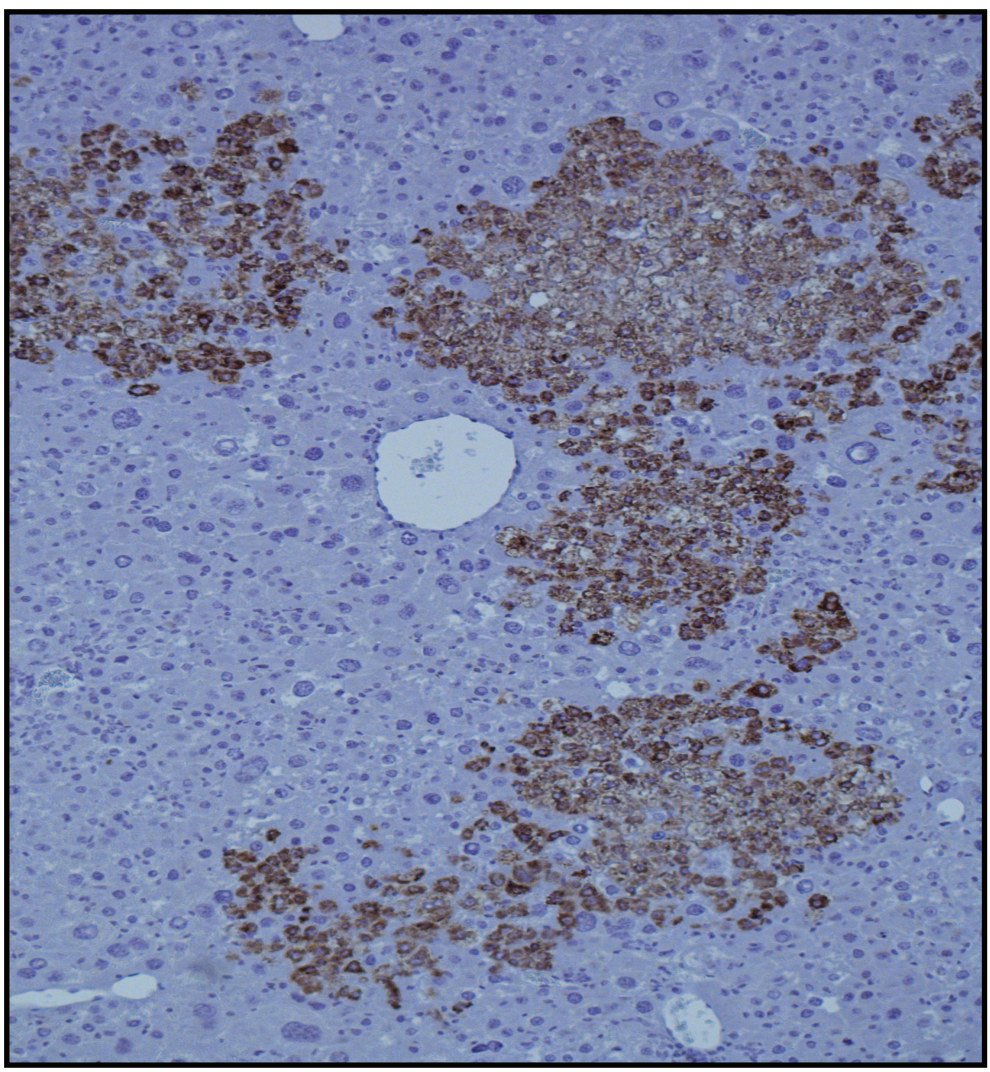

Human hepatocytes stained brown (anti-human mitochondria staining) in a mouse liver.

Hepatitis E virus genotype three infection of human liver chimeric mice as a model for chronic HEV infection

Martijn D.B. van de Garde[1], Suzan D. Pas[2], Guido van der Net[2], Robert A. de Man[1], Albert D.M.E. Osterhaus[2], Bart L. Haagmans[2], Andre Boonstra[1], Thomas Vanwolleghem[1,3]

Abstract

Genotype (gt) 3 hepatitis E virus (HEV) infections are emerging in Western countries. Immunosuppressed patients are at risk of chronic HEV infection and progressive liver damage, but no adequate model system currently mimics this disease course. Here we explore the possibilities of in vivo HEV studies in a human-liver chimeric mouse model (uPA+/+Nod-SCID-IL2Rγ-/-) next to the A549 cell culture system, using HEV RNA positive EDTA-plasma, feces or liver-biopsy specimens from 8 immunocompromised patients with chronic gt3 HEV. HEV from feces- or liver-derived inocula showed clear virus propagation within 2 weeks after inoculation onto A549 cells, compared to slow or no HEV propagation of HEV RNA positive, EDTA-plasma samples. These in vitro HEV infectivity differences were mirrored in human-liver chimeric mice after i.v. inoculation of selected samples. HEV RNA levels up to 8 log IU HEV RNA/gram, were consistently present in 100% of chimeric mouse livers from week 2-14 after inoculation with human feces or liver-derived HEV. Feces and bile of infected mice contained moderate to high amounts of HEV RNA, while HEV viremia was low and inconsistently detected. Mouse passaged HEV could subsequently be propagated for up to 100 days in vitro. In contrast, cell culture-derived or seronegative EDTA-plasma derived HEV was not infectious in inoculated animals. In conclusion, infectivity of feces-derived human HEV is higher compared to EDTA-plasma derived HEV both in vitro and in vivo. Persistent HEV gt3 infections in chimeric mice, show preferential viral shedding towards mouse bile and feces, paralleling the course of infection in humans.

[1]Department of Gastroenterology and Hepatology, [2]Department of Viroscience, Erasmus University Medical Center, Rotterdam, The Netherlands. [3]Department of Gastroenterology and Hepatology University Hospital Antwerp, Belgium

Introduction

Hepatitis E virus (HEV) is a non-enveloped positive-sense single-stranded RNA virus of the genus Orthohepevirus and family Hepeviridae (29). Four major HEV genotypes infecting humans have been described so far. Genotype (gt) 1 and 2 strains are only isolated from humans, whereas gt3 and gt4 strains are considered zoonotic viruses, present in both humans and several other species like pigs and wild game. HEV is spread through the oral-fecal route via contaminated water in developing countries or amongst others, via direct contact with animals or the consumption of undercooked meat in industrialized countries. In immunocompetent individuals, HEV infection is mainly self-limiting, often asymptomatic and thus remains largely underdiagnosed. HEV infections in immunosuppressed patients, such as solid-organ transplant recipients, often persist and can progress quickly to liver fibrosis and cirrhosis (158-160).

HEV gt3 infections are emerging in western countries, including France, the United Kingdom and the Netherlands (26-28). Despite an overall decrease in anti-HEV seroprevalence from 1996 to 2011, young adult blood donors demonstrated higher seroprevalences from 2000 to 2011 (161, 162). In addition, HEV RNA positive blood donations were reported to increase in the Netherlands since 2012 (163). Although the exact source of this HEV gt3 infection is unknown, it is likely that domestic swine and pig farming plays a critical role. HEV RNA gt3 was detected in approximately half of the pig farms in the Netherlands (164).

Human-liver chimeric mice have contributed significantly to our understanding of viral pathobiology, virus-host interactions and antiviral therapy for hepatitis B, C and D infections (40, 55, 61, 89, 165-167). Since no animal model for chronic HEV infection is available, we examined the infectivity of HEV gt3 samples of different clinical origins in the humanized liver urokinase-type plasminogen activator (uPA) transgenic mouse model on a severely immunodeficient NOD/Shi-scid/IL-2Rγnull background (uPA-NOG) and compared this to the established Adenocarcinoma human alveolar basal epithelial cells (A549) cell culture system (4, 168-170). We demonstrate that in vitro infectivity differences of feces, liver and plasma-derived HEV are paralleled in vivo. These differences are most apparent when inocula from a single patient are used with similar HEV RNA content. Once infected, persistent intrahepatic viral replication is seen in all chimeric mice, with preferential viral shedding to mouse bile and feces, reminiscent of human HEV infections. Human chimeric liver mice are therefore a suitable model for future studies on HEV transmission and pathobiology.

Material and Methods

Inoculum preparation

Inocula were obtained from heart- (n=4), liver- (n=1), and allogeneic hematopoietic stem cell (n=2) transplant recipients and one recipient who received both heart and kidney grafts (Table 1), treated either at the University Hospital Antwerp or the Erasmus Medical Center (4, 170). Clinical sequelae have been described elsewhere (4, 160, 170). All had detectable HEV RNA in their EDTA-plasma for more than 6 months (defined as chronic HEV infection). Table 1 shows the results of the anti-HEV IgM and IgG antibody determination in the EDTA-plasma inocula obtained with a commercially available enzyme-linked immunosorbent assay (ELISA, Wantai, Beijing, China). Open reading frame (ORF) 1 and 2 sequences of the inocula are available at GenBank (Table 1). Fecal suspensions were prepared as follows: 3 gram feces was vortexed thoroughly in 10 ml saline and centrifuged (450g, 3 min). After 2 additional centrifugation steps (14000g, 5 min), the supernatant was passed through a 0.45 µm filter. A cryopreserved liver biopsy fragment from one heart and one allogeneic hematopoietic stem cell-transplant patient was homogenized in 500 µl saline using ceramic beads. The supernatant was used as inoculum after centrifugation (5000g, 10 min). All inocula were kept at -80°C until use.

Hepatitis E virus propagation

A549 were seeded on a coverslip in 24-well plate, in A549 growth medium containing Dulbecco's modified Eagles Medium (DMEM, Lonza) supplemented with 10% fetal bovine serum (FBS, Greiner Bio-one, Kremsmünster, Austria), 0.08% NaHCO3, 2 mM L-glutamine (Lonza), 1% penicillin/streptomycin (pen/strep, Lonza) and 0.5 µg/µl amphotericin B (Pharmacy, ErasmusMC, Rotterdam, The Netherlands). Three days after seeding, cells were washed once with phosphate buffered saline (PBS, Oxoid, Hampshire, UK) and inoculated with either HEV derived from different sample types or mock and incubated for 1 hour at 36.5°C in a humidified 5% CO2 incubator. Liver-derived samples were diluted 1:10 prior to inoculation, to dilute toxic substances. The virus suspension was then removed and cells were washed three times with PBS before adding maintenance medium, containing 1:1 mixture of DMEM/Ham's F-12 (Life technologies), supplemented with 2% FBS, 20 mM HEPES (Lonza), 0.4% NaHCO3, 2 mM L-glutamine, 0.3% Bovine Albumin Fraction V (BSA, Lonza), 1% pen/strep and 2.5 µg/µl amphotericin B and incubated at 36.5°C in a humidified 5% CO2 incubator. Proper washing was documented by the absence of HEV RNA (Ct>38) in the last PBS supernatant. For monitoring virus propagation, every two to three days cells were inspected on cytophathogenic effect (CPE) and viability, culture medium was refreshed with maintenance medium (1:1) and supernatant was taken for HEV qPCR.

Mouse origin and genotyping

uPA-NOG mice were kindly provided by the Central Institute for Experimental Animals (Kawasaki, Japan) (168). Mice were bred at the Central Animal Facility of the Erasmus Medical Center. Offspring zygosity was identified using a copy-number duplex qPCR performed on phenol/chloroform/isoamyl-alcohol (Sigma Aldrich, St. Louis, MO, USA) extracted genomic mouse DNA from toe snip. TaqMan Genotyping Master Mix (Life technologies, Carlsbad, CA, USA) with TaqMan uPA genotyping assay (Mm00422051_cn, Life Technologies) and Tert gene references mix (Life technologies) were used according to the manufacturer's protocol. All animal work was conducted according to relevant Dutch national guidelines. The study protocol was approved by the animal ethics committee of the Erasmus Medical Center (DEC nr 141-12-11).

Human hepatocyte transplantation

uPA homozygous mice, 6-12 weeks of age, were transplanted as previously described (165). In short, mice were anesthetized and transplanted via intra-splenic injection with 0.5-2 x 106 viable commercially available cryopreserved human hepatocytes (Lonza, Basel, Switzerland and Corning, Corning, NY, USA). Graft take was determined by human albumin in mouse serum using ELISA with human albumin cross-adsorbed antibody (Bethyl laboratories, Montgomery, Tx, USA) as previously described (165).

Table 1. Inocula of chronic HEV gt3 patients for *in vitro* and *in vivo* infection

Case no.	1st year HEV+	age @ HEV+	Sex	Morbidity[#]	GenBank accession ORF1	GenBank accession ORF2	Serostatus Plasma[$]	HEV RNA (log IU/ml)			reference
							IgM/IgG	plasma	feces[¶]	liver	
HEV0008	2008	55	F	AlloHSCT	JQ015407	KT198654	+/+	6.18	6.09	5.31	(170)
HEV0014[*]	2011	40	F	AlloHSCT	KC171436	KP895853	-/-	5.46/6.84[*]	5.61	-	(170)
HEV0033	2010	51	M	HTx	JQ015427	KT198656	+/+	5.73	6.20	-	(4, 160)
HEV0047	2010	56	M	HTx	JQ015425	KT198657	-/+	6.72	6.69	-	(4, 160)
HEV0063	2010	19	M	LTX	JQ015426	KT198658	+/+	4.96	5.18	-	(4, 160)
HEV0069[*]	2010	62	M	HTx	JQ015423	KP895854	-/-	6,23	6.37/8.80[*]	-	(4, 160)
HEV0081	2009	50	M	HTx + KTx	JQ015418	KT198659	+/+	4.91	5.15	-	(4, 160)
HEV0122[*]	2014	63	M	HTX	KP895856	KP895855	-/-	5.83/6.74[*]	6.12/8.80[*]	4.87/6.26[*]	this publication

[*]Undiluted Inocula used for in vivo infection; [#]AlloHSCT allogeneic hematopoietic stem cell transplantation; HTx heart transplantation; LTx liver transplantation; KTx kidney transplantation; [$]as determined by anti-HEV IgM and anti-HEV IgG ELISA (Wantai, Beijing, China); [¶]Feces inocula were diluted to the plasma HEV RNA level in order to use an identical HEV RNA level for infection of the A549 cells.

Mouse infection

Mice were inoculated intravenously (i.v.) with 135-200 µl pooled patient EDTA-plasma (6.8 log international units (IU/ml), individual patient EDTA-plasma (6.7 log IU/ml), a homogenized liver biopsy fragment (6.3 log IU/ml), feces (8.8 log IU/ml or diluted to 6.8 log IU/ml) or 7th passage (P7) culture supernatant initially derived from feces (7.4 log IU/ml) containing HEV gt3 as denoted in Table 1 and Supp. Fig. 1. The use of patient material was approved by the medical ethical committees of Erasmus MC and Antwerp University Hospital.

Histology, immunohistochemistry and HEV ORF2 immunofluorescence

Mouse livers were fixed in 4% formaldehyde solution (Merck-Millipore). Standard H&E staining was performed and human hepatocytes were identified using goat anti-human albumin cross-adsorbed antibody (Bethyl laboratories) or mouse anti-human mitochondria antibody (Merck). To visualize the detected antigens, 3,3'-diaminobenzidine (DAB, DAKO, Copenhagen, Denmark) was added as a substrate and slides were counterstained with hematoxylin. To confirm in vitro HEV replication after 7 to 14 days post infection, cells were fixed in 80% acetone (Sigma-Aldrich) for 10 minutes, washed 3 times with PBS and air-dried. Cells were then blocked for 30 min at 36.5°C with 10% normal goat serum (MP Biomedicals, Santa Ana, CA, USA), followed by three times washing in PBS. Subsequently cells were stained for 1 hour at 36.5°C with a 1:200 0.5% BSA/PBS diluted mouse-α-HEV ORF 2 aa434-547 antibody (MAB8002, Merck-Millipore, Billerica, Massachusetts, USA), followed by staining with 1:200 0.5% BSA/PBS diluted goat anti mouse IgG conjugated with Alexa Fluor 488 (Life Technologies) for 1 hour at 37°C. After washing with PBS, cells were counterstained with 4,6-diamidino-2-phenylindole (DAPI) and pictures were taken using a confocal microscopy (ZEISS LSM700).

HEV RNA detection

All samples were screened for the presence of HEV RNA by an ISO15189:2012 validated, internally controlled quantitative real-time RT-PCR, described previously (4). Ct values above 38 were considered background. HEV RNA detection in samples with Ct values below 38 are indicated with their calculated values. Feces was pre-treated with transport and recovery buffer (STAR buffer, Roche, Almere, The Netherlands) and chloroform. Liver tissues were homogenized using ceramic beads in 500 µl RPMI (Lonza). Mouse serum, bile and liver homogenate supernatants, were diluted 10x before extraction due to limited sample volume or to dilute any impurities inhibiting the qPCR.

Statistics

Graphpad Prism 5.01 was used for statistical analysis. Non-normally distributed data were log-transformed. Continuous variables are presented as mean ± SD. Michaelis-Menten non-linear test was used to determine goodness of fit, Kruskal-Wallis one-way Anova and Mann-Whitney test were used to calculate the p-value. Significance was set at $P<0.05$.

Results

Infectivity differences of HEV gt3 from patient plasma, feces or liver on A549 cells in vitro

Different clinical isolates from 8 chronic HEV gt3 patients were used to infect cultured A549 cells (Table 1). Feces samples were diluted, in order to load an identical HEV RNA amount of both plasma and feces derived inocula on the A549 cells. A549 cells were efficiently infected with HEV derived from feces and liver biopsies with increasing HEV RNA titers in supernatant up to 5.05 log IU/ml within 7 days (Fig 1A-H). HEV propagation was less efficient when using HEV RNA positive EDTA-plasma specimens, with 4 (HEV0008, HEV0014, HEV0033 and HEV0122) out of 8 samples showing increasing HEV RNA titers after 10 or 15 days post exposure regardless of their serostatus (Fig 1A-H, Table 1). The different in vitro replication kinetics of feces vs plasma-derived HEV is evident from the calculated slopes during the first 2 weeks after inoculation on A549 cells (Fig 1I; mean slope 0.151 versus 0.028 log HEV RNA IU per day, respectively, $P<0.01$). HEV gt3 derived from patient HEV0069 feces was passaged seven times onto new cells, which resulted in increasing HEV RNA titers after each passage up to 8 log IU/ml (Fig. 1J). Anti-HEV ORF2 fluorescence staining confirmed HEV protein expression in feces-but not in plasma-inoculated A549 cells at day 7 and day 14 (Fig. 1K). HEV is visualized in cytoplasm of clustered infected cells without obvious cytopathogenic effects. The percentage of infected cells was counted at 3-5% of total cells.

Successful infection of chimeric mice with feces-derived HEV gt3

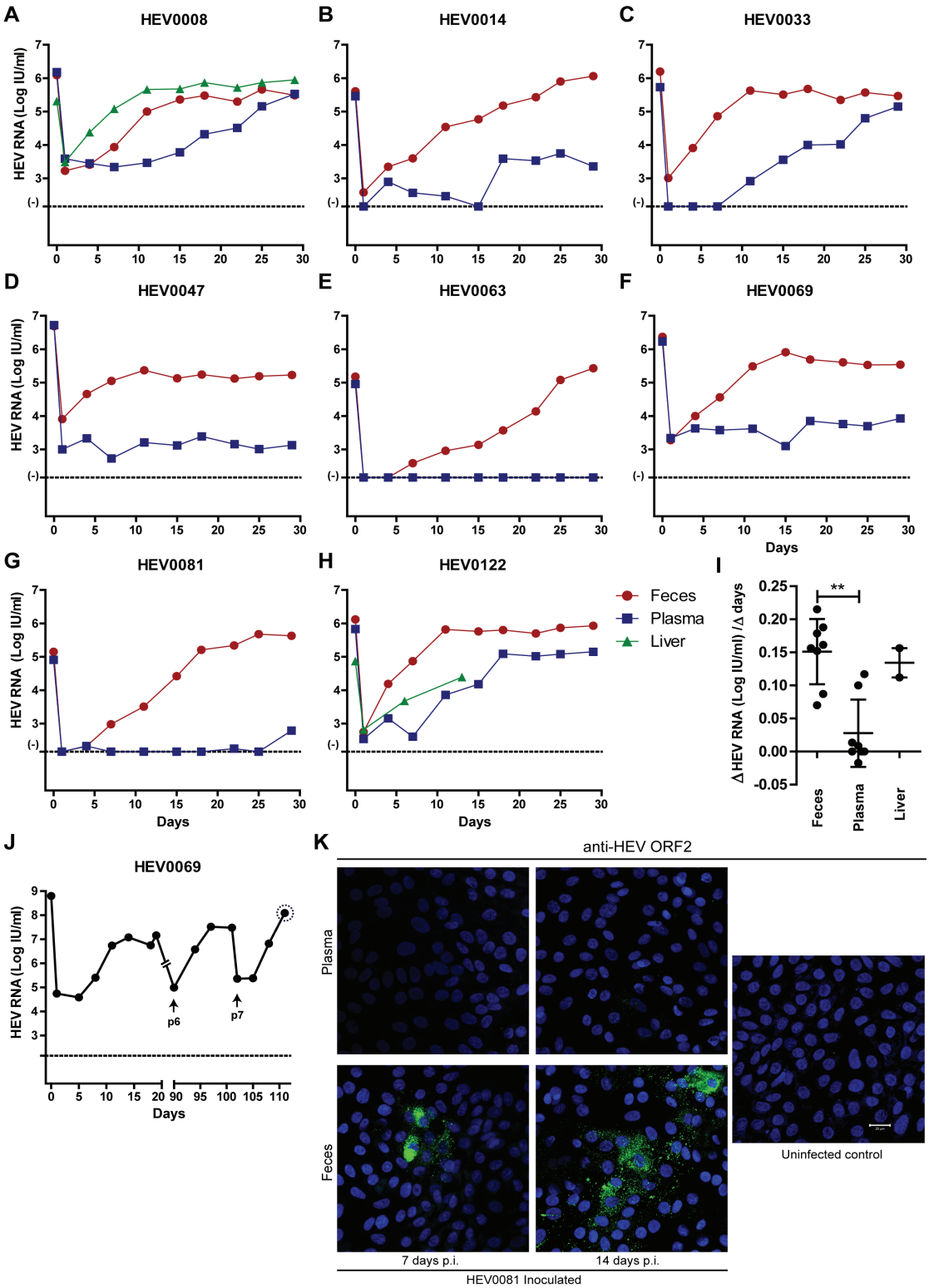

Figure 1. Differences in in vitro infectivity of HEV gt3 containing clinical samples on A549 cells. Gradual increase in HEV RNA levels in supernatant of A549 cells after inoculation of feces- (A-H) or liver-derived (A, H) HEV (Red and green line, respectively). No or slower increase in HEV RNA levels in supernatants of A549 cells after inoculation of EDTA plasma derived HEV (A-H, blue line). I) Log HEV RNA increase per day within the first two weeks after inoculation with feces, plasma and liver derived HEV as depicted in A-H. J) Increasing HEV RNA titers after prolonged culture. Arrows indicated first measurement after passage. Dotted circle around the last P7 viral load, indicates the inoculum used for in vivo challenge described in Fig 3A.K) HEV ORF2 immunofluorescence of HEV infected A549 cells, 7 and 14 days after inoculation of HEV0081 feces and plasma derived virus, and uninfected control A549 cells. HEV RNA was quantified with qRT-PCR and Ct-values above 38 are considered background (-) (A-H, J) . The HEV RNA concentrations of the initial inocula are indicated on time point 0 (A-H, J) . Error bars indicated mean±SD, ** P-value <0.01 (I).

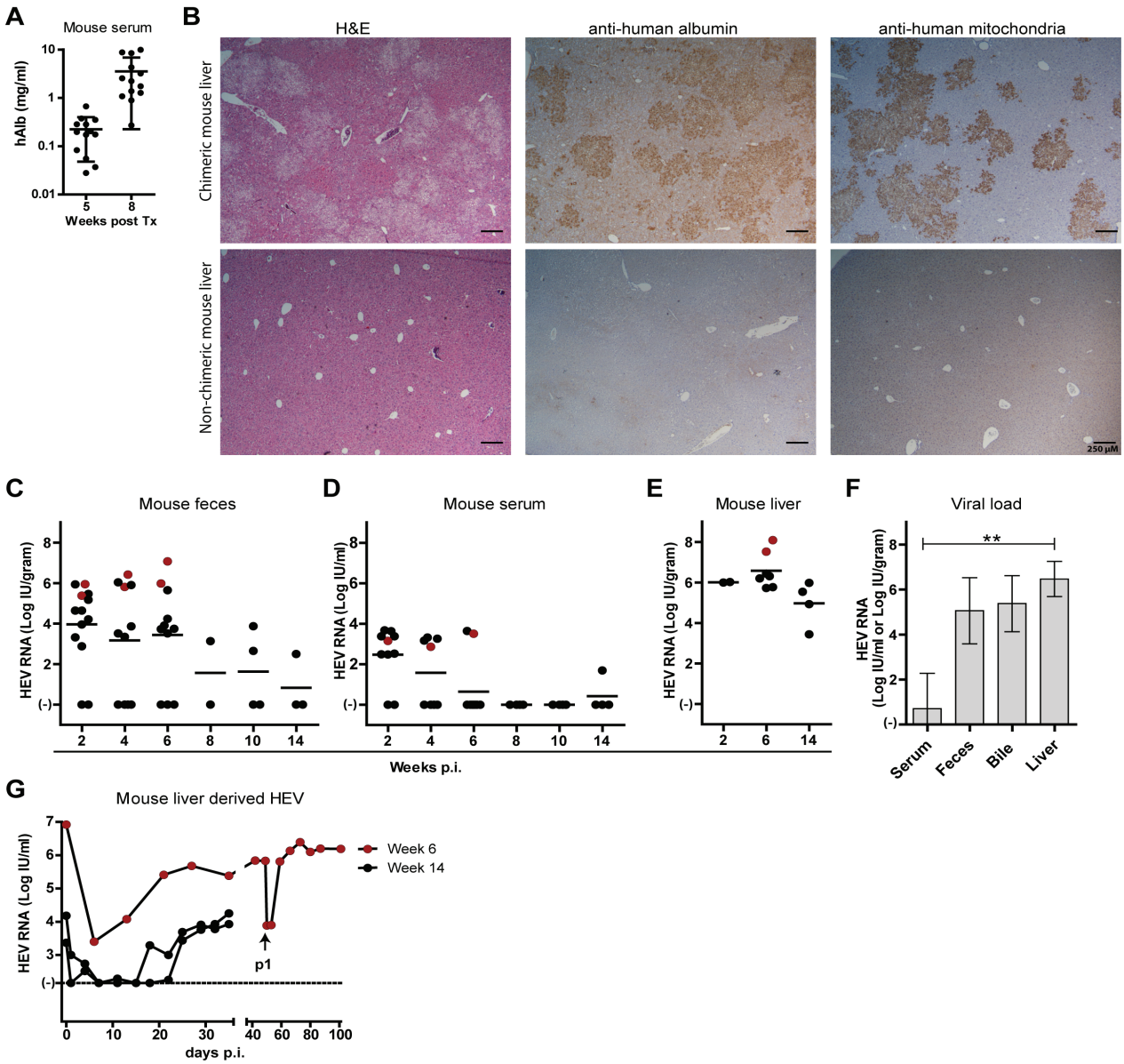

Figure 2. Persistent infection of human liver-chimeric mice with feces-derived HEV gt3 from two chronic HEV patients. A) Human albumin levels were measured in mouse serum via ELISA to quantify the hepatocyte graft take at 5 and 8 weeks post transplantation (n=13, geometric mean ± SD). B) Liver histology of chimeric mouse livers at 8 weeks post transplantation (upper panels) and non-chimeric mouse liver (lower panels); H&E (left panel), anti-human albumin (middle panel), and anti-human mitochondria staining (right panel). Chimeric mice (n=13) were challenged i.v. with 8 log IU HEV RNA derived from human feces from patient HEV0069 (black dots) or patient HEV0122 (red dots) for 2, 6 or 14 weeks (n=2; 7; 4 respectively) (C-E). HEV RNA levels were measured by qPCR in mouse feces (C), mouse serum (D), and in mouse liver (E). F) Comparison of HEV viral load in serum, feces, bile, and liver at week 6 post infection (n=5, mean ± SD). G) In vitro HEV propagation in A549 cells of mouse liver-derived HEV0122 (red dots) or HEV0069 (black dots) after in vivo replication for 6 or 14 weeks, respectively. Arrow indicates first new data point after passage onto new A549 cells. ** P-value <0.01

uPA-NOG mice, successfully transplanted with human hepatocytes had increasing human albumin levels in serum (Fig. 2A), which correlated with liver repopulation by human hepatocytes as demonstrated by H&E; specific human albumin and human mitochondria staining (Fig. 2B) (165). To corroborate the observed feces-derived HEV in vitro infectivity, filtered undiluted fecal suspensions (see Methods) from patients HEV0069 and HEV0122 were i.v. inoculated into chimeric mice and the infection course was documented for 2, 6 or 14 weeks until sacrifice. During follow-up, HEV RNA was detected in feces of these mice with titers up to 7 log IU/gram (3.1±2.4 log IU HEV RNA/gram, Fig. 2C), while HEV viremia was low and inconsistently detectable, with maximum viral loads of 3.6 log IU/ml (1.1±1.5 log IU HEV RNA/ml, Fig. 2D). All 13 inoculated animals had high intrahepatic HEV RNA titers at sacrifice (6.0±1.1 log IU HEV RNA/gram, mean±SD, Fig. 2E). HEV is preferentially secreted via feces in infected individuals. In fact, HEV seroconverted patients continue to shed HEV in feces for several weeks, even when HEV serum titers drop to undetectable levels (159). We found that in infected animals serum titers were lower compared to feces, bile and liver titers. In 5 infected mice at 6 weeks post infection, the mean HEV RNA titers in serum, feces, bile and liver were 0.7±1.6 log IU/ml, 5.1±1.5 log IU/gram, 5.4±1.2 log IU/ml, 6.5±0.8 log IU/gram, respectively (mean±SD; P-value 0.004 for difference, Kruskall-Wallis test, Fig. 2F). These

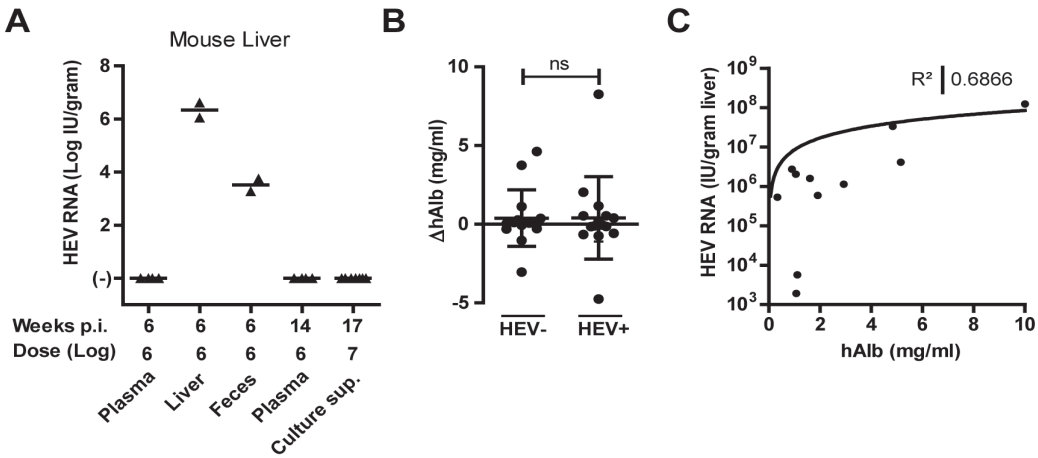

Figure 3. Differences in in vivo infectivity of HEV gt 3 containing clinical samples in human liver chimeric mice. Chimeric mice (n=19) were challenged i.v. with HEV RNA containing inocula derived from EDTA plasma (patient HEV0014 and HEV0122; n=4 respectively), a cryopreserved liver biopsy (patient HEV0122; n=2), feces (patient HEV0069; n=2), or P7 culture supernatant of patient HEV0069 feces (n=7) (see Methods). The respective infectious doses are indicated below the X-axis, as well as the duration of the infection in weeks. HEV RNA levels were measured by qPCR in mouse liver at sacrifice (A). B) Changes in serum human albumin levels from HEV inoculation to end of follow up of HEV RNA negative and HEV RNA positive mice (n=23, P=0.9339). C) Non-linear regression of chimerism, indicated by human albumin level in mouse serum (X-axis), versus the HEV titer in the liver (Y-axis) at week 6 post infection (n=11).

data suggests that virions are secreted preferentially through the biliary canaliculi, instead of basolaterally in the liver sinusoids. In addition, HEV0069 and HEV0122 viruses isolated from mouse livers after 6 or 14 weeks of in vivo replication respectively, could be propagated in vitro after exposure to A549 cells (Fig. 2G). The HEV0122 isolate was passaged further and could be maintained for over 3 months reaching high HEV RNA levels (>6 log IU/ml) in the culture supernatant (Fig. 2G). Taken together, these data confirm the in vivo infectivity of feces-derived HEV gt3 with establishment of 100% persistent and productive HEV infections in chimeric mice.

Differences in in vitro HEV gt3 infectivity are reflected in vivo

In order to assess the infectivity differences of HEV RNA containing clinical samples a total of 19 chimeric mice were challenged with EDTA-plasma samples from patients HEV0014 and HEV0122, with liver homogenate from patient HEV0122, with feces of patient HEV0069 or with a high titre P7 culture supernatant of this patient's feces (Fig. 1J, Fig. 3A, Table 1). Care was taken to inject animals with similar HEV RNA containing inocula, with some variation due to differences in injected volumes (135 to 200 µL). The respective inocula are indicated below the X-axis (Fig. 3A). Given the need for liver HEV RNA determination to demonstrate or rule out HEV infectivity, large liver fragments of sacrificed animals were collected at week 6 to week 17 after inoculation. Only liver- and feces-derived inocula proved to be infectious in chimeric mice. EDTA-plasma or A549 cell culture-derived inocula did not result in detectable HEV RNA levels at 6, 14 or 17 weeks after inoculation in any of the examined biological matrices (feces, sera, bile and liver; Fig. 3A and data not shown). In addition, untransplanted uPA+/-NOG mice inoculated with undiluted fecal suspensions from patient HEV0069 (8 log IU HEV RNA) remained HEV RNA negative in liver, serum and feces, indicating that human hepatocytes are HEV target cells in vivo (n=3; data not shown).

The absence of detectable HEV RNA could not be ascribed to loss of chimerism, as the variation of human albumin levels during the course of the experiment was similar in HEV-positive and HEV-negative mice (Fig. 3B). Intrahepatic HEV RNA titers do vary and correlate with the degree of liver chimerism, as reflected by the human albumin levels in mouse serum (R2 0.6866) (Fig. 3C). However, the latter does not explain the infectivity differences observed between the different HEV containing samples, as the animal with lowest human albumin values at end of follow-up (50 µg/ml) still had detectable intrahepatic HEV RNA levels. These data therefore corroborate a genuine biological difference in infectivity of HEV containing samples of different origins.

Discussion

Human HEV gt3 are emerging in Western countries and immunosuppressed patients are at risk of developing chronic HEV with progressive liver fibrosis. In this study we establish the human-liver chimeric mouse as model for chronic HEV gt 3 infections and demonstrate intrinsic in vitro A549 cell culture and in vivo infectivity differences of HEV gt3 containing clinical samples. Our data show that human liver-chimeric mice can develop a 100% chronic HEV infection, mimicking the infection course in solid organ and bone marrow transplant recipients. HEV in these mice is preferentially shed in bile and feces, which corresponds to the secretion pattern seen in humans.

Feces- and liver-derived inocula led to rapid HEV RNA increases in the A549 cell culture system. The plateauing viral titers early after plasma inoculation, may be ascribed to HEV cell surface detachment and gradual release into the supernatant as HEV ORF2 staining remained negative after 7 days of culture (Fig. 1K). We observed intrinsic HEV infectivity differences that were most apparent when plasma-, feces- and liver- HEV isolates from the same patient (HEV0008 and HEV0122) were examined: plasma-derived HEV demonstrated slower or no replication in vitro and in vivo respectively. HEV virions from plasma and feces have been found to differ in virion density, ascribed to a divergent lipid membrane content. In addition, culture derived HEV has comparable characteristics to plasma derived HEV (171, 172). Differences between these viruses might be caused by the detergent activity of bile acids, which could strip the HEV virions from their lipid membrane upon their passage towards the intestinal system (173). This different buoyant density may influence in vivo infectivity, as has previously been shown for the

hepatitis C virus (167). Circulating inhibiting factors, including virus-specific antibodies, on the other hand may also negatively influence the infectivity of the virus preparations. Nevertheless, we used only pre-seroconversion plasma samples in our in vivo infectivity assays.

Similar to 4 late resurgences of HEV RNA levels in vitro demonstrated here, others found productive in vitro infections with insertions in the ORF1 region after 5 to 6 weeks of culture of chronic HEV gt3 sera, but not acute phase sera (174-177).

The observation that human plasma-derived virus is less infectious in vivo may be relevant for the infectivity and epidemiology of HEV in humans. Indeed, only a limited number of cases of transfusion transmitted HEV have been reported despite administration of contaminated blood products (28, 159, 178, 179). In addition, a recent retrospective survey of United Kingdom's plasma pool, surprisingly showed that only half of HEV viremic British blood donors infected their recipients (28). The HEV transmission rate seemed to be dependent on the HEV RNA load and anti-HEV antibodies status in donor plasma. Ultimate proof of intrinsic infectivity differences of membranous or antibody coated HEV particles will require delipidation and antibody depletion of plasma derived inocula. While recent reports have shown HEV gt3 viremia among blood donors (163), Dutch national blood safety guidelines do not require NAT testing of the donor pool (180). This is of concern for solid organ transplant patients who are prone to develop chronic infections.

In conclusion, we have shown that feces- and liver-derived HEV gt3 induces a sustained infection in human liver-chimeric mice with preferential viral shedding towards mouse bile and feces, mimicking the course of infection in humans. This novel small animal model offers new avenues to study chronic HEV infections.

Acknowledgements

We would like to thank Vincent Vaes from the Erasmus MC animal care facility for his assistance in performing biotechnical manipulations and Jolanda Voermans, Jolanda Maaskant, Kim Kreefft, Debby van Eck-Schipper, Marwa Karim and Stalin Raj for excellent technical assistance.

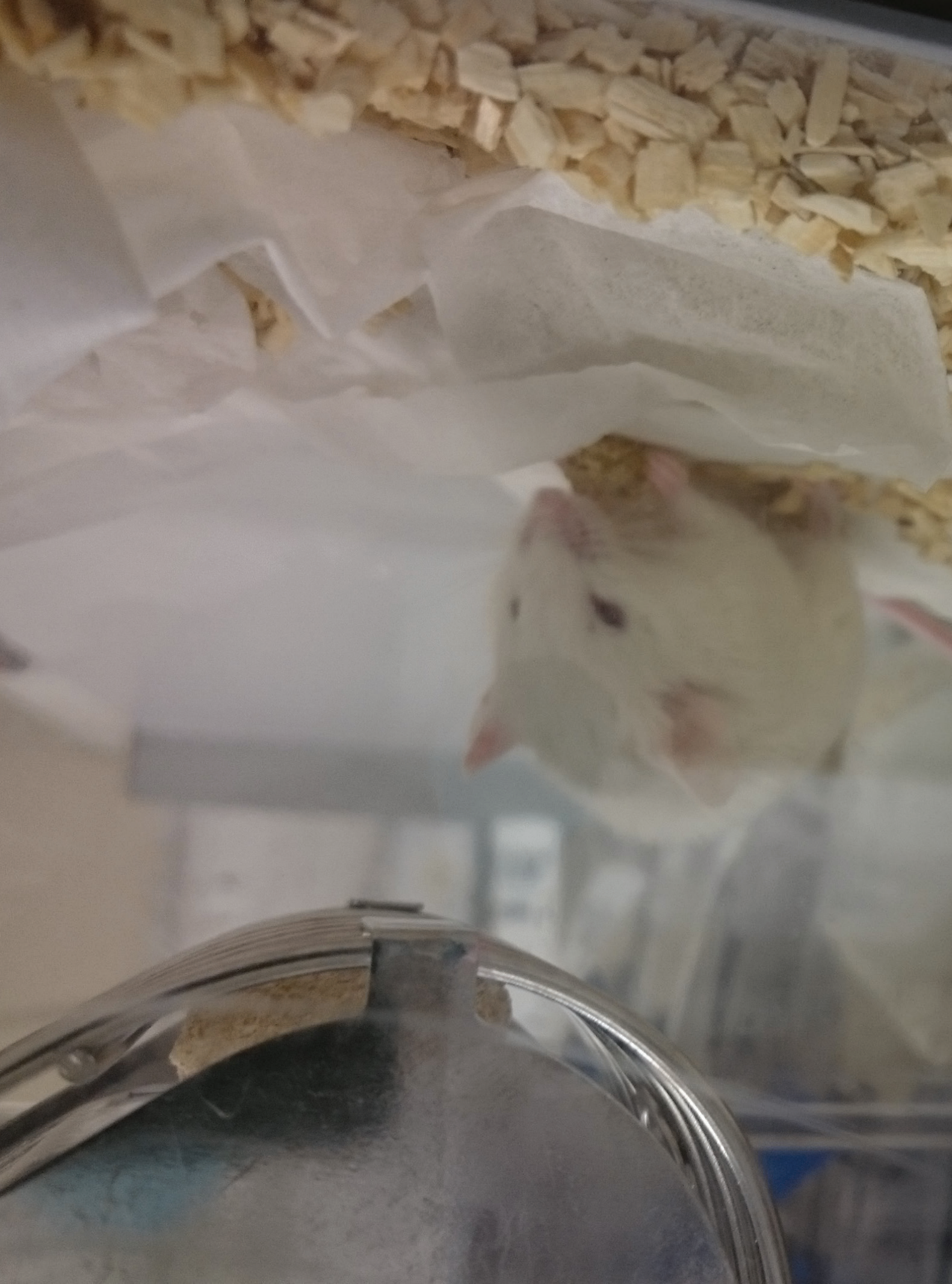

Chapter 5

Manuscript in preparation

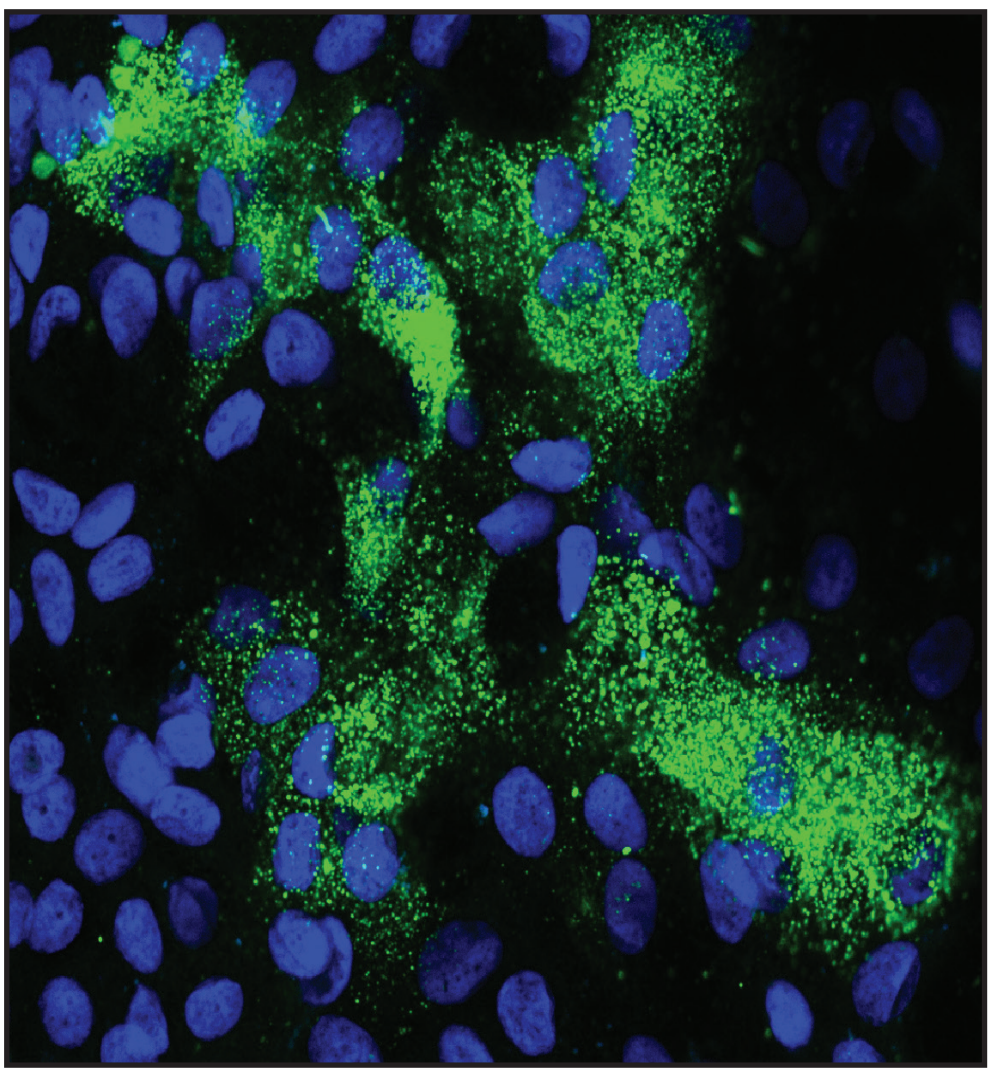

Hepatitis E virus (ORF2) stained green in infected A549 cells with blue cell nucleus (DAPI).

The hepatitis E virus genotype three genome adapts to in vitro conditions, but shows limited mutagenesis in immunocompromised hosts

Martijn D.B. van de Garde[1,*], Anne van Schoonhoven[1,*], Robert A. de Man[1], Andre Boonstra[1], Thomas Vanwolleghem[1,2,#], Suzan D. Pas[3,#]

Abstract

The hepatitis E virus (HEV) genotype (gt) 3 genome is predominantly detected in blood, feces and liver of an infected host. These sample types have in vivo and in vitro infectivity differences, in part ascribed to biophysical differences of the virions. However, less is known about the selection of viral quasispecies/clones in these different body compartments. Since extrahepatic manifestations have been described and single nucleotide variants have been suggested to alter HEV virulence, we examined the genomic stability of HEV virions in different clinical samples and experimental conditions, including propagation in immunodeficient humanized mice and in A549 cells. Near full HEV genome Sanger sequences of serum- and feces samples from two immunocompromised chronic HEV gt3 patients were obtained. After prolonged in vitro culture, a clinical HEV gt3 strain acquired 19 nucleotide mutations, leading to 7 non-synonymous amino acids changes in the papain-like cystein protease, variable, viroporin and capsid regions. The same clinical HEV gt3 strain showed only 4 nucleotide mutations without alterations in the amino acid sequence after prolonged infection in a human liver-chimeric mouse model with impaired adaptive and innate immune responses. Similarly, intra-patient comparison of feces- and serum-derived HEV gt3 showed 7 and 2 nucleotide mutations with 2 and 0 amino acid changes, in two patients respectively. Overall, our data suggest that in vivo selection pressure in immunodeficient hosts is minimal, but adaptation to in vitro culture occurs.

[1]Department of Gastroenterology and Hepatology, [2]Laboratory of Experimental Medicine and Pediatrics, Faculty of Medicine and Health Sciences, University of Antwerp and Department of Gastroenterology and Hepatology, Antwerp University Hospital, Antwerp, Belgium. [3]Department of Viroscience, Erasmus University Medical Center, Rotterdam, The Netherlands. *,#These authors contributed equally to this work

Introduction

Hepatitis E virus (HEV) is a non-enveloped positive-sense single-stranded RNA virus, belonging to the family Hepeviridae within the genus Orthohepevirus (29). The genome of HEV is approximately 7.2 kb and contains three open reading frames (ORF). ORF1 encodes several non-structural proteins including a methyltransferase, a y-domain, a papain-like cysteine protease, a helicase, and the RNA-dependent RNA polymerase. ORF2 encodes for structural proteins forming the viral capsid and ORF3, which overlaps with ORF2, encodes a viroporin essential for the release of infectious particles (30, 158).

In an infected host, a virus can compartmentalize in different locations and tissues, resulting in intra-host viral variants. Indeed, genomic viral variants of hepatitis C virus (HCV), human immunodeficiency virus (HIV) and Epstein-barr virus (EBV) have been observed in different compartments with altered viral entry, viral replication and treatment response (181-186). In addition to the liver, HEV is also found in blood, feces, and sporadically in cerebrospinal fluid of infected patients. Furthermore, in some cases HEV infection resulted in extra-hepatic manifestations (187). HEV's mutational drift in vivo is not well studied, except for genomic alterations of blood-derived HEV, with respect to emergence of treatment resistant strains (188). It therefore remains unknown whether genomic viral variants of HEV are selected in different physiological compartments in a patient.

Previous studies have identified single nucleotide substitutions in the viral genome of strains that resulted in more severe clinical phenotypes compared to strains lacking these substitutions, and suggested that these single nucleotide variants could be associated with increased virulence (189-191). Whether such mutations can affect HEV infectivity has never been investigated. We recently showed that HEV gt3 derived from feces and liver was more infectious in humanized mice and A549 cells compared to HEV gt3 from serum (192). The contribution of viral variants to these observed infectivity differences in vitro and in vivo remains elusive.

Here we examine HEV gt3's mutational drift in different compartments of two chronically infected hosts and compare mutagenesis of one clinical strain after experimental in vivo and in vitro propagation. We show up to two nonsynonymous of total seven nucleotide differences in intra-patient sample types, four synonymous mutations after in vivo passage, and seven nonsynonymous of total 19 nucleotide mutations after the 7th in vitro passage on A549 cells. Overall this demonstrates minimal in vivo selection pressure on HEV gt3 genomes in an immunocompromised host, but greater selection pressure during in vitro propagation.

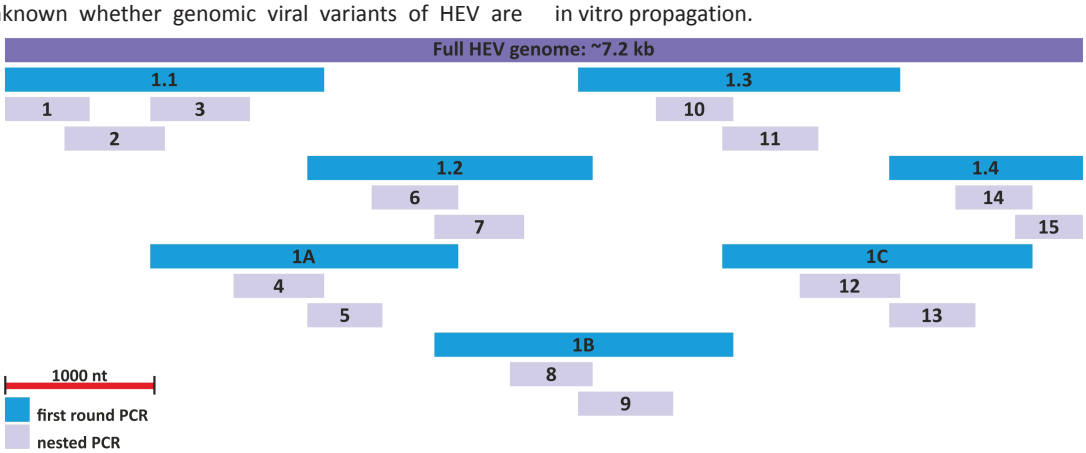

Figure 1. Schematic representation of size and location of the amplicons of PCR amplification. PCR fragment coverage was determined by primer alignment to the wbGER27 reference genome (purple bar). Blue bars represent first round PCR fragments; grey bars represent nested PCR fragments. Red scale bar indicates approximate size of 1000 nt. Fragment names correspond to primer pairs in Table 1 and Table 2.

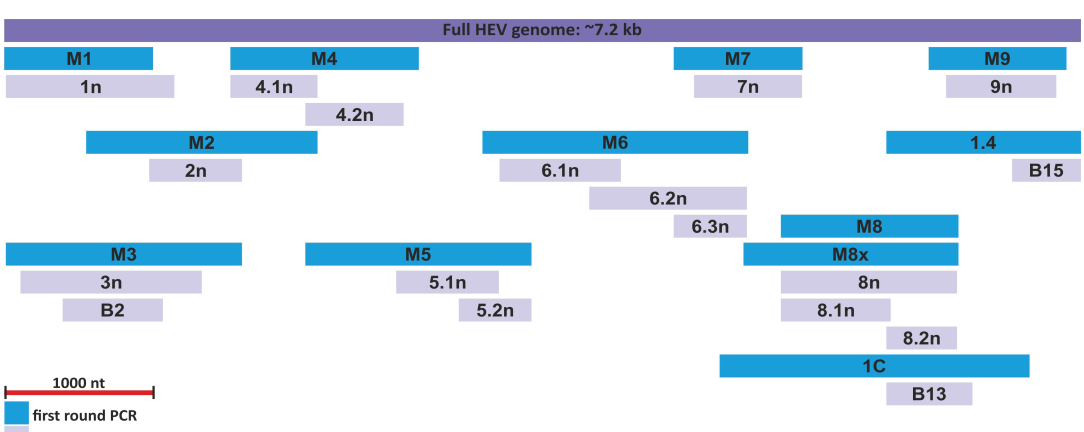

Figure 2. Schematic representation of size and location of the amplicons of alternate PCR amplification. PCR fragment coverage was determined by primer alignment to the wbGER27 reference genome (purple bar). Blue bars represent first round PCR fragments; grey bars represent nested PCR fragments. Red scale bar indicates approximate size of 1000 nt. Fragment names correspond to primer pairs in Table 3 and Table 4.

Table 1. Sequences and details of primers used for first round of PCR amplification method 1.

Amplicon/Primer name	Sequence 5'- 3'	Size amplicon (nt)	Tm (°C)
1.1: FW1	GCAGACCACGTATGTGGTCGATGCC	2136	58
RV4*	GTCCGGGTGTACAARGTTCCCTC		56
1.2: FW5	TTGTGGCTGCAYCCTGAGGGG	1912	55
RV8*	CAGTGGACTATGTCCGTGAGTTC		52
1.3: FW9	TGCCCTGAACTTGAGCAAGGC	2118	51
RV12*	ACCAAACCRGAAGTAGCCTCCTC		54
1.4: FW13	TATCGTAACCAGGGYTGGCGCTCTGT	1302	58
RV15*	GTTTTCCTCATGACGACCTA		60
1A: FW3	GTTCATATYTGGGACCGGCTYATGCT	2381	54
RV6	CCACYACRTCAACATCCCCCTGCTGTA		58
1B: FW7	GCCAACCTAGCACTGGAGATCGATGC	2263	58
RV10	CCGGCCGGCAAAGCGCACCACATC		61
1C: FW11	GGTTGTATGCTGGCGTGGTGGTGGC	2349	59
RV14	CAATCAGAATCTGATCAC		50

*Primers used for cDNA synthesis

Table 2. Sequences and details of primers used for nested PCR amplification method 1 and Sanger sequencing of resulting fragments.

Amplicon/primer name	Template	Sequence 5' - 3'	Size amplicon (nt)	Tm (°C)
1: FW1*	1.1	GCAGACCACGTATGTGGTCGATGCC	564	58
1: RV1		CGGGCCATRGCCTCCGCAACATC		59
2: FW2	1.1	GCCCTGCGGCTAACTGCCGCCG	669	61
2: RV2		CTAATCCCGCGGAGGTAGGTCATAAG		56
3: FW3*	1.1	GTTCATATYTGGGACCGGCTYATGCT	664	54
3: RV3		GGGATGTTAAGYGCCCTATACAG		52
4: FW4	1A	GAGGGCTCTGAGGTCGAYCAGGC	604	59
4: RV4*		GTCCGGGTGTACAARGTTCCCTC		56
5: FW5*	1A	TTGTGGCTGCAYCCTGAGGGG	500	55
5: RV5		GCGYTGGTAGAAGGCATGGCAAAG		56
6: FW6	1.2	TTGGCTGGTYAAYGCGTCGAATCC	613	54
6: RV6*		CCACYACRTCAACATCCCCCTGCTGTA		58
7: FW7*	1.2	GCCAACCTAGCACTGGAGATCGATGC	598	58
7: RV7		TGGACYGTAATCGCACCGGGGTT		54
8: FW8	1B	GCGGTCTTTATTCTGGAATGAGCC	554	52
8: RV8*		CAGTGGACTATGTCCGTGAGTTC		52
9: FW9*	1B	TGCCCTGAACTTGAGCAAGGC	596	51
9: RV9		CCAAGGGAGAAGTTATTTTGRGTGCTATC		55
10: FW10	1.3	GACGCATAYGAGGAGTCTGTGTT	515	52
10: RV10*		CCGGCCGGCAAAGCGCACCACATC		61
11: FW11*	1.3	GGTTGTATGCTGGCGTGGTGGTGGC	640	59
11: RV11		CGCTGGGAYTGATCACGCCAAG		55
12: FW12	1C	CTCCCCTATATTCATCCAACCAACC	622	53
12: RV12*		ACCAAACCRGAAGTAGCCTCCTC		54
13: FW13*	1C	TATCGTAACCAGGGYTGGCGCTCTGT	574	58
13: RV13		TCATAGTCTTGGATGACCACACG		50
14: FW14	1.4	GTCGTCTCAGCCAATGGCGAGC	513	55
14: RV14*		CAATCAGAATCTGATCAC		50
15: FW15	1.4	AAACATTCTATGTTCTCCCGC	458	43
15: RV15*		TTTTTTTTCCAGGGAGCGCG		60

*Primers also used in first round PCR (Table 1)

Material and Methods

Virus isolates

Clinical samples were obtained from two heart transplant recipients (HEV0069 and HEV0122) (192), before treatment at either the Erasmus Medical Center or the University Hospital Antwerp. Both patients had detectable HEV RNA in their EDTA-plasma for more than 6 months (defined as chronic HEV infection). Feces and plasma were collected for HEV0069 at 45 and 64 days respectively, and for HEV0122 at 8 months after estimated time of infection. In vitro derived HEV was obtained from A549 cell culture supernatant after seven passages of HEV0069 feces-derived HEV, showing increased replication capacity over other passages. In vivo derived HEV was obtained from a human-chimeric mouse liver 6 weeks after inoculation with feces-derived HEV0069. More details about the in vitro and in vivo experiments have recently been described (192).

Viral RNA isolation

HEV RNA was isolated using the QIAamp Viral RNA Mini kit according to manufacturer's instructions. Viral RNA was eluted in 2 x 30 µl elution buffer.

cDNA synthesis

cDNA of HEV0069 feces, serum and in vitro culture supernatant was synthesized using 1 µM HEV-specific primer Rv4, Rv8, Rv12 and Rv15 (Table 1) , 0.5 mM dNTP nucleotide mix (Roche) and 44 µl HEV RNA. Before cDNA synthesis potential secondary RNA structures were removed by heating to 65°C for 5 minutes followed by 1 minute incubation on ice. Subsequently, 2 U/µl RNasin (Promega), 5 mM Dithiothreitol (DTT) (Invitrogen), 0.25x First Strand buffer (Invitrogen), and 10 U/µl Superscript III RT (Invitrogen) were added to a total volume of 80 µl and incubated for 60 minutes at 50°C. HEV0122 feces and serum, and HEV0069 derived from mouse liver HEV RNA was made to cDNA with a Transcriptor First Strand cDNA Synthesis kit (Roche) following manufacturer's instructions, with 10 µl HEV RNA input for each 20 µl reaction, using a combination of random hexamers and an oligo-dT primer.

PCR amplification

HEV primer design of method 1 was done on basis 113 GenBank gt3 genomes, taking into mind that HEV gt3 genome FJ705359.1| Hepatitis E virus isolate wbGER27 is the closest related genome to most prevalent HEV genomes within our chronic HEV gt3 patient population according to HEV genotyping method described before (193).

cDNA of HEV0069 feces, serum and in vitro culture supernatant was used to generate seven overlapping amplicons in first round PCR (Figure 1) of each ~2000bp. Subsequently, two or three amplicons per primary product were generated using nested primers to cover the full HEV genome, with each ~100bp overlap and ~500bp length (Figure 1). Table 1 and Table 2 depict primer sequences for primary PCR and nested PCR, respectively. Primary PCR mixture contained 10 µl HEV cDNA with 0.4 µM primers, 1x PCR buffer (Qiagen), 1mM MgCl2 (Qiagen), 0.2 mM dNTP mix (Roche), and 2.5 U Hotstar polymerase (Qiagen), filled up to 50 µl with RNase/DNase free water. PCR program started with a 15

Table 3. Sequences and details of primers used for first round PCR amplification method 2.

Amplicon/Primer name	Sequence 5' - 3'	Size amplicon (nt)	Tm (°C)
M1*: 1-F	GCAGACCACGTATGTGGTCGATGCC	975	60
1-R	GTCCGGGTGTACAARGTTCCCTC		
M2*: 2-F	TTGTGGCTGCAYCCTGAGGGG	1530	60
2-R	CAGTGGACTATGTCCGTGAGTTC		
M3*: 3-F	TGCCCTGAACTTGAGCAAGGC	1562	60
3-R	ACCAAACCRGAAGTAGCCTCCTC		
M4*: 4-F	TATCGTAACCAGGGYTGGCGCTCTGT	1498	57
4-R	GTTTTCCTCATGACGACCTA		
M5*: 5-F	GTTCATATYTGGGACCGGCTYATGCT	1749	57
5-R	CCACYACRTCAACATCCCCCTGCTGTA		
M6*: 6-F	GCCAACCTAGCACTGGAGATCGATGC	1761	50
6-R	CCGGCCGGCAAAGCGCACCACATC		
M7*: 7-F	GGTTGTATGCTGGCGTGGTGGTGGC	838	57
7-R	CAATCAGAATCTGATCAC		
M8*: 8-F	TGCCTATGYTGCCCGCGC	1412	57
8-R	ACWGYYGGCTCACCATTGGC		
M8x*: 6.2n-R	CARACCTGCGCIACRTTCGT	1439	50
8-R	ACWGYYGGCTCACCATTGGC		
M9*: 9-F	GCIGCYACRCGITTYATGAA	897	57
M*9: 9-R	TTYTAAGRCGCTGAAGYTCAG		
1.4#: FW13	TATCGTAACCAGGGYTGGCGCTCTGT	1302	50
RV15	GTTTTCCTCATGACGACCTA		
1C#: FW11	GGTTGTATGCTGGCGTGGTGGTGGC	2349	50
RV14	CAATCAGAATCTGATCAC		

*Amplicons are based on the primer set described by Muñoz-Chimeno, et al. (194); #Amplicons derived from method 1 (Table 2)

Table 4. Sequences and details of primers used for nested PCR amplification method 2 and Sanger sequencing of resulting fragments.

Amplicon/Primer name	Template	Sequence 5' - 3'	Size amplicon (nt)	Tm (°C)
1n*: 1n-F	M1	TCGAWGCCATGGAGGCCCA	539	60
1n-R		GTCATCCCRTGICGRGCCAT		
2n*: 2n-F	M2	ATYTGGGAYCGGCTYATGCT	600	60
2n-R		CCRTGRACIGCRTARGTCCC		
3n*: 3n-F	M3	GCTGTGGTGGTYCGGCCGTT	1194	57
3n-R		CGRCAYTGIGCRTARAACTG		
4.1n*: 4.1-F	M4	GGCYTAYGARGGITCIGARGT	564	54
4.1-R		AAIGGRTTIGCIGAYTCCCA		
4.2n*: 4.2-F	M4	TRTGGYTRCAYCCYGAGGG	891	54
4.2-R		GTYTCICGRTAYGCYGCCTC		
5.1n*: 5.1n-F	M5	AGGRTYGARCAGAAYCCIAAGAG	667	54
5.1n-R		CGRTGIGTIACRTGCCACCA		
5.2n*: 5.2n-F	M5	GAGCTYCGIAAYAGYTGGCG	465	54
5.2n-R		CTRGCRTCRGCYGTRGCTAT		
6.1n*: 6.1n-F	M6	GAYGTITGYGARCTYATACG	792	50
* 6.1n-R		TCCTGRCCCTTYTCIACCAT		
6.2n*: 6.2n-F	M6	ATAGTYCAYTGYCGIATGGC	1035	50
6.2n-R		CARACCTGCGCIACRTTCGT		
6.3n*: 7n-R	M6	TTGGTTGGATGAATATAGGGGAGGG	351	50
* 6.2n-R		CARACCTGCGCIACRTTCGT		
7n*: 7n-F	M7	GGAAYACYGTYTGGAAYATGGC	697	57
7n-R		TTGGTTGGATGAATATAGGGGAGGG		
8n*: 8n-F	M8x	TGCCTATGYTGCCCGCGC	1178	57
8n-R		CCCGCGCGGCYGARACRACIGGGCGGG		
8.1n: 8n-F*	M8x	TGCCTATGYTGCCCGCGC	736	50
FW13#		TATCGTAACCAGGGYTGGCGCTCTGT		
8.2n: FW13*	M8x	TATCGTAACCAGGGYTGGCGCTCTGT	462	50
8n-R#		CCCGCGCGGCYGARACRACIGGGCGGG		
9n*: 9n-F	M9	CCGACAGAATTRATTTCGTCGGC	715	57
9n-R		TCMGGRCARAAATCATCRAAAGT		
B2#: FW2	M3	GCCCTGCGGCTAACTGCCGCCG	669	50
RV2		CTAATCCCGCGGAGGTAGGTCATAAG		
B13#: FW13	1C	TATCGTAACCAGGGYTGGCGCTCTGT	574	50
RV13		TCATAGTCTTGGATGACCACACG		
B15#: FW15	1.4	AAACATTCTATGTTCTCCCGC	458	45
RV15		TTTTTTTTCCAGGGAGCGCG		

*Primer set described by Muñoz-Chimeno, et al.(194); #Amplicons derived from method 1 (Table 2)

minute hot start at 95°C, followed by 40 cycles of 1 minute at 95°C, 1 minute at 50°C, and 3 minutes at 72°C, and finalized by 10 minutes at 72°C. Nested PCR conditions were identical to first round PCR, except the template was 2 µl of corresponding first PCR product, and the 40 cycles of the PCR program consisted of 30 seconds at 95°C, 30 seconds at 50°C, and 1 minute at 72°C. Amplicon 15 was amplified using altered annealing temperature of 45°C instead of 50°C. RNase/DNase free water served as a negative control.

In order to amplify cDNA from serum and feces-derived HEV0122, and HEV0069 mouse liver, an alternative method using 12 amplicons in primary PCR, which served as template for a total of 18 nested PCR products was adapted from Munoz-chimeno et al. (Figure 2) (194). Table 3 and Table 4 depict primer sequences for primary PCR and nested PCR, respectively. PCR conditions were identical as described above, except 5 µl cDNA was used as input for first round PCR, and 2.5 µl first PCR product served as template for nested PCR. The annealing temperature in the PCR program was adjusted to match each primer set (Tables 3 and 4). RNase/DNase free water served as a negative control.

Fragment detection and purification

Presence and purity of the nested amplicons was assessed by gel electrophoresis on a 2% agarose gel. UV exposure was kept to minimum. Amplified nested amplicon was extracted using the GeneJET MinElute kit (QIAGEN) according to manufacturer's instructions. DNA concentrations were determined using Nanodrop, and samples were diluted to 0.5 ng/µl – 20 ng/µl.

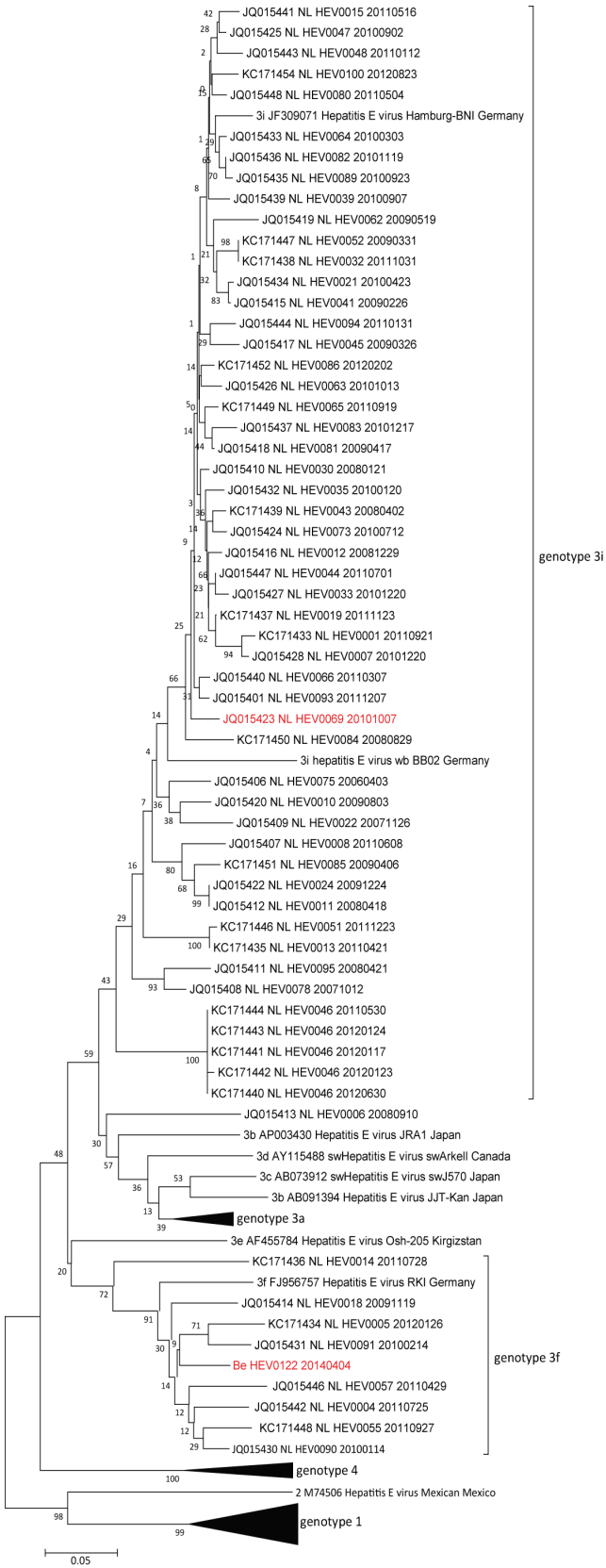

Figure 3. Neighbour-joining phylogenetic tree of ORF1 HEV gt3 sequences. Phylogenetic relationships of a (224bp) part of ORF1 were calculated using Kimura2parameter and Neighbour-Joining Method, with 500 bootstrapping steps. Total of 111 sequences, including HEV0069 and HEV0122 (in red) are depicted. Different subtypes and genotypes are indicated within the tree.

Sanger sequencing

Sequence PCR was performed on 1 - 40 ng purified HEV DNA amplicon using 0.4 µM nested PCR primers (Table 2 and 4), 2 µl Big Dye Terminator V3.1 reaction mix (Applied Biosystems), and 3 µl Big Dye 5x sequence buffer (Applied Biosystems), filled up to 22 µl with RNase free water. The PCR program started with 1 minute at 96°C, followed by 25 cycles of 30 seconds at 96°C, 30 seconds at 45°C, and 1 minute at 60°C. Enzymes and superfluous reactants were removed using a Performa DTR V3 96-well short plate kit (EdgeBio) following manufacturer's instructions. Sequence data and base calling were acquired through an ABI PRISM 3130XL genetic analyzer with POP7 polymer and 50 cm capillaries.

Data analysis

Sequences were assembled using SeqMan Pro v10.1.2 (Lasergene, DNA star) by aligning fragment sequences against the wbGER27 full HEV genome as reference (GenBank accession number: FJ05359) for HEV0069 and HEV RKI strain (GenBank accession number FJ956757) for HEV0122. Assembled sequences were aligned using the ClustalW Multiple alignment algorithm in BioEdit v7.2.0. Comparison of samples were performed using pairwise nucleotide distance and amino acid distances. Phylogenetic relationships of a (224bp) part of ORF1 were calculated using Kimura2parameter and Neighbour-Joining Method, with 500 bootstrapping steps using MEGA6 software. A total of 111 nucleotide sequences, including HEV0069 and HEV0122 were used to generate a neighbor-joining phylogenetic tree.

Results

Feces- and serum-derived HEV sequences are not completely identical

Serum and feces HEV RNA was extracted from two chronic HEV patients (HEV0069 and HEV0122), from in vitro A549 passaged (P7) fecal-HEV0069 supernatant, and in vivo passaged (P1) fecal-HEV0069, in human-liver chimeric mice. Using primers from Table 1 and Table 2, 15/15 and 8/15 amplicons were amplified for HEV0069 and HEV0122 isolates, respectively. Increasing genome coverage could be obtained with 16/18 amplicons for HEV0122 using extra and alternated primers (Table 3 and 4). Similarly, fragments (8n and 8.1n, Table 4) did not amplify HEV0069 derived from chimeric mouse livers. Full genome coverage could be obtained for HEV0069, but not HEV0122, using amplicon primers 11 and 12 (Table 2) from the initial set up. All amplified fragments were purified and sequenced. All HEV0069 and HEV0122 sequences were assembled by aligning fragment sequences against the wbGER27 or HEV RKI full HEV genomes, respectively. Sequenced HEV0069 samples resulted in a genomic coverage of 98.3-100%, whereas for HEV0122 only 85.4-88.9% genomic coverage could be obtained. The sequenced regions of HEV0122 completely covered ORF1, but lacked the first part of ORF2 and ORF3. The pairwise nucleotide identity of feces-derived HEV ORF1 sequences from HEV0069 and HEV0122 was calculated at 80.1%, whereas the pairwise amino acid identity was 93.7%. A neighbour-joining phylogenetic tree analyses of a (224bp) part of ORF1 revealed that HEV0069 and HEV0122 are divergent strains belonging to different genotype subtypes, namely genotype 3i and 3f respectively (Figure 3). The sequences obtained were used to compare serum and feces derived HEV. Intra-patient comparison of HEV0069 isolates revealed 5 synonymous and 2 nonsynonymous nucleotide mutations (one in the variable and one in the capsid region), whereas HEV0122 isolates revealed only

Table 5. Genomic differences of HEV0069 isolates and after in vitro and in vivo passage.

HEV0069								
Nucleotide changes						Corresponding (non)synonymous amino acid changes.		
nucleotide position*	feces$	serum	A549 Culture	mouse liver	mutation#	ORF1	ORF3	ORF2
1409	Y	Y	C	Y	Y1409C	FL462L		
1474	C	C	Y	C	C1474Y	C483C		
1591	C	C	T	C	C1591T	A522A		
1900	C	C	Y	C	C1900Y	G625G		
2070	T	Y	T	T	T2070Y	F682S		
2122	Y	C	Y	C	Y2122C	T699T		
2246	T	T	C	T	T2246C	W741R		
2710	C	C	Y	C	C2710Y	L895L		
2962	C	C	Y	C	C2962Y	H979H		
3577	S	C	C	C	S3577C	L1184L		
3610	C	C	Y	C	C3610Y	D1195D		
3931	Y	T	Y	T	Y3931T	V1302V		
4951	T	T	Y	T	T4951Y	L1642L		
5373	C	C	Y	C	C5373Y		Y71Y	P68S
5378	A	A	G	A	A5378G		N73S	Q69Q
5456	C	C	Y	C	C5456Y		P99L	S95S
5980	A	W	A	A	A5980W			E270V
5990	T	C	T	T	T5990C			S273S
6071	T	T	Y	T	T6071Y			L300L
6323	S	G	G	G	S6323G			P384P
6503	C	C	Y	C	C6503Y			D444D
6596	C	C	Y	C	C6596Y			L475L
6765	T	T	Y	T	T6765Y			Y532D
7045	A	A	T	A	A7045T			D625V
nt changes to feces	n/a	7	19	4	24	13	3	11
aa changes to feces	n/a	2	7	0	9	3	2	4

*Relative to HEV wbGER27 (GenBank accession number: FJ05359), $Feces strain is used as reference sequence, #feces nt_nt position_changed nt; nt, nucleotide; aa, amino acid; n/a, not applicable; ORF, open reading frame; Yellow marks nucleotide mutations, green marks synonymous aa changes, red marks nonsynonymous aa changes.

2 synonymous nucleotide changes (Table 5 and Table 6).

HEV adapts to cell culture, but shows only synonymous nucleotide changes during in vivo passage

RNA viruses are known to have relative high mutation rates, resulting in fast adaptation and evolutionary more distant strains (195). To assess the mutational drift of HEV, A549 cells were infected in vitro, and a human-liver chimeric mouse in vivo with HEV derived from feces of patient HEV0069. Infection in A549 cells was maintained for 7 passages and culture supernatant was harvested 10 days after last passage, covering a total of 111 days of in vitro propagation, as shown before (192). HEV from culture supernatant was sequenced and showed 19 single nucleotide mutations compared to the initial feces-derived HEV inoculum (Table 5). Seven of these mutations resulted in amino acid selection or substitutions; FL462L, W741R in ORF1, N73S, P99L in ORF3, and P68S, E270V, Y532D, D625V in ORF2. We next investigated viral mutagenesis in differentiated human hepatocytes without interference of immune pressure. Therefore, humanized NOG mice harbouring differentiated human hepatocytes were infected with the same patient derived HEV0069 strain and humanized mouse liver was isolated 6 weeks later. HEV derived from chimeric-mouse liver showed 4 synonymous nucleotide mutations Y2122C, S3577C, Y3931T in ORF1, and S6323G in ORF2 (Table 5).

Discussion

In an HEV-infected host, virus concentrations are higher in bile, liver and feces than in blood. It is not known whether this compartmentalization results in different viral variants. HEV single nucleotide variants in blood have been shown to alter clinical virulence (189-191). Furthermore, we have previously shown that the in vivo and in vitro infectivity of HEV from blood and feces differs substantially. Finally, the presence of extrahepatic manifestations in selected patients suggests viral selection or adaptation to different tissues. Therefore, we performed intra-patient comparison of full genome sequences of HEV gt3 isolates from serum and feces of two chronic HEV patients. In addition, to assess mutation rate we examined the HEV sequences after in vitro and in vivo passage of HEV0069 feces-derived virus.

Table 6. Genomic differences of HEV0122 isolates

HEV0122						
Nucleotide changes				Corresponding (non)synonymous amino acid changes.		
nucleotide position*	feces$	serum	Mutation#	ORF1	ORF3	ORF2
4984	Y	T	Y4984T	V1652V		
6416	T	C	T6416C			V409V

*Relative to HEV RKI (Genbank accession no. FJ956757.1); $Feces strain is used as reference sequence; #feces nt_nt position_changed nt; ORF, open reading frame; green marks synonymous aa changes;

HEV RNA was isolated and sequenced from serum and feces of two chronic HEV patients. Intra-patient HEV nucleotide sequences showed five synonymous and two nonsynonymous differences between feces and serum isolates from HEV0069, whereas only two synonymous mutations were found in HEV0122 isolates. The two amino acid changes occurred in the ORF1 in a region of unknown function, and ORF2 encoding the capsid, thereby possibly impacting viral entry. This illustrates that compartmentalized viral variants may exhibit distinct intrinsic viral properties. Whether the identified nonsynonymous mutations are the cause for altered infectivity remains to be determined.

In addition to inter- and intra-patient comparison of serum- and feces-derived HEV gt3 strains, the genomic alterations after in vitro and in vivo passage were assessed. HEV0069 feces-derived virus was used to infected A549 cells in vitro and human hepatocytes in immunocompromised human-liver chimeric mouse. The latter host precludes immune selection pressure, due to the absent T, B and NK cells, and therefore allows to compare the mutagenesis between HEV replication in a lung adenocarcinoma cell-line and differentiated hepatocytes. A four nucleotide-different viral variant, without amino acid alterations, was identified in HEV derived from humanized mouse liver 6 weeks after inoculation. The absence of immune cells may explain the limited mutational drift of HEV in these mice. In addition, we recently showed no induction of intra-cellular innate immune response in HEV infected human hepatocytes, minimizing the intra-cellular immune pressure (255). The fact that only few viral variants are seen in patients between serum and feces supports this relatively low compartment-specific mutation rate.

However, when we culture HEV for 111 days (seven serial passages), 7 out of 19 mutations, which were identified, resulted in amino acid changes (2 occurred in ORF1, and 5 in ORF2/3) (Table 5). Previous studies have identified single nucleotide variants that displayed altered viral fitness (189-191). In addition, one study showed significant increased infectivity in HepG2/C3A cells upon insertion of a 171-nucleotide sequence of human S17 ribosomal protein into a HEV gt3 cDNA clone (176). We did not detect any nucleotide insertions after 111 days of propagation in A549 cells with patient derived HEV. Whether the mutations found after culture in A549 cells influence viral fitness is subject for further study.

The observed genomic alterations after in vitro culture and in vivo infection in humanized mice illustrate important model differences. Occurrence of several nucleotide substitutions can alter viral fitness and responsiveness to treatment. Therefore, it is important to identify viral mutations and selection with the models used to study HEV. Based on our results the in vivo model is most representative for genuine infection with no nonsynonymous mutations after 6 weeks of infection. Whether the in vitro acquired nucleotide substitutions are due to the in vitro setting or the adaptation of the virus to non-hepatic cell line remains to be determined.

Our observations showed clear differences between the major populations identified using Sanger sequencing, which is able to detect viral variants that comprise at least 20% of the total viral population (196). Therefore, we are not able to conclude on possible minority populations present. Future research could use Next generation sequencing (NGS) for detection of minority populations, which has a detection limit of as low as 1% (196)

In conclusion, our data suggest that HEV gt3 genomically adapts to in vitro culture, but that in vivo selection pressure in immune deficient hosts is minimal. However, possible genomic adaptation to compartmentalization in chronically infected patient can ensue.

Acknowledgements

We would like to thank Bo van der Heuvel for her excellent technical assistance.

Chapter 6

Published in: Scientific Reports, 2017, 7:8267.

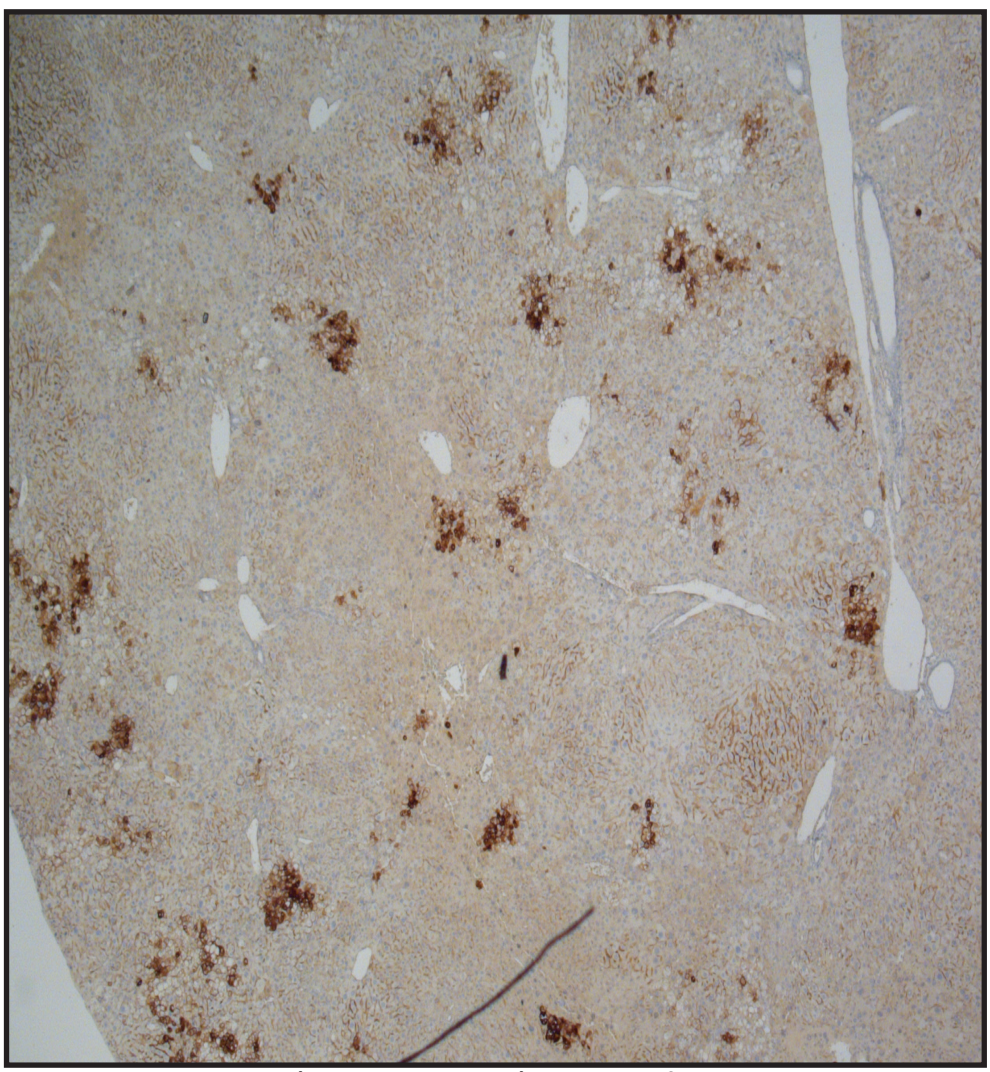

Hepatitis B virus in brown (anti-HBsAg staining) in clusters of human hepatocytes in the mouse liver.

Interferon-alpha treatment rapidly clears hepatitis E virus infection in humanized mice

Martijn D.B. van de Garde[1], Suzan D. Pas[2], Gertine W. van Oord[1], Lucio Gama[4], Youkyung Choi[5], Robert A. de Man[1], Andre Boonstra[1], Thomas Vanwolleghem[1,3]

Abstract

Antiviral treatment options for chronic Hepatitis E Virus (HEV) infections are limited and immunological determinants of viral persistence remain largely unexplored. We studied the antiviral potency of pegylated interferon-α (pegIFNα) against HEV infections in humanized mice and modelled intrahepatic interferon stimulated gene (ISG) responses. Human gene expression levels in humanized mouse livers were analyzed by qPCR and Nanostring. Human CXCL10 was measured in mouse serum. HEV genotype 3 (gt3) infections were cleared from liver and feces within 8 pegIFNα doses in all mice and relapsed after a single pegIFNα injection in only half of treated animals. Rapid viral clearance by pegIFNα was confirmed in HEV gt1, but not in Hepatitis B Virus infected animals. No ISG induction was observed in untreated HEV gt3 and gt1 infected humanized livers compared to control chimeric mice, irrespective of the human hepatocyte donor, viral isolate or HEV infection duration. Human specific ISG transcript levels in mouse liver increased significantly after pegIFNα treatment and induced high circulating human CXCL10 in mouse serum. In conclusion, HEV gt1 and gt3 infections do not elicit innate intrahepatic immune responses and remain highly sensitive to pegIFNα in immunocompromised humanized mice.

[1]Department of Gastroenterology and Hepatology, [2]Department of Viroscience, Erasmus University Medical Center, Rotterdam, The Netherlands. [3]Laboratory of Experimental Medicine and Pediatrics, Faculty of Medicine and Health Sciences, University of Antwerp and Department of Gastroenterology and Hepatology, Antwerp University Hospital, Antwerp, Belgium. [4]Department of Molecular and Comparative Pathobiology, The Johns Hopkins University School of Medicine, Baltimore, Maryland, USA. [5]Division of Viral Hepatitis, The Center for Disease Control and Prevention, Atlanta, Georgia, USA

Introduction

Hepatitis E Virus (HEV) infections are emerging in western countries (197). HEV is a non-enveloped positive-sense single-stranded RNA virus, belonging to the family Hepeviridae within the genus Orthohepevirus (29). Transmission mainly occurs through the fecal-oral route via contaminated water in developing countries or through the consumption of undercooked meat in industrialized countries (158). Seven different genotypes have been described so far, of which genotype (gt) 1 and 3 are most prevalent in humans (29). In healthy individuals, HEV mostly resolves spontaneously without severe symptoms, but pregnant women seem to be at risk of developing fulminant liver failure by HEV gt1 with mortality rates up to 25% (198, 199). On the other hand, increasing rates of chronic gt3 infections have been described in immunocompromised patients in Europe, resulting in progressive liver fibrosis and cirrhosis (3-5). These data indicate that host pathogen interactions differ between both genotypes.

Antiviral treatment options for chronic HEV infected immunocompromised patients are limited. Ribavirin (RBV) leads to sustained viral responses in roughly 75% of patients, but is hampered by RBV-induced anemia and the need for recombinant erythropoietin injections or transfusions in more than half of patients (47, 200). As an alternative, pegylated interferon-alpha (pegIFNα) has been administered to a few patients in doses comparable to Hepatitis C virus (HCV) treatment regimens (47, 48). However, factors associated with interferon (IFN)-susceptibility, the optimal pegIFNα dose or treatment duration have not been investigated in vivo.

The anti-HEV effects of IFNα in vitro differ according to the target cell and viral strain used. In vitro HEV models consist of human hepatoma and lung adenocarcinoma cell-lines, in which replication of subgenomic or full length replicons and seldom intact patient-derived viruses are studied (169, 175, 192, 201, 202). Patient-derived HEV gt3 cultures show slow viral propagation, whereas HEV gt1 can only be cultured in vitro after induction of endoplasmic reticulum stress in the host cell line (169, 192, 203). While HEV gt1 replication has been shown to be adequately suppressed by exogenous IFNα, HEV gt3 replication has not (204-206). In addition, viral inhibition of the interferon stimulated gene (ISG) responses have been described as a determining factor for IFNα susceptibility in vitro (207). As the studied host cells are either no target cells in vivo (A549 cells) or are hampered by defects in their innate immune signaling (Huh7 and Huh7.5), the host response towards genuine patient-derived HEV in differentiated human hepatocytes remains to be established (204, 208). In addition, several clinical observations are not matched by in vitro viral replication data. HEV containing an in vivo RBV acquired mutation (K1383N), showed conflicting results in vitro with decreased viral replication and increased RBV-sensitivity (191). Furthermore, the antiviral efficacy of sofosbuvir against HEV showed discrepancies in different in vitro and in vivo studies (209-212).

Recently, we and others have shown that human-liver chimeric mice can be used to study HEV infection in differentiated human hepatocytes in vivo (192, 213, 214). Here, we examined baseline ISG expression levels and susceptibility to pegIFNα in HEV gt1 and gt3 infected humanized mice. We demonstrate that HEV gt1 infections lead to higher virus loads in mouse feces, bile and liver compared to HEV gt3 infections, without the induction of intrahepatic human innate immune responses. Both HEV genotypes, but not Hepatitis B virus (HBV), are cleared after a few doses of pegIFNα in vivo, an effect accompanied by a clear increase of human ISG transcript levels in liver and of circulating human CXCL10 levels in mouse serum.

Material and Methods

Ethics, consent and permissions

The use of patient material was approved by the medical ethical committees of Erasmus Medical Center and Antwerp University Hospital. Informed consent was obtained from all subjects. All animal work was conducted according to relevant Dutch national guidelines. The study protocol was approved by the animal ethics committee of the Erasmus Medical Center (DEC nr. 141-12-11).

Mouse origin and genotyping

Urokinase-type plasminogen activator (uPA)/NOD/Shi-scid/IL-2Rγnull(NOG) mice were kindly provided by the Central Institute for Experimental Animals (Kawasaki, Japan) (53). Mice were bred at the Central Animal Facility of the Erasmus Medical Center. Zygosity of mice was determined as described previously (192). Mice were co-housed with a maximum of 4 mice per individually ventilated cage and were fed normal chow ad libitum.

Human hepatocyte transplantation

Six to twelve week old male uPA-homozygous mice were transplanted as described previously (215). In short, mice were anesthetized and transplanted via intrasplenic injection with 0.5 x 106 to 2 x 106 viable commercially available cryopreserved human hepatocytes from 1 of 3 donors (Corning, NY, USA; Lonza, Basel, Switzerland; Table 1). Graft take was determined by human albumin in mouse serum using an ELISA with human albumin cross-adsorbed antibody (Bethyl laboratories, Montgomery, TX, USA) as previously described (192).

Table 1. Hepatocyte donors

Donor ID	Gender	Age	Race
HD1	Male	2 years	Caucasian
HD2	Female	2 years	Caucasian
HD3	Female	7 months	Caucasian

Viral strains, mouse infection and treatment

HEV gt3 was derived from feces of one of two chronic HEV patients (HEV0069 and HEV0122) as described previously (192). HEV gt1 Sar-55 was derived from feces of a Rhesus macaque that had been originally inoculated with the human Sar-55 strain (216). Eight weeks after transplantation human-liver chimeric mice were inoculated intravenously (i.v.) with 200 µl feces suspension containing HEV gt3 (8.8 log IU/ml or diluted to 6.8 log IU/ml), HEV gt1 (7.9 log IU/ml or diluted to 6.2 log IU/ml) or 200 µl patient serum containing HBV gtA (7.7 log IU/ml). After viral inoculation, mice were housed individually. Mice were treated with a single subcutaneous pegIFNα-2a (30 µg/kg unless stated otherwise, Pegasys, Roche, Basal, Switzerland) injection or every 3-4 days for 2 or 4 weeks. Overview of viral isolates are shown in Table 2. An overview of experimental groups is shown in Table 3 and Suppl. Fig. 4.

HEV RNA and HBV DNA detection

The presence of HEV RNA in mouse serum, feces, bile and liver was determined by an ISO15189:2012-validated, internally controlled quantitative real-time RT-PCR, described previously (4, 192). Cycle threshold (Ct) values above 38 were considered

Table 2. Viral isolates

Virus	Genotype	Strain/ Isolate*	Source	Inoculum
HEV	1	Sar-55	Rhesus macaque feces	feces suspension
HEV	3	HEV0069*	Chronic HEV patient feces	feces suspension
HEV	3	HEV0122*	Chronic HEV patient feces	feces suspension
HBV	A		Chronic HBV patient serum	serum

background, which corresponds to a lower limit of detection of 2.16 log10 HEV RNA units/ml in undiluted human serum. HEV RNAs detected in samples with Ct values below 38 are indicated with their calculated values. HBV viral load was measured in mouse serum and liver using a dual target approach, using primers and probes targeting preS-gen, as described before (217, 218), and the X gene (HBV XJfwd12 5'-ggtctgtgccaagtgtttgst-3', HBV XJprobe 5'-FAM-acgcaacccccactggctggg-BHQ1-3', HBV XJrev12, 5'-tycgcagtatggatcgsc-3').

RNA isolation of whole liver, generation of cDNA and real-time qPCR

Whole liver RNA was isolated using RNeasy mini kit (Qiagen, Hilden, Germany) including DNAse treatment according to manufacturer's protocol starting with homogenization of liver tissue in RLT buffer. cDNA was generated by using an iScript cDNA synthesis kit (Bio-Rad Laboratories, Hercules, CA, USA) according to the manufacturer's protocol. Human specific gene expression was measured using Taqman primer/probe quantitative PCR, in TaqMan® Gene Expression Master Mix (Thermo Fisher Scientific, Waltham, MA, USA). Primer/probe combinations were purchased from Thermo Fisher Scientific; CXCL10 (Hs01124251_g1), CXCL9 (Hs00171065_m1), DDX58 (Hs01061436_m1), GAPDH (Hs00266705_g1), IFIT1 (Hs01911452_s1), ISG15 (Hs01921425_s1), IFNA1 (Hs00855471_g1), IFNA4 (Hs01681284_sh), IFNB1 (Hs01077958_s1), MX1 (Hs00895608_m1), OAS1 (Hs00973637_m1), RSAD2 (Hs00369813_m1), STAT1 (Hs01013996_m1), TLR3 (Hs01551078_m1). Expression of target genes was normalized to the expression of GAPDH using the formula 2-ΔCt, ΔCt = Cttarget-CtGADPH. cDNA from non-chimeric mouse livers was used as control to test cross-reactivity of housekeeping and target genes. Due to the difference in hepatocyte donor baseline expression levels of examined genes (Suppl. Fig. 1), fold changes of transcripts were calculated to those of non-infected humanized livers from mice transplanted with the identical hepatocyte donor.

Cytokine measurement

Human CXCL10 was measured in 1:5 diluted mouse serum samples using the Human CXCL10/IP10 Quantikine ELISA Kit (R&D Systems, Minneapolis, MN, USA) according to manufacturer's protocol.

Nanostring analyses

RNA was isolated from chimeric mouse livers as described above. The nCounter GX human Immunology V2 Kit (NanoString Technologies, Seattle,WA, USA) was used to measure the expression of 594 human genes in the RNA of these samples. Following hybridization, transcripts were quantitated using the nCounter Digital Analyzer. Samples were run at the Johns Hopkins Deep Sequencing & Microarray Core facility. To correct for background levels, the highest negative control value for each sample was subtracted from each count value of that sample, as described previously (137, 219). Following background subtraction, any negative count values were considered as 0. The geometric mean of 5 housekeeping genes provided by the company panel was calculated and used to normalize expression values. RNA from non-chimeric mouse livers was used as control to test cross-reactivity of genes. Fifty cross-reactive genes were removed prior to analyses of the data set. Non-expressed genes were defined as <100 relative RNA counts and below four times the standard deviation in all samples.

Statistics

Differences between groups were calculated using two tailed Mann-Whitney test or Kruskal-Wallis one-way ANOVA with Dunn's all column comparison post-test (GraphPad Prism version 5.01; GraphPad Software). Differences were considered significant when $P<0.05$. Results are presented as the mean ± SEM. Principal component analyses was performed on log 2 transformed data set and heatmap of IFN signaling/response genes was generated using Multi-experiment viewer (MeV) software version 4.9.

Results

Higher viral burden in HEV gt1 compared to gt3 infected human-liver chimeric mice

Humanized UPA+/+NOG mice were i.v. inoculated with a filtered feces suspension containing either HEV gt3 or HEV gt1 and were observed for 2, 6 or 14 weeks until euthanization. Infected mice were housed individually to prevent inter-mice contamination. During the infection course a higher percentage of HEV gt1 infected mice presented viremia, but the peak viral load in serum was similar to HEV gt3 infected mice (2.6 ± 0.4 and 1.4 ± 0.4 log HEV RNA IU/ml, respectively, Fig. 1a). The peak HEV RNA load in feces was significantly higher in HEV gt1, compared to HEV gt3 infected mice (5.9 ± 0.2 and 4.2 ± 0.5 log HEV RNA IU/gram, respectively, P = 0.029; Fig. 1b). HEV gt1 infected mice also had higher viral loads in bile (6.1 ± 0.2 vs. 5.2 ± 0.4 log HEV RNA IU/ml, respectively, P = 0.038; Fig. 1c) and liver (6.8 ± 0.2 vs 5.8 ± 0.3 log HEV RNA IU/gram, respectively, P = 0.015; Fig. 1d) at euthanasia, despite similar levels of serum human albumin compared to HEV gt3 infected mice, indicative for similar degrees

Table 3. Overview of experimental groups

Treatment	Chimeric liver	Virus	n=	Hepatocyte donor
None	no	None	3	n/a*
	yes	None	8	HD1, HD2
	yes	HEV gt1	10	HD1
	yes	HEV gt3 (HEV0069)	16	HD1, HD2, HD3
	yes	HEV gt3 (HEV0122)	4	HD1
	yes	HBV gtA	5	HD3
pegIFNα-2a	no	None	2	n/a*
	yes	None	2	HD2
	yes	HEV gt1	3	HD2
	yes	HEV gt3 (HEV0069)	11	HD2
	yes	HBV gtA	6	HD2

*n/a, not applicable

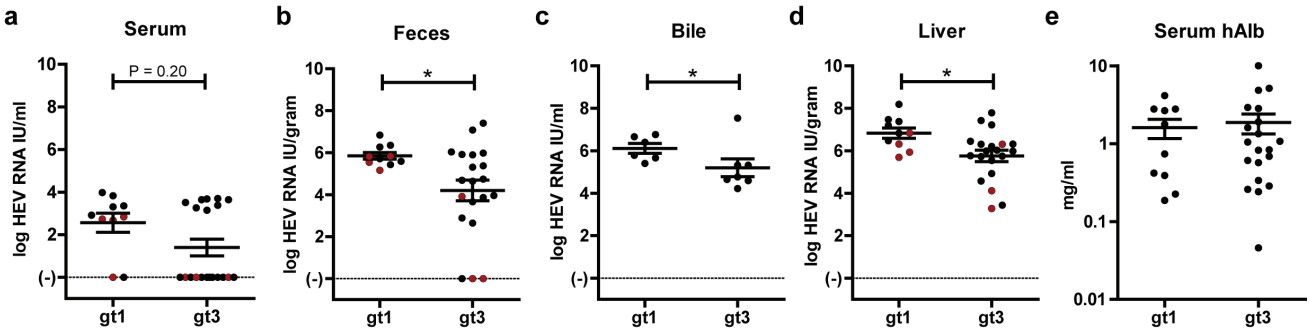

Figure 1. Higher viral loads in HEV gt1 compared to HEV gt3 infected mice despite similar degrees of human chimerism. Comparison of peak HEV RNA levels as measured by qRT-PCR in serum (a) and in feces (b). At sacrifice viral titers of HEV gt3 and gt1 infected mice were compared in bile (c, n=7 and n=6, respectively) and in liver (d). Human albumin levels were determined in mouse serum to quantify degree of chimerism at euthanasia (e). *, P < 0.05, n=20 for HEV gt3 and n=10 for HEV gt1 (a, b, d, e). Data are pooled from 2, 6, and 14 weeks infection experiments. Red dots indicate mice who received a diluted HEV inoculum (a-d).

of human chimerism (1.6 ± 0.4 and 1.9 ± 0.5 mg/ml, respectively, Fig. 1e). Despite lower absolute HEV gt1 inocula compared to HEV gt3, animals challenged with undiluted feces suspensions demonstrated similar results reaching higher HEV gt1 RNA levels in bile (P=0.038), liver (P=0.006), and feces (P=0.06) compared to HEV gt3 RNA levels. These results point to a higher in vivo virulence of HEV genotype 1 compared genotype 3.

No induction of intrahepatic innate immune responses in HEV gt1 or gt3 infected human-liver chimeric mice

Because of the HEV gt1 and gt3 clinical differences (3-5, 198) and different viral burdens in humanized mice, we examined the human host response in chimeric livers 2, 6, or 14 weeks after infection with either HEV gt1 or gt3. Using qRT-PCR we could not detect a significant increase in transcript levels of alpha or beta IFNs (data not shown), pathogen recognition receptors TLR3 and DDX58 (Fig. 2a), transcription factor STAT1 (Fig. 2b), or ISGs CXCL9, CXCL10, ISG15, RSAD2, OAS1, MX1, and IFIT1 (Fig. 2c). Furthermore, longer duration of HEV gt3, but not HEV gt1 infection led to significantly decreased STAT1, RSAD2 and MX1 expression levels in the liver (Fig. 2b+c). None of these human transcripts were detected in non-chimeric mouse livers.

In order to evaluate a broader number of genes, Nanostring analysis of 594 human specific immunology-related genes was performed on chimeric (serum hAlb 2.5 ± 0.8 mg/ml) gt3 HEV-infected livers (6.1 ± 0.25 log HEV RNA IU/gr) at different time points post infection. Human transcript specificity was confirmed by including RNA from 3 non-chimeric livers and led to the removal of 50 cross-reactive genes from further analyses. Based on set criteria (<100 relative RNA counts and below four times the standard deviation in all samples), 255 genes were defined as non-expressed. Principal component analyses did not reveal clustering of samples (Fig. 2d). Of 18 genes related to interferon signaling and response, none showed consistent upregulation compared to non-infected chimeric mice (Fig. 2e). Down regulation of STAT1 and MX1 as observed by qRT-PCR, was confirmed in the Nanostring gene expression data (Fig. 2b+c, e). Taken together, these data show that ongoing HEV gt1 or gt3 replication for up to 14 weeks does not elicit an innate immune response in human hepatocytes in vivo.

HEV but not HBV is sensitive to pegIFNα-2a treatment in human-liver chimeric mice

Baseline ISG expression in hepatocytes has been shown to predict the response to IFNα treatment in chronic HCV infected patients (43, 44, 220). As HEV did not induce an ISG response in vivo, we examined the HEV-sensitivity to pegIFNα treatment. As a negative antiviral control, we applied the same treatment to HBV gtA infected mice, which has been shown to only slightly reduce serum HBV DNA levels in a similar humanized mouse model (221). After 1 to 2 pegIFNα injections, HEV gt3 RNA became undetectable in feces of all treated animals (Fig. 3a-c). Complete viral clearance in liver and bile was observed in all mice at euthanasia 24 hours after 4 or 8 pegIFNα injections (Fig. 3d). To examine whether a single dose of 30 µg/kg pegIFNα would suffice to clear HEV gt3 in vivo, 4 animals received one injection after 6 weeks of ongoing HEV gt3 replication and were observed for an additional 4 weeks. This led to a complete viral clearance in 2 out of 4 mice and relapse in feces in the remainder 2 (Fig. 3c+d). Four weeks after the initial single pegIFNα dose, the latter 2 animals received repetitive 10-fold lower pegIFNα doses for 2 weeks. Again a steep decline in fecal HEV RNA loads was noted, but HEV RNA reemerged in feces and was detectable in bile and liver at euthanasia one day after the second pegIFNα treatment course (Fig. 3c+d). The high in vivo HEV IFNα sensitivity was corroborated in HEV gt1 infected animals. Again rapid suppression of HEV replication was noted in feces (Fig. 3e), liver and bile (data not shown) after a 2 week treatment course with 30 µg/kg pegIFNα. In contrast, a similar treatment regimen of HBV gtA infected mice induced a maximum decline of 0.7 ± 0.2 log HBV DNA copies/ml in serum with high intrahepatic viral loads at necropsy (6.9 ± 0.6 log HBV DNA copies/gr liver) (Fig. 3f). Non-treated HEV gt1, HEV gt3 and HBV infected mice never showed spontaneous viral clearance (Fig. 1b-d and Suppl. Fig. 2a-c), nor was loss of human chimerism in pegIFNα-treated animals observed, based on persistent detection of human albumin levels in mouse serum (data not shown). These data indicate that HEV, but not HBV is highly sensitive to pegIFNα in humanized mice.

Upregulation of intrahepatic ISG and serum CXCL10 upon pegIFNα treatment

To examine whether pegIFNα induced HEV clearance was associated with an induction of human hepatocyte ISG responses, human specific transcript levels of several innate immune response genes were studied in chimeric livers of HEV gt3, HEV gt1 and HBV gtA infected and pegIFNα treated animals. PegIFNα treatment led to an 20-fold increase of CXCL10 transcription, conjointly with induction of TLR3, DDX58, STAT1, CXCL9, ISG15, RSAD2, OAS1, MX1, and IFIT1 genes in the livers of HEV infected humanized mice (Fig. 4a and Suppl. Fig. 3). In addition, treatment was associated with an increase in serum human CXCL10 levels of HEV gt1 and

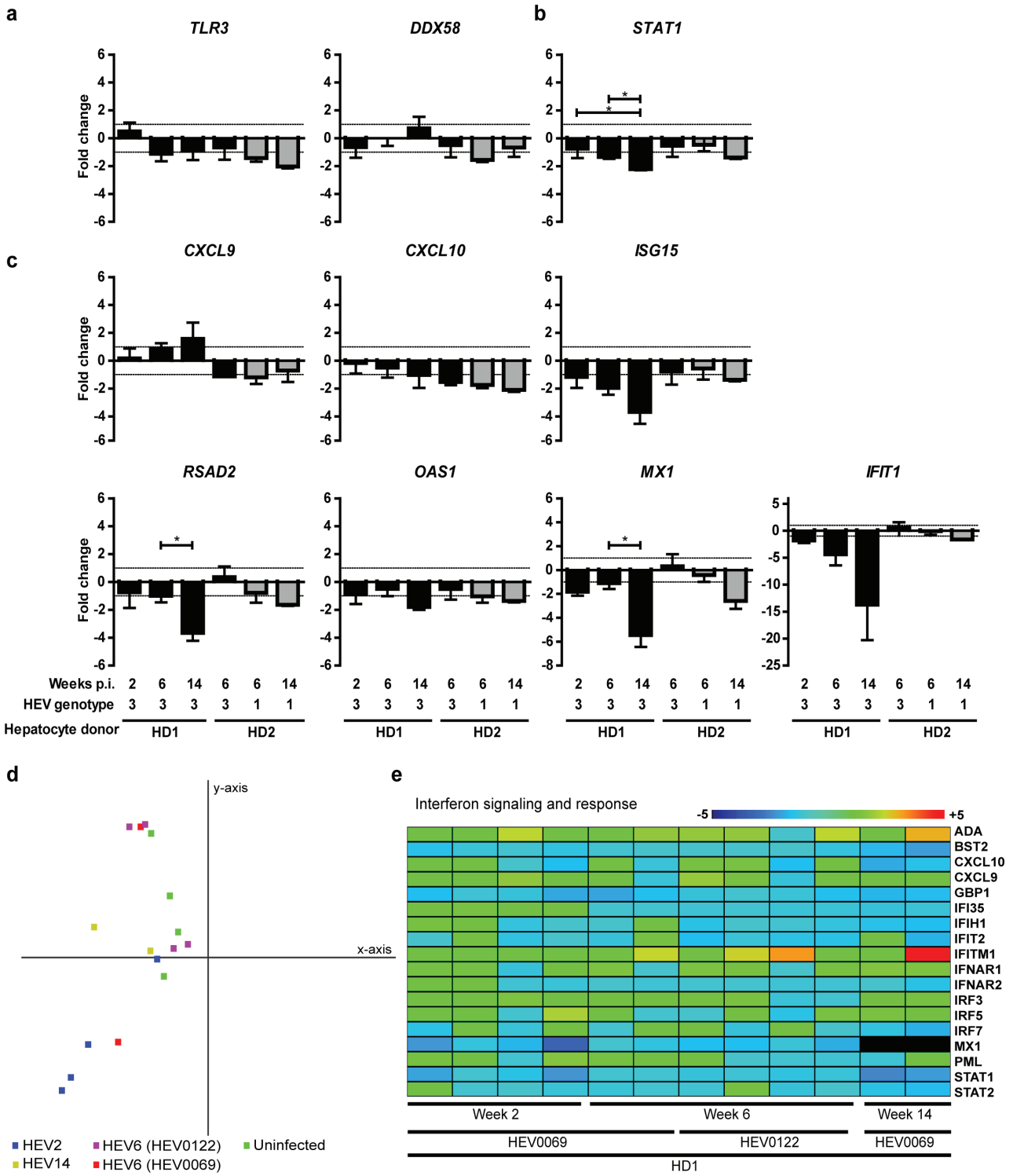

Figure 2. Minimal intrahepatic interferon-stimulated gene induction in HEV infected human-liver chimeric mice, between weeks 2 to 14 post infection. Whole chimeric-liver RNA was isolated from HEV gt3 and gt1 infected mice and analyzed for the human specific gene expression of sensing molecules TLR3 and DDX58 (a), transcription factor STAT1 (b), and interferon stimulated genes CXCL9, CXCL10, ISG15, RSAD2, OAS1, MX1 and IFIT1 (c) using qRT-PCR. Groups consist of n= 4, 6, 4, 3, 6 and 4 mice from left to right (a-c). Given values on y-axes are fold changes over HEV RNA negative chimeric-livers transplanted with the same hepatocyte donor. X-axes shows weeks post infection, HEV genotype, and hepatocyte donor. Significance was assessed within groups of the same hepatocyte donor using Krukskal-Wallis one-way Anova with Dunnett's Multiple comparison test. *, $P < 0.05$, Gray bars indicate HEV gt1, black bars HEV gt3 (a-c). In-depth human gene expression analysis was performed on RNA from chimeric mouse livers before infection, and after 2, 6 and 14 weeks of HEV gt3 infection using nCounter® Human Immunology V2 panel. Principal component 1 (x-axis) and 2 (y-axis) comprise 49% of the variance between samples using all non-cross reactive genes (d). Uninfected samples are indicated in green, infected samples are indicated in blue, red (HEV0069), purple (HEV0122) and yellow and by the number of weeks infected HEV2, HEV6, HEV6, HEV14, respectively (d). Heatmap shows fold change over average of 4 uninfected mice for interferon signaling and response genes (e). Gene legend is indicated on the right side and sample legend below the heatmap (e). Dark red indicates ≥ 5 fold change, and dark blue ≤ 5 fold change (e).

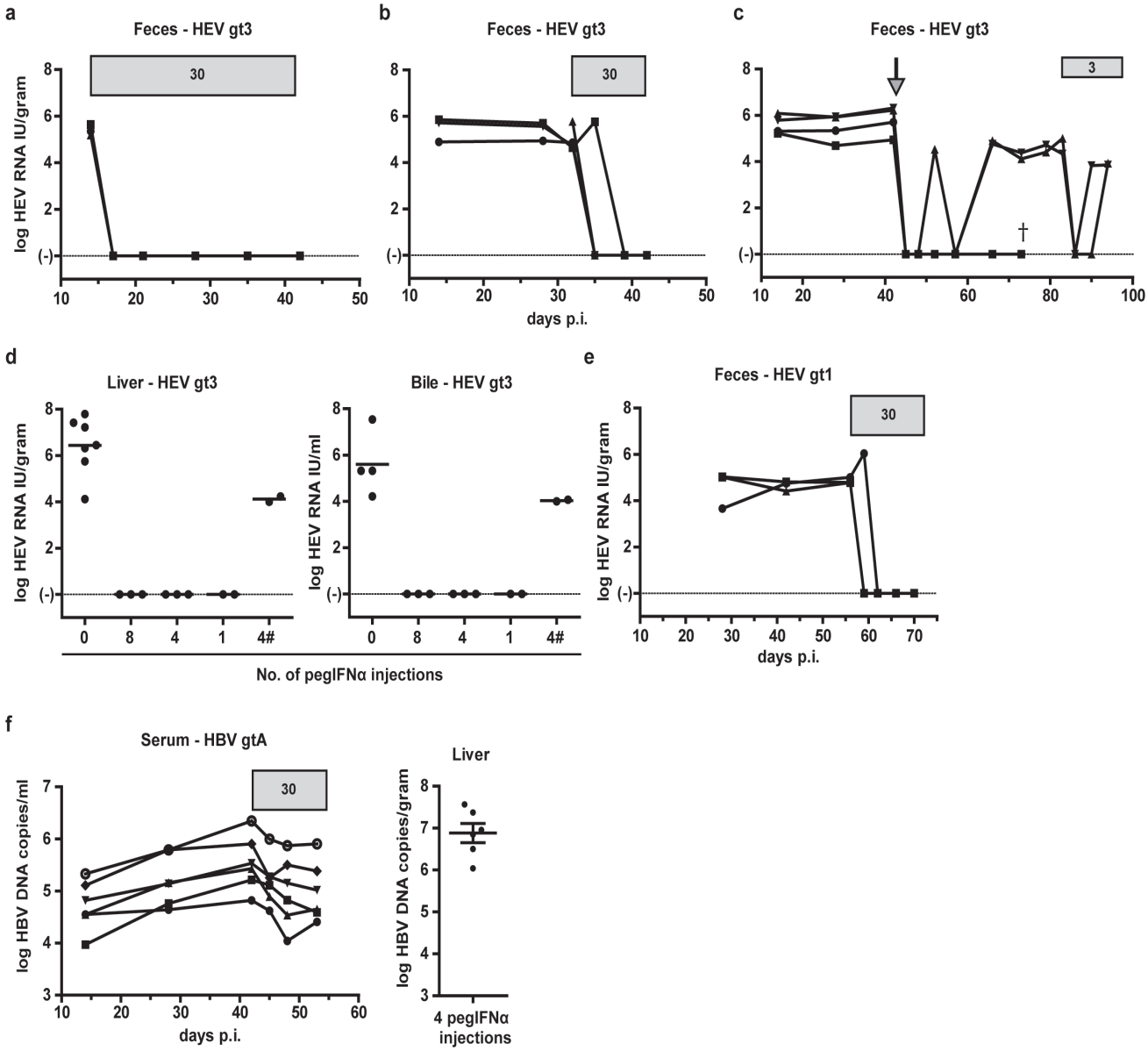

Figure 3. HEV is more sensitive than HBV to pegIFNα treatment in human-liver chimeric mice. HEV RNA was measured by qRT-PCR in feces of human-liver chimeric mice infected with HEV gt3 or HEV gt1 before and during 4 weeks (a, n=3), 2 weeks (b, n=4; e, n=3). and single (c, n=4) pegIFNα treatment. Horizontal gray bars indicate pegIFNα treatment duration and dosage in µg/kg (a, b). Arrow indicates time point of the single 30 µg/kg pegIFNα injection (c). One day after last dosage mice were sacrificed and viral load was determined in liver and bile (d). Non-treated infected mice were added as control (d). X-axes indicates number of pegIFNα injections (d). HBV DNA was measured in serum of HBV gtA infected human-liver chimeric mice before and during pegIFNα treatment, and one day after last treatment mice were euthanized and intrahepatic HBV DNA was measured (f, n=6). # indicates 3 µg/kg pegIFNα dosages. All mice were transplanted with the same hepatocyte donor (HD2, a-f). Y-axes indicate log HEV RNA IU/gram (a-c, d left panel, e), log HEV RNA IU/ml (d right panel), and log HBV DNA copies/ml (f). X-axes indicate days post infection (a-c, e-f).

gt3 infected mice (59 ± 10 and 108 ± 14 pg/ml, respectively, Fig. 4b). Interestingly, intrahepatic CXCL10 expression levels remained elevated (3.4-fold compared to HEV-infected non-treated mice) 4 weeks after a single pegIFNα dose in the two mice that cleared HEV. Similar to previous reports, HBV persistence in vivo was not due to absence of an ISG response, as IFIT1, ISG15, MX1, STAT1, and CXCL10 all were strongly induced (Fig. 4a and data not shown) (221). Overall, HEV but not HBV was found to be sensitive to pegIFNα induced hepatocyte-specific innate responses in vivo.

Discussion

Despite increasing reports on acute and chronic Hepatitis E Virus infections in Europe, antiviral treatment options are limited and immunological determinants of viral persistence remain largely unexplored (199). Here we aimed to study baseline and therapeutically induced innate immune responses in a recently established humanized mouse model for chronic HEV infection. We demonstrate that (1) HEV is highly sensitive to pegIFNα treatment in vivo; (2) HEV infection in human hepatocytes doesn't elicit an innate immune response; (3) HEV gt1 presents higher

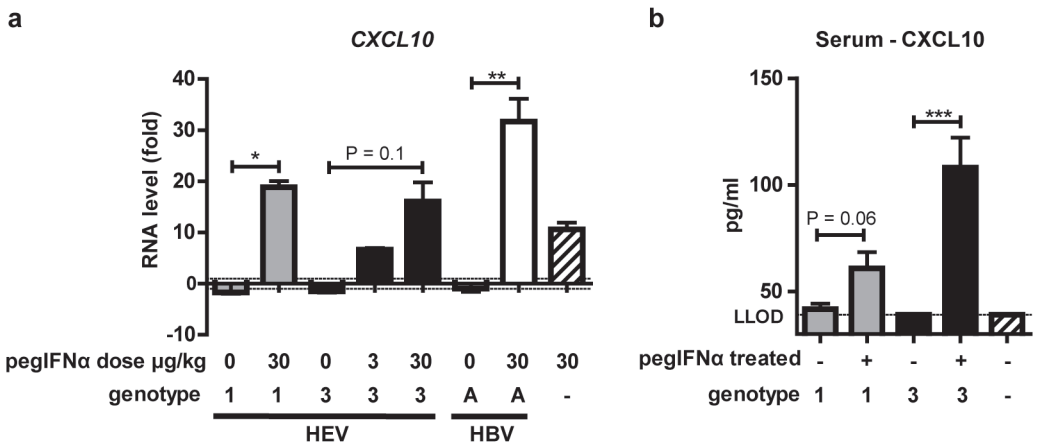

Figure 4. CXCL10 transcripts and protein are induced after pegIFNα treatment in HEV infected mice. RNA was isolated from non-treated and 2 weeks pegIFNα treated HEV gt1, gt3 and HBV infected mouse livers and was analyzed for the expression of human CXCL10 (a). X-axes indicate treatment dosage and virus genotype (a). Given values on y-axes are RNA levels in fold changes over uninfected non-treated mice (a). Human CXCL10 levels were measured using ELISA in mouse serum of uninfected, HEV-infected and HEV-infected pegIFNα treated mice (b). Dotted line indicates lower limit of detection (LLOD) (b). Gray bars indicate HEV gt1, black bars HEV gt3 and striped bar uninfected (a+b).

viral loads compared to HEV gt3.

HEV gt1 and gt3, but not HBV, showed to be highly sensitive to pegIFNα treatment in immune deficient human liver chimeric uPA+/+NOG mice. Viral clearance in feces, liver and bile was achieved after 4 and 2 weeks treatment and even after a single pegIFNα injection in 2/4 mice. PegIFNα associated viral clearance was accompanied by an increase of intrahepatic human ISGs and serum CXCL10 levels. In line with our data (Fig. 3f), the antiviral potency of pegIFNα against other hepatotropic viruses was less pronounced in similar humanized mouse models. PegIFNα reduced HBV viremia by 2.5 log IU/ml and HCV loads with 2.3 log IU/ml after 12 and 4 weeks of treatment respectively, without clearing the infection (221-223). Successful IFNα treatment in immunocompetent woodchucks chronically infected with woodchuck hepatitis virus (a model for chronic HBV infection), is associated with an intrahepatic IFN-γ and NK/T cell gene signature, but not an ISG signature (224). All together this suggests that pegIFNα has a strong direct anti-viral effect against HEV, whereas HBV and HCV require the immune system to achieve viral clearance or complete suppression.

Ongoing HEV gt1 or gt3 replication did not elicit human-innate immune responses in humanized livers of 30 uPA+/+NOG mice, irrespective of the infection duration, the human hepatocyte donor or viral isolate used. We specifically addressed the genomic response of human hepatocytes to HEV without that of infiltrating immune cells in our profound immune deficient uPA+/+NOG mice. In addition, we carefully eliminated cross hybridizing probes by including non-chimeric mice. After prolonged HEV gt3 infection for more than 3 months, significantly lower expression levels of STAT1, RSAD2 and MX1 compared to uninfected controls were observed, suggesting possible viral interference with the host's cell innate immune signaling. Hepatotropic pathogens have developed different methods to evade innate immune defenses (225). In our model, expression of TLR3 and DDX58 was detected in all HEV-infected chimeric livers indicating that these host sensing molecules were not counteracted at the transcription level (Fig. 2a). Several studies in HEK293T, A549 and Huh7 cells have suggested that HEV can directly interfere with phosphorylation of STAT1 and the induction of IFNα (206, 207, 226). However, most of these studies use non-physiological HEV-infection models or are influenced by defects in the innate signaling of target cells (208). Our findings indicate possible HEV mediated innate immune inhibitory effects in primary human hepatocytes. Further studies in differentiated human hepatocytes are required to determine how HEV is able to prevent immune sensing or disrupt innate signaling and how this influences viral fitness.

In contrast to our findings, one recent study infected a similar, but less profound immunodeficient uPA-SCID mouse model with the same HEV gt1 strain (Sar-55) and showed elevated ISG expression in 2 HEV-infected mice compared to one control animal (213). While the impact of the hepatocyte donor type on expression levels cannot be disregarded as shown here (Suppl. Fig. 1), remnant mouse natural killer cell and Kupffer cell activity in the SCID compared to the NOG background might have contributed to the observed differences (227, 228). The role of infiltrating innate immune cells in the liver during HEV-clearance was recently shown in the chimpanzee model (229). In HEV-infected chimpanzees the intrahepatic expression levels of BST2 (present in monocytes, macrophages and dendritic cells) and not those of the adaptive immune system, corresponded with the expression kinetics of several ISG's, including CXCL10, ISG15 and OAS1 (229, 230).

An important finding of our study was that during both HEV gt1 and gt3 infections, no innate immune responses were induced despite higher HEV gt1 viral loads in mouse feces, bile and liver. These observations point to an intrinsic phenotypical difference of the distinct HEV genotypes, but cannot explain the different immune pathogenesis seen in patients, who have a strikingly different clinical presentation. Not only is disease severity higher in HEV gt1 infections, but also chronicity rates for HEV gt1 are found to be low or even zero. Possibly, different amounts of viral antigens or epitopes, could induce different magnitudes of natural killer cell or HEV-specific T cell responses resulting in respectively more clinical disease or less chronic infections for the different genotypes (231, 232).

The clinical experience with pegIFN based therapies for chronic HEV is minimal. Eight cases have been published of which 5 showed a suppression of viremia at the first measured timepoint after initiation of pegIFNα treatment. PegIFNα treatment in HEV infected humanized mice modelled the viral decline seen in these 5 patients. It remains however unclear why some chronic HEV patients show slow viral declines upon IFN-treatment. We observed a viral relapse in feces, liver and bile of 2 humanized

mice after a second pegIFNα treatment course (Fig 3c+d). While animals received a 10-fold lower pegIFNα dose, the relapse might be partially ascribed to elevated intrahepatic ISG levels before retreatment. Increased CXCL10 levels were measured in the liver of 2 mice 4 weeks after a single pegIFNα injection, which corresponds to the timepoint at which retreatment was given to the remainder mice of that group. Since in chronic HCV patients the virologic response to pegIFNα is associated with low baseline ISG expression levels (44), it would be interesting to examine whether this holds true for chronic HEV patients as well.
In conclusion, despite higher viral loads for HEV gt1 in human-liver chimeric mice, both HEV gt1 and gt3 do not induce an intrahepatic innate immune response. HEV, but not HBV, is highly sensitive to pegIFNα treatment in humanized mice.

Acknowledgements
We would like to thank Vincent Vaes and Vincent Duiverman for their assistance in performing biotechnical manipulations, and Jolanda Voermans and Claudia Mulders for excellent technical assistance.

Supplemental information

Supplemental figures 1-4

Supporting Table is available on request
Supplemental Table 1. Relative RNA counts of HEV RNA negative and HEV RNA positive human-chimeric mouse livers

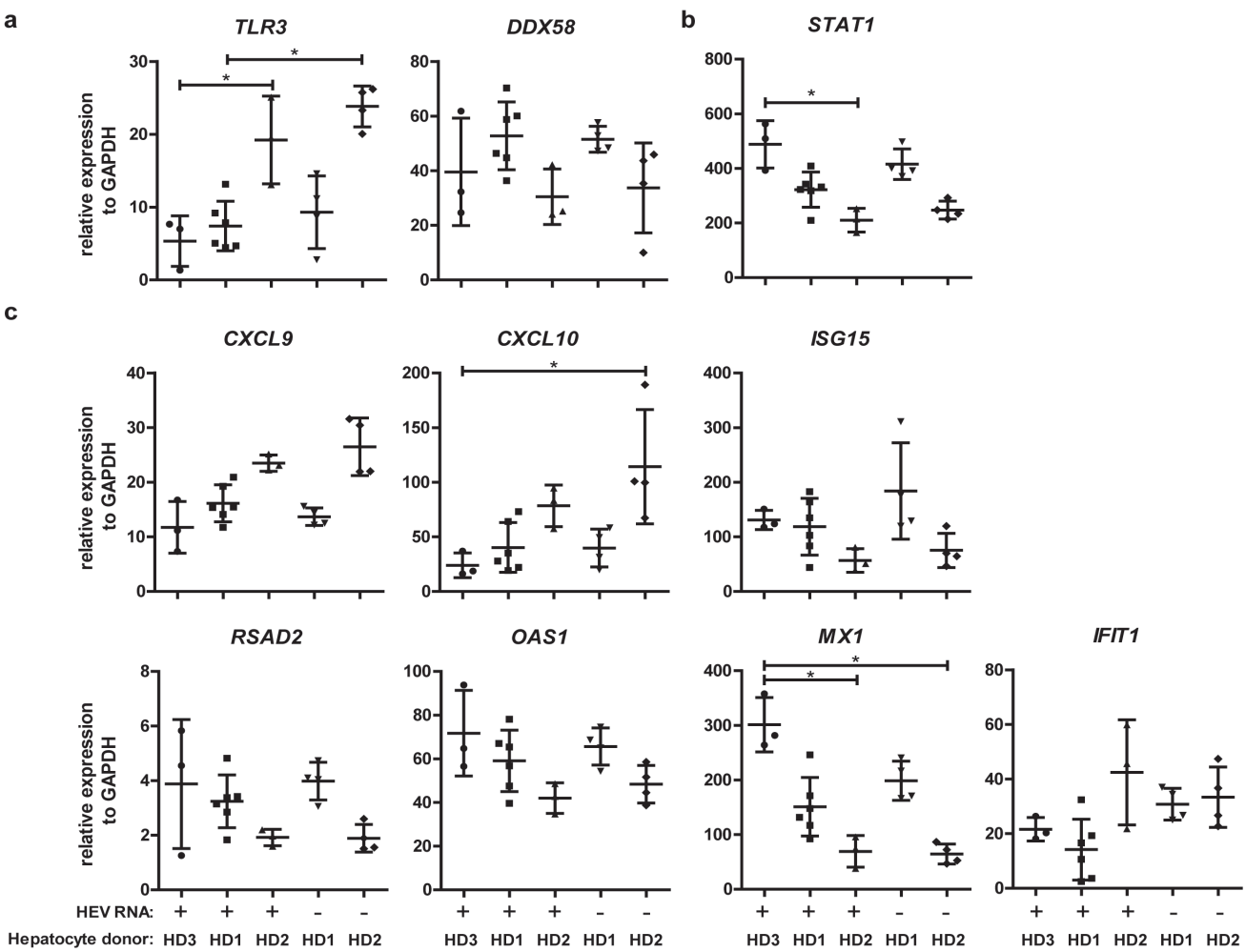

Supplemental figure 1. Hepatocytes donor is an important variable in the baseline gene expression profile. UPA+/+NOG mice were transplanted with hepatocytes from one of three available donors (HD1, HD2, or HD3). Whole liver RNA was isolated from HEV infected and uninfected chimeric-mice (HEV RNA+ or – below X axis), and was analyzed for human specific gene expression of sensing molecules TLR3 and DDX58 (a), transcription factor STAT1 (b), and interferon stimulated genes CXCL9, CXCL10, ISG15, RSAD2, OAS1, MX1 and IFIT1 (c) using qRT-PCR. Given values on y-axes are relative expression to GAPDH. X-axes shows HEV RNA presence and hepatocyte donor (a-c). Significance was assessed between all samples using Krukskal-Wallis one-way Anova with Dunnett's Multiple comparison test. * $P < 0.05$

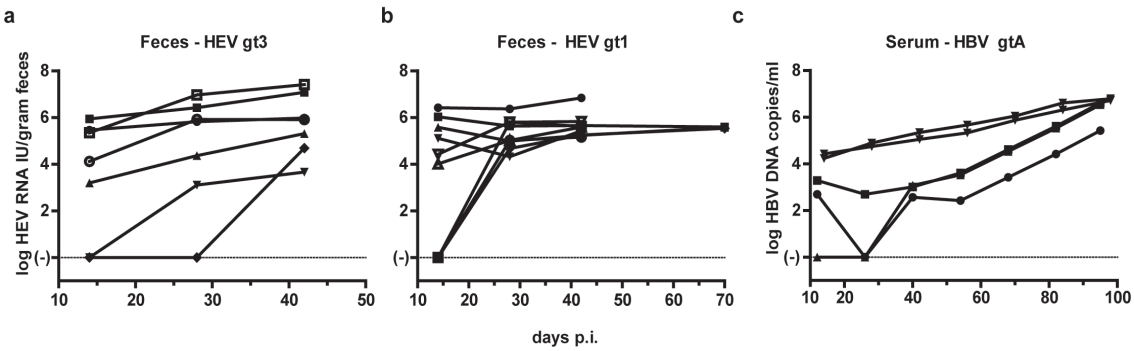

Supplemental figure 2. No drop in HEV RNA or viral clearance in gt1 or gt3 HEV, and HBV infected mice without pegIFNα treatment. HEV RNA was measured in feces of HEV gt3 (a, n=7) and HEV gt1 (b, n=9) inoculated mice. HBV DNA was measured in serum of mice challenged with HBV gtA (c, n=5). X-axes indicate days post infection until euthanasia (a-c). Y-axes indicated log HEV RNA IU/gram feces (a-b) or log HBV DNA copies/ml (c).

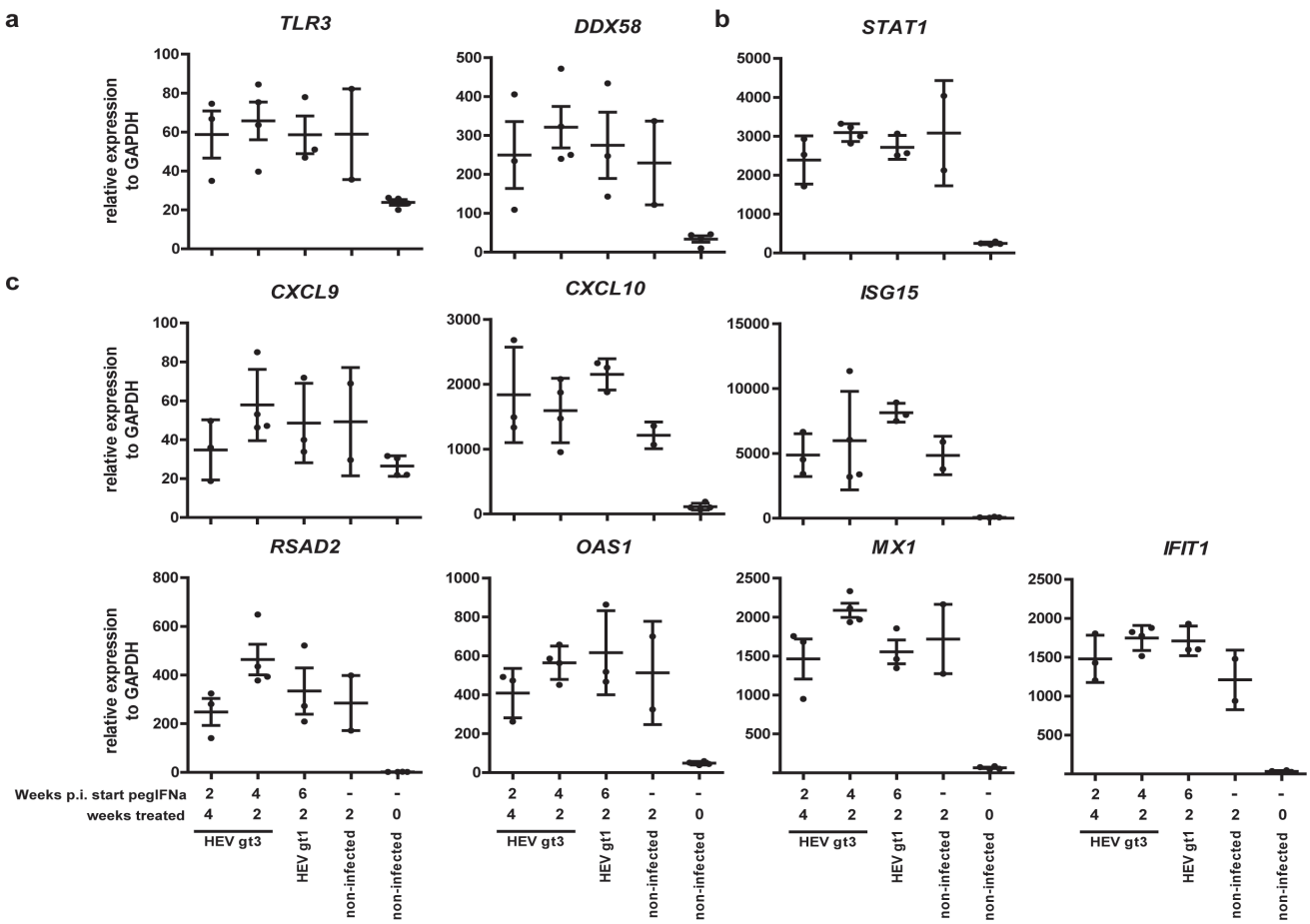

Supplemental figure 3. Genes related to interferon signaling and response are strongly upregulated after pegIFNα treatment in human-liver chimeric mice. Whole liver RNA was isolated from non-infected (n=4), non-infected treated (n=2), and HEV gt3 (n=7) and gt1 (n=4) infected pegIFNα treated chimeric mice, and was analyzed for human specific gene expression of sensing molecules TLR3 and DDX58 (a), transcription factor STAT1 (b), and interferon stimulated genes CXCL9, CXCL10, ISG15, RSAD2, OAS1, MX1 and IFIT1 (c) using qRT-PCR. Given values on y-axes are relative expression to GAPDH. X-axes shows virus used for infection, time after infection at which treatment was started, and the duration of treatment in weeks (a-c).

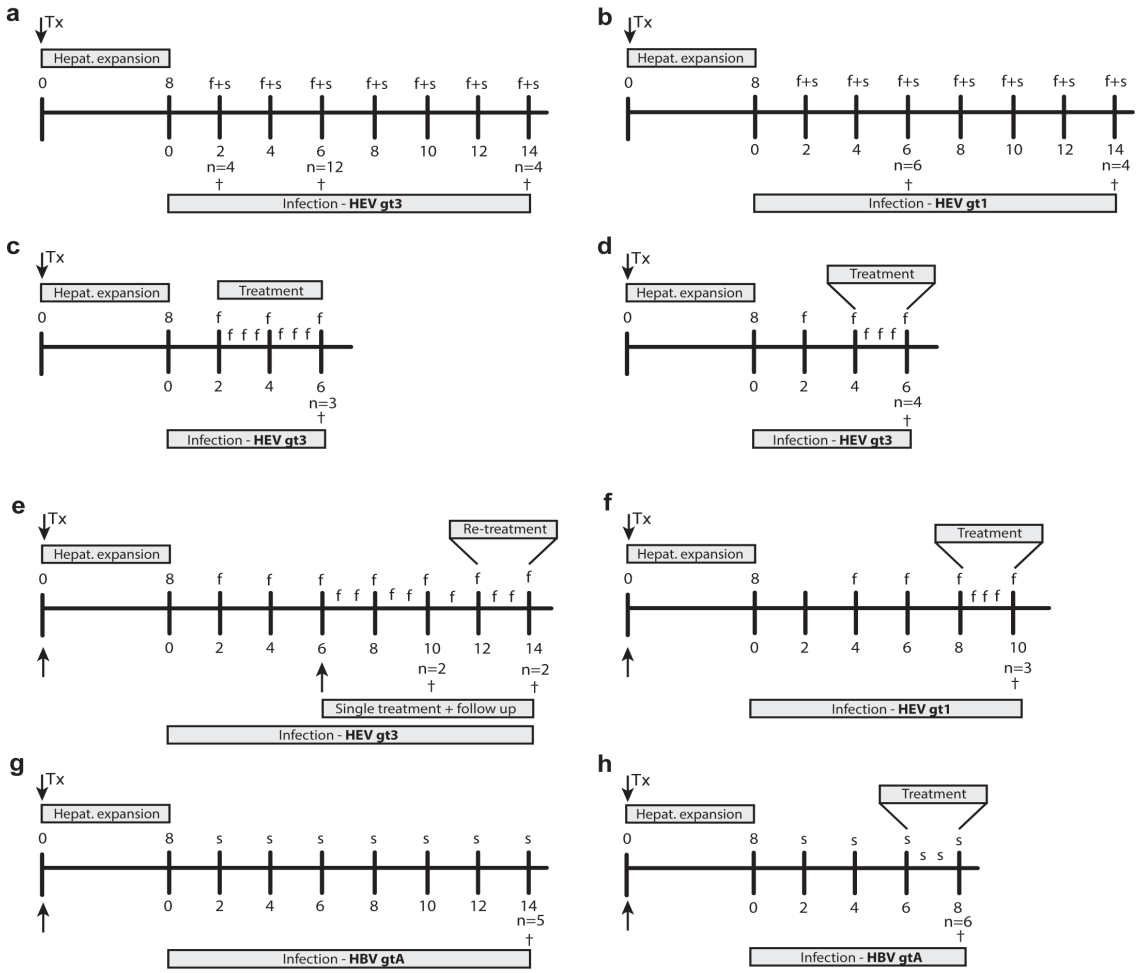

Supplemental figure 4. Overview of experimental groups of untreated and pegIFNα-treated infected mice. HEV gt3 infection experiment is illustrated and described in figure 1a-d, figure 2a-e and supplemental figures 1+2 (a). HEV gt3 treatment experiments are illustrated and described in figures 3a-d, figure 4a+b, and supplemental figure 3 (b-d). HEV gt1 infection experiment is illustrated and described in figure 1a-d, figure 2a, and supplemental figure 2 (e). HEV gt1 treatment experiment is illustrated and described in figure 3e, figure 4a+b, and supplemental figure 3 (f). HBV gtA infection experiment is illustrated and described in figure 4a, and supplemental figure 2 (g). HBV gtA treatment experiment is illustrated and described in figure 3f, and figure 4a (h). 'Tx' indicates human hepatocytes transplantation, 'f' indicates feces collection (a-f), 's' indicates serum collection (a-b, g-h). † indicates time of euthanization at which serum, feces, bile and liver were collected for HEV quantification, qPCR analysis, Nanostring analysis or serum hAlbumin/cytokine quantification (a-h). Arrow below X-axes indicates single pegIFNα treatment dosage (d). Numbers above X-axes refer to weeks after human hepatocyte transplantation (transplantation time=0). Numbers below X-axes refer to weeks after HEV or HBV inoculation (inoculation time =0).

Chapter 7

General discussion and future perspectives

Discussion

Liver-residing leukocytes are essential in determining the outcome of infection with hepatitis viruses. In hepatitis patients, liver leukocytes are mainly studied during chronic infection using core needle biopsies or the less invasive fine needle aspiration biopsy (233-235). Despite successful studies of liver innate immune cells during chronic infection, these studies are hampered by the lack of baseline samples and unknown variable time point of infection. Furthermore, it is very difficult to obtain these samples during initial acute phase of infection in which these cells play a very important role. In addition, number of cells isolated is low allowing phenotypical studies, but functional studies are more restricted. Therefore, animal models are essential to study of innate immune responses in viral hepatitis.

The restricted host range of the hepatitis viruses has hampered the development of suitable animal models for years. The development of human-liver chimeric mouse models was a big leap forward in the study of human hepatitis C virus (HCV), hepatitis B virus (HBV), and hepatitis D virus (HDV) infections. Models to study chronic hepatitis E virus (HEV) were not available, therefore in this thesis we established the use of humanized mice as attractive model to study this emerging virus. In the same year, different labs have shown the use of comparable animal models, which indicates the urgent need for models to study this virus. Using this in vivo model for the study of HEV, we have shown that direct interaction of the virus with the primary human hepatocyte does not induce an intracellular innate immune response. This indicates that the virus is either not sensed by the host cell or that the virus has evasive measures in place to prevent immune activation. Treatment of chronically HEV-infected mice with pegylated interferon-alpha (pegIFNα), a drug that activates the intracellular immune response, showed to be very potent and was able to clear the virus after 1-4 dosages. These results suggest that HEV is very sensitive to the pegIFNα-induced intracellular immunity. The use of pegIFNα to treat these mice may pave the way for further study of pegIFNα treatment in specific groups of chronic HEV patients.

The immune-deficient background of these humanized mice precludes studies focusing on the immune pathogenesis. Therefore, in this thesis we used an immunocompetent surrogate model for the study of innate cellular immunity in viral hepatitis based on lymphocytic choriomeningitis virus (LCMV) infection in C57BL/6 mice. The role of Kupffer cell (KCs) and monocytes during early and chronic liver inflammation is not well understood. Difficulty in studying these cells arises with their high plasticity and their strong phenotypical resemblance to each other. Using the LCMV- infected mice, we were able to perform transcriptome analyses on cell-sorted KCs and liver monocytes before, during and after chronic LCMV-induced hepatitis. Despite the strong resemblance between both cell types, our data nicely illustrate that both KC and monocytes remain distinct cell types at all stages of infection. Our study strongly points to distinct roles for KC and monocytes during viral hepatitis.

Cellular immunity

KCs are cells with high plasticity and can exert diverse functions depending on their environment. The main function of KCs is to screen the blood flowing through the liver as part of the immune surveillance. In a steady state condition, liver immune cells are

mainly exposed to microbial products derived from the intestine. Despite possible binding of microbial antigens to surface TLRs in the liver these cells do not initiate a full-blown immune response. Regulatory cytokines such as interleukin (IL)10 and transforming growth factor (TGF)-β, have shown to be essential in maintaining the balance between inflammation and tolerance. During viral infection of the liver, intrahepatic immune cells should get activated to prevent viral spread and initiate adaptive immune responses to eventually clear the infection. Limited information is available on the orchestration of the intrahepatic immunity, the phenotype, and function of liver immune cells during viral infection. We studied the KCs during the early phases of LCMV infection in chapter 2 and during the chronic phase of infection in chapter 3.

In steady-state condition KCs act as specialized phagocytes with only marginal cytokine production ex vivo (125), and are among the first to stain positive for the LCMV nucleoprotein thereby limiting viral spread (77, 83, 102). Therefore, KCs likely play a role in shaping the immune response, and thereby affect the outcome of a viral infection in the liver. Indeed, we showed that within 24 hours after infection KCs produce various inflammatory cytokines (TNF, IL6, MCP-1, CXCL10, RANTES), interferon-beta, and regulatory cytokine IL10. Interestingly, KC showed no or minimal inflammatory cytokine production 24 hours after exposure to LPS, indicating disruption of the steady state 'tolerance' balance upon viral infection but not after high dose bacterial products.

Regulatory cytokines, such as IL10, are able to dampen inflammatory responses. The production of IL10 by KCs during viral infection might indicate that KCs remain instigators of tolerance in the liver. Furthermore, KCs largely maintained their filtering function, as indicated by the uptake of dextran ex vivo after infection. Next to maintaining their phagocytic functions, KCs also showed stable or upregulated expression of complement genes and surface receptors (FcyR1, F4/80, and Marco). Overall, these data show that within 24 hours of infection KCs are able to initiate an inflammatory response but in essence these cells try to maintain their steady state functions. Possibly, KCs are 'allowed' to largely maintain their steady state function due to the vast recruitment of inflammatory monocytes to the liver upon viral infection.

Monocytes are one of the first cells to respond and infiltrate inflamed tissue. Within the first day after LCMV infection we already observed a vast influx of these monocytes into the liver. In the inflamed tissue, monocytes can either be regulatory or exert inflammatory responses. Monocytes showed a strong plasticity dependent on the nature of the inflammatory signal, either viral or sterile. In contrast to KC, liver monocytes completely lost their ability to take up dextran during LCMV infection, but increased dextran uptake after LPS challenge. Furthermore, monocytes sorted from LCMV-infected liver showed strong transcript induciton of inflammatory cytokines (*Tnf, Il6, Mcp1, Cxcl10* and *Rantes*), but not *Il10* as KCs did. Our data support the pro-inflammatory role of recruited monocytes in the setting of early virus-induced liver disease.

The distinctive roles of intrahepatic monocytes and KC are also present during chronic virus-induced hepatitis. During chronic infection, monocytes were still activated and transcribed *Tnf*, but the complete gene expression profile did not reveal clear functional specializations for these cells. We found elevated serum IL10 levels during chronic LCMV infection and an exclusive transcription of *Il10* in sorted KC and not monocytes suggesting a cell-specific regulation of immune responses. Similarly, in HBV patients the anti-inflammatory IL10 in serum has also been shown to be elevated and may play a role in the decreased cytokine production by monocytes (140, 155, 156). This suggests that their function might be tightly regulated between a pro- or non-inflammatory state. Further insight will require a selective depletion of either KC or monocytes during or before LCMV, without disturbing the entire mononuclear phagocyte system. Until recently, it was impossible to selectively deplete only one population of tissue-resident macrophages, without disturbing the entire mononuclear phagocyte system. Current depletion methods target all immune cells (e.g. irradiation), all phagocytic cells (e.g. clodronate liposomes), or require specific markers expressed on cell surface (e.g. CD11b-DTR mice) (236-238). The latter has proven to be challenging due to large overlap in surface proteins between cells of the myeloid lineage (239). The identification of Clec4f as KC-specific gene enabled the development of a KC-Knock out mouse, which poses an interesting mouse model to study the innate cellular immune response in the absence of KC during early and chronic LCMV infection (157).

Intracellular immunity

Innate and adaptive cellular immunity are required to clear viral pathogens from an organism. However, the first line of defense is set in the target host cell of the virus. Each cell is equipped with sensors, which are able to recognize foreign molecules, the so -called pattern recognition receptors (PRR). Upon recognition of viral molecules, these receptors can initiate intracellular immunity to counteract the virus. Previous research has shown that these defense mechanisms are not well activated in hepatocytes upon infection with HBV, which is therefore regarded as a 'stealth' virus (240). In contrast, HCV infection in hepatocytes does elicit a strong defense response (241, 242). However, despite the host cell's innate immune response, most individuals do not clear the infection and become chronically infected. The current knowledge on HEV infection in host cells is limited to in vitro cell lines. In chapter 6, we investigated the interaction of HEV with primary human hepatocytes in infected human-liver chimeric mice. We did not detect any upregulation of genes related to the intracellular immunity during chronic HEV genotype (gt) 3 and gt1 infection, despite the presence of PRRs. Whether HEV is not sensed by the host cell or if viral counteractive mechanisms prevent immune activation is not known. In vitro studies have suggested that HEV is able to counteract the downstream signaling of the PRRs. To confirm the in vitro findings, the humanized mouse model may contribute to unravel HEV's counteractive mechanisms in primary human hepatocytes. Understanding the interaction of HEV with the host cells is crucial in understanding current pathology and the development of possible intervention strategies.

Cellular Immunity against HEV

Despite the fact that HEV does not induce intracellular innate immune responses, most HEV infected individuals clear the virus. The cellular immunity against HEV has been suggested to play a major role in HEV clearance. It has been shown that strong and multi HEV-specific CD4+ and CD8+ T cell responses are present in seropositive patients, but not in chronic HEV solid organ transplant (SOT) patients (231). In addition, in HEV gt1 patients with acute liver failure a massive influx of cytotoxic CD8+ T cells has been observed (243). Exposure to HEV also induces the development of a humoral response, which may contribute to the clearance of the infection. Cynomolgus monkeys showed no or less signs of HEV gt1 (Sar-55) infection after passive or active immunization, indicating a virus-neutralizing role for anti-HEV antibodies (244). The human-liver chimeric mouse model may be an interesting

model to test whether passive immunization or pre-incubation of viral stock with anti-HEV gt3 antibodies can block infection in these mice. In addition, T cell transfers into humanized mice can help us to further elucidate the role of epitope-specific CD4+ and CD8+ anti-HEV T cells.

As discussed above, innate immune cell responses are a determining factor for good adaptive immune responses. The roles of innate immune cells in HEV infections are so far elusive. It would be interesting to determine whether KCs take up the virus, are able to orchestrate the initial inflammatory response, and recruit inflammatory monocytes to the liver during acute HEV infection. Moreover, the impact of immunosuppressing drugs on the function of these cells is subject for future study. In addition, intra-genotype comparison of innate immune cell function during HEV infection may unravel important differences in immunopathology. Preliminary studies on innate immune cells during HEV infection could be studied using liver biopsies. Using flow cytometric analysis, immune histochemical stainings or gene expression profiling, the role of these cells can be elucidated. The here applied mouse models are either not susceptible to HEV (C57BL/6) or lack immune cells (UPANOG). However, recent development allowed reconstitution of the mouse bone-marrow with human immune cells, followed by the engraftment of human hepatocytes to generate a human-liver chimeric mouse with a human immune system (HIS-HUHEP mice) (245). This model may enable the study of HEV gt1 and gt3 immune pathobiology.

HEV isolate infectivity differences

HEV gt3 infections are emerging in west European countries, including France, the United Kingdom and the Netherlands (26-28). While recent reports have shown HEV gt3 viremia among blood donors (246), Dutch national blood safety guidelines do not require nucleic acid testing of the donor pool (180). This is of concern for immune-compromised and SOT patients, who are prone to develop chronic infections, which may quickly progress to severe liver fibrosis. Interestingly, only a limited number of cases of transfusion-transmitted HEV have been reported despite administration of contaminated blood products (28, 178, 179, 199). In addition, a recent retrospective survey of United Kingdom's plasma pool, surprisingly showed that only half of HEV-viremic British blood donors infected their recipients (28). Determinants of HEV transmission rate are not well studied yet, but seemed to be dependent on the HEV RNA load and anti-HEV antibodies status in donor plasma.

We observed intrinsic HEV infectivity differences that were most apparent when plasma-, feces- and liver-HEV isolates from the same patient were examined: plasma-derived HEV demonstrated slower or no replication in vitro and in vivo, respectively (Chapter 3). The determining factor for these infectivity differences is not completely understood. In chapter 4 we showed limited genomic differences between HEV derived from plasma and feces of two chronic HEV patients, minimizing genomic alterations as the cause for the observed differences. Other studies described that HEV virions from plasma and feces differ in virion density, ascribed to the presence or absence of a lipid membrane content. This different buoyant density may influence in vivo infectivity, as has previously been shown for HCV (167). The detergent activity of bile acids could strip HEV virions of their lipid content upon passage towards the intestinal system, which may explain the observed difference between plasma and feces viruses (173). In addition, circulating inhibiting factors in blood, such as virus-specific antibodies, can also act as negative influencers of infectivity of virus preparations. However, for HEV it has not been proven yet that presence of anti-HEV antibodies reduces infectivity in vivo . In vitro studies have shown that HEV serum samples can still initiate efficient replication despite the presence of HEV antibodies (247). Ultimate proof of intrinsic infectivity differences of membranous or antibody-coated HEV particles will require delipidation and antibody depletion of plasma derived inocula. Nevertheless, we used only pre-seroconversion plasma samples in our in vivo infectivity assays, excluding any inhibitory effects of anti-HEV antibodies. Overall, the observation that human plasma-derived virus is less infectious in vivo may be relevant for the infectivity and epidemiology of HEV in humans. Future studies should aim at unravelling the determinants of infectivity for HEV.

The differences in clinical presentation between HEV gt1 and 3 are so far not understood. HEV gt1 infections in pregnant women occur in countries in south-east Asia, whereas HEV gt3 infections result in clinical disease mainly for immunocompromised patients, but not for pregnant women, in Europe. Possible intrinsic viral differences may play a role, such as the observed increased replication described in chapter 6. All mice inoculated with either high or low HEV gt1 or gt3 inocula, all animals became chronically infected. Irrespective of lower absolute inocula for HEV gt1 compared to gt3, higher viral loads were detected in feces, bile and liver of HEV gt1-inoculated animals. These results corroborate a higher intrinsic virulence of HEV gt1 compared to gt3. However, the molecular mechanisms associated with enhanced HEV gt1 replication remain to be determined.

Treatment of chronic HEV

Current antiviral treatment options for chronic HEV-infected immunocompromised patients are limited, and consist of two strategies. First, a reduction of immunosuppressive drugs is opted, and second, anti-viral treatment with either pegIFNα or ribavirin can be used. The latter are based on safety and efficacy treatment studies for chronic HCV infections, as no such study has been performed in chronic HEV patients. No universal definition for HEV treatment outcome exists, therefore the current sustained virological response (SVR) is considered as HEV RNA-negative PCR result in the period of follow-up after end of treatment (47).

Reducing the dose of immunosuppressive drugs in SOT patients has shown to result in HEV clearance in up to one third of the patients (3, 248). PegIFNα has been administered to eight patients, in doses comparable to HCV treatment regimens, and resulted in SVR in 75% of the patients treated (47, 48). Despite the treatment success, reduction of immunosuppressive drugs and the use of pegIFNα in kidney and heart transplant recipients are not preferred, due to concerns for acute graft rejection. Currently, the preferred treatment is the use of ribavirin (RBV) for these patients. Similar to pegIFNα treatment, SVR was achieved in 74% of the patients, despite any knowledge on optimal dose and treatment duration (47). RBV is quite well tolerated in most patients, however anaemia has been described as the main side effect. Patients suffering from RBV-induced anaemia require a dose reduction, administration of erythropoietin, or eventually need a blood transfusion (47). The precise mechanisms of RBV treatment are not completely understood and should be subject to further study, especially in the context of HEV. In addition, the emergence of HEV strains non-responding to RBV treatment has been described. The RBV-resistant strains have been linked to mutations in their polymerase gene (G1634R) (191, 249, 250).

Treatment possibilities for chronic HEV patients developing a RBV-resistant HEV strain are limited to the non-preferred reduction of immunosuppressive drugs or treatment with pegIFNα. In chapter 6 we investigated the effect of pegIFNα on HEV in humanized mice.

We showed that HEV, but not HBV, was highly sensitive to pegIFNα treatment, with viral clearance in feces, liver and bile after 4 and 2 weeks treatment and even after a single pegIFNα dose in 2/4 mice. PegIFNα-associated viral clearance was accompanied by an increase of intrahepatic human interferon-stimulated genes (ISGs) and serum CXCL10 levels. In line with our data, in similar chimeric mouse models, pegIFNα reduced HBV viremia and HCV loads after 12 and 4 weeks of treatment, respectively, without clearing the infection (62, 221, 223). All together, this suggests that pegIFNα has a strong direct anti-viral effect against HEV, whereas HBV and HCV require the immune system to achieve viral clearance or complete suppression. The comparative effectiveness of pegIFNα treatment for HEV, HBV and HCV infection in humanized mice, should incite further studies on the optimal antiviral pegIFNα dose and treatment duration without increased risk for rejection in SOT patients.

In chronic HCV patients, the virologic response to pegIFNα is associated with low baseline ISG expression levels. Whether this can also be used as prognostic marker for treatment success of pegIFNα for HEV remains to be determined. However, in chapter 6 we observed a viral relapse in feces, liver and bile of two humanized mice after a second pegIFNα treatment course. While animals received a 10-fold lower pegIFNα dose, the relapse might be partially ascribed to elevated intrahepatic ISG levels before retreatment. Increased CXCL10 levels were measured in the liver of 2 mice 4 weeks after a single pegIFNα injection, which corresponds to the time point at which retreatment was started for the remainder mice of that group. Interestingly, the cases described of chronic HEV patients treated with pegIFNα, showed a rapid viral response within 1 month in 5/8 patients (47). This indicates that chronic HEV patients may be categorized in rapid responders and non-responders. The determinants that distinguish rapid responders and non-responders to pegIFNα should carefully be examined.

The use of pegIFNα is not preferred in SOT patients due to concerns for acute graft rejection. Alternatively, other intracellular innate immune-activating compounds should be explored. Type III interferons (Interferon lambda (IFNλ)) have shown to induce antiviral genes similar to IFNα, but signals through a different receptor (251). The IFNλ receptor is less widely expressed and distributed compared to the IFNα receptor, implying that IFNλ may induce fewer side-effects such as off-target immune activation. Another treatment option could be the use of immune-stimulating compounds targeting the Toll-Like Receptors (TLR). The use of TLR agonist has been investigated to treat HBV and HIV infections in vitro and in vivo (252-254). In our mice, HEV was much more susceptible to pegIFNα-stimulated innate immune activation compared to HBV. Therefore, HEV may also be vulnerable to TLR agonist-induced immune responses. However, as discussed above, HEV might have counteractive mechanisms to prevent immune activation, which may block down-stream TLR signaling and thus prevent upregulation of anti-viral genes. These treatment options pose interesting alternatives to treat chronic HEV infections in SOT patients. However, future studies are required to determine the effectiveness, the possible side-effects, and the off-target immune activation.

Conclusions

The work described in this thesis contributes to our understanding of the cellular and intracellular innate immune responses in the liver. We have established the use of human-liver chimeric mice for the study of chronic HEV infection and used LCMV infection in C57BL/6 as immunocompetent model for viral hepatitis. Our LCMV data indicate that KC and liver monocytes should always be considered as separate cell populations that play distinct roles during viral infections. Humanized mice could be productively infected with HEV isolated from feces, but not from plasma. HEV gt3 genomically adapts to in vitro culture, but the in vivo selection pressure in immune-deficient hosts is minimal. HEV infection of human hepatocytes did not activate the intracellular innate immune responses, but activation of these responses via pegIFNα treatment resulted in quick clearance of the virus.

Future perspectives

The first documented outbreak of HEV was in 1955 in New Delhi, India. Since then, our knowledge on this virus has advanced, but is still limited. With the emergence of HEV gt3 in Europe more research has been performed on this virus including our work described in this thesis. However, with all the new knowledge generated, more questions arise and Europe's new Hepatitis problem is not solved yet. Future research on HEV should focus around several questions: 1) How can we prevent HEV infection? What are all the infectious sources of human HEV and how can we eliminate HEV from these sources? 2) How can we efficiently and safely treat chronic HEV gt3 SOT patients and acute pregnant HEV gt1 patients? 3) What viral epitopes are recognized by T and B cells after HEV infection, and are the responses evoked protective against other genotypes? 4) What are the intrinsic differences between HEV genotypes? Why do gt1 HEV infections result in acute liver failure (ALF) in pregnant women but gt3 HEV infections do not? 5) How does the complete immune system orchestrate a successful immune response against HEV and what are the determinants for chronicity in gt3 or ALF in gt1 infections? Next to studies in patients, our mouse models can contribute in future attempts to find answers to these questions. The LCMV infection model can contribute to our general understanding in immune pathobiology of chronic (liver) infections unravelling potential essential factors for the development of chronicity. The human-liver chimeric mouse is useful in infectivity studies, including the comparison of different HEV isolates (HEV gt4, gt2, or other animal HEV strains), testing the neutralization effect of anti-HEV polyclonal and monoclonal antibodies, and test the effect of delipidation on infectivity. Moreover, this model shows great potential for treatment studies including intracellular immune-activating drugs (IFNλ, TLR3 agonists), and may contribute as a model for testing new direct-acting antivirals. Furthermore, the anti-viral effect of adoptively transferred immune cells (e.g. HEV-specific T cells) can be studied. Lastly, the human-liver chimeric mouse will contribute to the ability to study the direct interaction of the virus with differentiated primary human hepatocytes and to in vivo efficacy studies of new direct acting antivirals.

Chapter 8

Summary

Liver-residing leukocytes are essential in determining the outcome of infection with hepatitis viruses. Patient studies of liver innate immune cells during chronic viral hepatitis have been performed but are hampered by, amongst others, a lack of baseline data and unknown time of infection. Therefore, animal models are essential for the study of the innate immune response in viral hepatitis. In the studies presented in this thesis, we aimed to better understand the cellular innate immune responses in the liver during lymphocytic choriomeningitis virus (LCMV) clone 13 induced chronic hepatitis, and to establish the human-liver chimeric mice as model for chronic Hepatitis E virus (HEV) infections in order to study the intracellular innate immune mechanisms upon HEV infection.

In chapter 2 and 3, we aimed to unravel how the cellular innate immune system deals with chronic viral infection in the liver using the LCMV infection mouse model. In chapter 2, we described that early after LCMV infection a functional dichotomy is observed for inflammatory monocytes and F4/80high-Kupffer cells with respect to endocytosis, but their activation and cytokine gene expression profiles exhibit a strong resemblance. In addition, inflammatory monocytes exhibit a huge capacity for recruitment to the liver and plasticity dependent on the nature of the inflammatory signal, either viral or sterile. This suggests that inflammatory monocytes play a crucial role in shaping the inflammatory environment in the liver early after infection. In chapter 3, we showed that LCMV induces chronic viral hepatitis with limited intrahepatic cytokine and interferon responses during the chronic infection. Furthermore, we identified KC and IM as distinct cell populations before, during, and after chronic infection, with important differences in activation status, antigen presentation, and gene expression profile correlating with the presence of viral antigens. Overall, these data suggest that intrahepatic monocytes and KC play distinctive roles during chronic virus-induced hepatitis, which is crucial knowledge in order to develop new antiviral strategies aimed at eradicating chronic viral infection.

In chapters 4, 5, and 6, we investigated Europe's new hepatitis threat. Increasing numbers of endemic infections with genotype (gt) 3 HEV are observed in European countries. Unfortunately, no adequate in vivo model system exists to mimic this disease course, which hampers studies on HEV infectivity, transmission, and antiviral drug development. Therefore, in chapter 4, we explored and showed that human-liver chimeric mice can model chronic HEV infections. Humanized mice could productively be infected with clinical fecal, but not plasma, samples from several chronic HEV patients. In chapter 5, we described that HEV gt3 genomically adapted to in vitro culture, but that in vivo selection pressure in immune-deficient hosts was minimal. In chapter 6, we compared infection of HEV gt1 and HEV gt3 in human liver chimeric mice, and examined the intracellular innate immune responses in human hepatocytes upon infection. Despite higher viral loads for HEV gt1 in human-liver chimeric mice, neither HEV gt1 nor gt3 induced an intrahepatic innate immune response. Interestingly, treatment of infected chimeric mice with intracellular innate immune activating drugs pegIFNα, showed rapid clearance of HEV. Overall, these data show that humanized mice could be productively infected with HEV isolated from feces, and that HEV does not induce intracellular innate immune responses in human hepatocytes, but is very sensitive to these immune mechanisms induced by pegIFNα.

Samenvatting

Afweercellen in de lever zijn essentieel om een hepatitis virus infectie onder controle te houden. Door beperkingen in patiëntenstudies kunnen de aangeboren niet-specifieke directe afweercellen in lever niet altijd even goed bestudeerd worden. Daarom zijn diermodellen essentieel in het bestuderen van de aangeboren directe immuunrespons in de lever tijdens een virale infectie. In de studies beschreven in dit proefschrift hebben wij de aangeboren directe afweercellen bestudeerd in de lever tijdens virale hepatitis door gebruik te maken van het Lymphocytic Choriomeningitis Virus (LCMV) infectie muismodel. Daarnaast hebben wij intracellulaire directe immuunmechanisme onderzocht in muizen met een chimeren humane lever geïnfecteerd met hepatitis E virussen (HEV). In hoofdstuk 2 en 3 van dit proefschrift hebben wij het LCMV infectiemodel gebruikt om in de lever de aangeboren niet-specifieke directe immuunrespons te onderzoeken tijdens infectie. In hoofdstuk 2 beschrijven we dat dat tijdens de initiële infectie er een functionele dichotomie bestaat tussen twee verschillende aangeboren afweercellen, de monocyten en Kupffer cellen. Desondanks vertonen beide cellen wel een vergelijkbaar activatie en cytokine genexpressieprofiel. Daarnaast, beschrijven wij dat de inflammatoire monocyten snel naar de lever gerekruteerd worden tijdens de initiële infectie, en dat deze cellen zich goed kunnen aanpassen aan verschillende ontstekingssignalen. Deze data suggereren een belangrijke rol voor de inflammatoire monocyten in het vormen van de ontstekingsreactie in de lever kort na infectie. In hoofdstuk 3 laten we zien dat LCMV infectie zorgt voor een duidelijke chronische virale leverontsteking, maar met beperkte cytokine en interferon activatie tijdens de chronische fase. Tevens laten wij zien dat Kupffer cellen en inflammatoire monocyten verschillende cellen zijn voor, tijdens, en na de chronische lever infectie. Beide cellen laten belangrijke verschillen zien in activatiestatus, antigeenpresentatie, en in het genexpressieprofiel dat correleert aan de aanwezigheid van het virus. Algeheel laten deze data zien dat Kupffer cellen en monocyten een verschillende rol spelen tijdens chronische virale hepatitis. Deze kennis is van belang om mogelijke nieuwe behandel strategieën te ontwikkelen die zich richten op het genezen van chronische virusinfecties.

In hoofdstukken 4, 5, en 6, hebben we onderzoek gedaan naar de nieuwe hepatitis dreiging van Europa. Laatste jaren zijn het aantal endemische infecties met genotype 3 HEV zijn gestegen in Europa. Helaas worden studies naar HEV besmettelijkheid, transmissie, en behandel methode beperkt door de afwezigheid van goede diermodellen die het ziekteverloop nabootsen. In hoofdstuk 4 beschrijven we ons onderzoek naar de mogelijkheid om een muis met een chimeren humane lever te gebruiken als model voor chronische HEV infecties. Deze gehumaniseerde muizen bleken vatbaar te zijn voor het virus uit feces, maar niet bloed, van chronische HEV patiënten. In hoofdstuk 5 laten wij zien dat het genotype 3 HEV zich genetisch aanpast aan celkweek condities, maar dat deze genetische aanpassingen beperkt blijven in de immuundeficiëntie gastheer. In hoofdstuk 6 vergelijken wij genotype 3 HEV en genotype 1 HEV infecties in de gehumaniseerde muis, tevens onderzoeken wij de directe afweermechanisme van de cel tijdens infectie. Ondanks het hoger aantal genotype 1 virussen in de gehumaniseerde muis, activeren beide virussen niet het directe afweermechanisme van de levercel tijdens chronische infectie. Echter genezen muizen snel van het virus wanneer we deze behandelden met een geneesmiddel (pegIFNα) dat deze immuunmechanisme aanzet. Algeheel laten deze studies zien dat het gehumaniseerde muismodel gebruikt kan worden voor onderzoek naar chronische HEV infecties met minimale genetische aanpassing van het virus. Daarnaast laten we zien dat pegIFNα behandeling het virus succesvol klaard in dit muismodel. Dit bied nieuwe inzichten voor de behandeling van chronische HEV patiënten.

Chapter 9

Appendix

Word of thanks

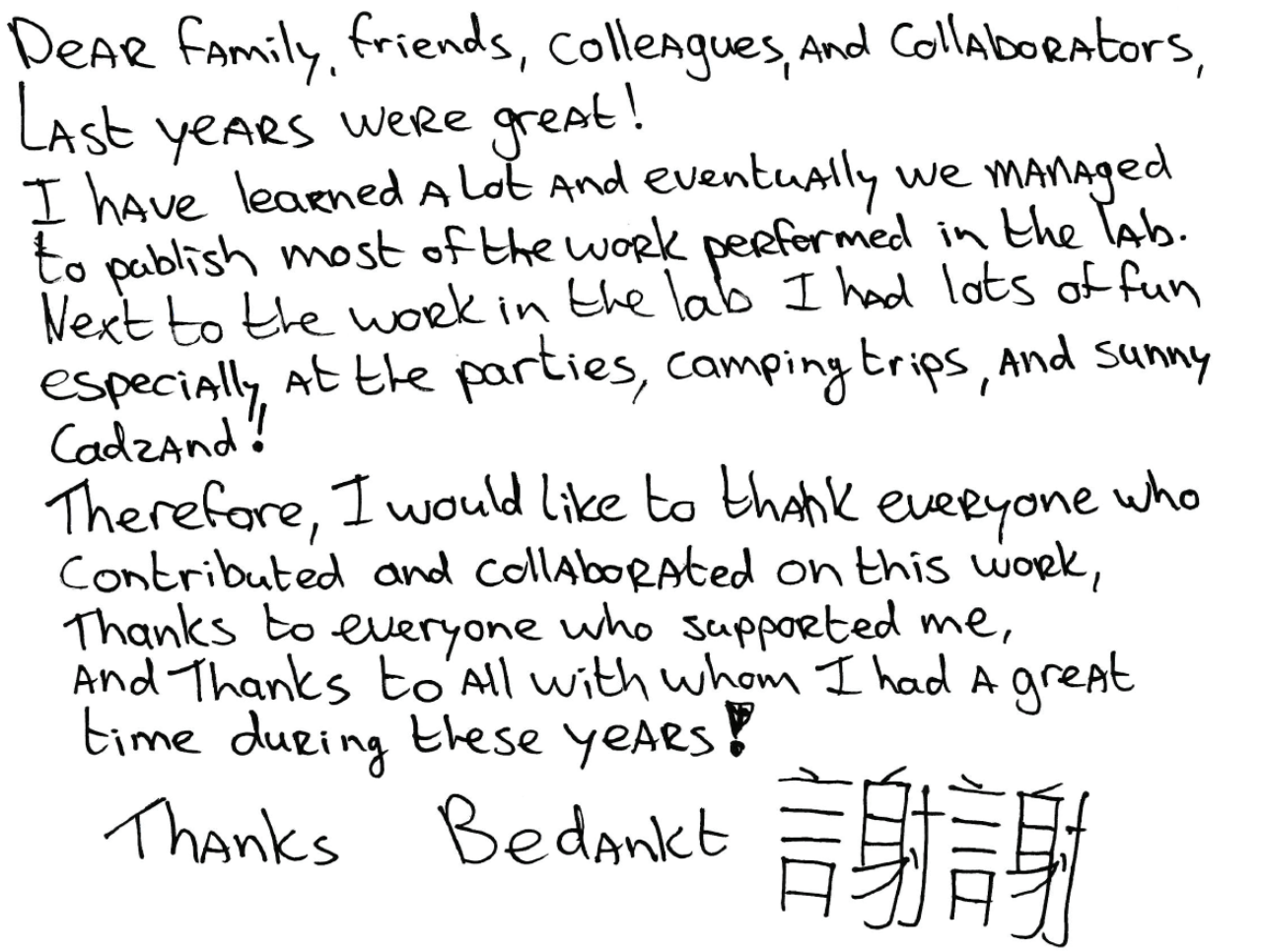

Curriculum Vitae

Martijn D.B. van de Garde was born in Rijen, Noord-Brabant, The Netherlands, on 28th of November 1985. In 2003 he graduated from high school obtaining his HAVO degree, with Nature and Technical profile including Informatics, at The Nassau in Breda. The same year he started his bachelor studies in Life Sciences and Chemistry at the University of Applied Sciences in Utrecht. He performed his bachelor internships at the Department of Medical Microbiology and Immunology of the Meander Medical Center in Amersfoort and at the National Institute for Public Health and the Environment. In 2007, he obtained his Bachelor of Applied Sciences degree in Life Sciences with specialization in Microbiology.

He started his Master studies in Biomedical Sciences at the VU University in Amsterdam in 2008 after a year working as a technician at the Department of Medical Microbiology and Immunology of the Meander Medical Center. During his master studies he performed both his research internships at the Academic Medical Center (AMC) in Amsterdam. The first research project was focused on optimizing a technique developed for the discovery of unknown viruses in the group of Dr. L. van der Hoek at the Department of Experimental Virology. He performed his second research project at the Department of Experimental Immunology with Dr. J. Hamann, where he investigated the expression of the GPR56 on different lymphocyte (sub)populations. After finishing his Master Thesis under supervision of Dr. M. Pegtel and Prof. Dr. J. Middeldorp, he obtained his Master degree in Biomedical Sciences with specialization in Immunology in 2011.

Before starting his PhD training he worked as a researcher in the AMC at the Department of Experimental Immunology for 1,5 year. During this time he investigated the effect of chronic exposure of glucocorticoids in Macrophages, which was published in journal of immunology. In February 2013, he started his PhD training at the department of Gastroenterology and Hepatology and was supervised by Dr. T. Vanwolleghem and Dr. A. Boonstra. His training was a great opportunity to get well acquainted within the research areas of immunology, virology and the use of animal models related to both subjects. During the last year of his training Prof. dr. R.A. de Man joined in this work and acted as promotor.

After obtaining his PhD, Martijn continued his work in the field of immunology and is appointed as postdoctoral researcher in bacterial immunity at the National Institute for Public Health and the Environment in Bilthoven, The Netherlands.

PhD Portofolio

Name PhD student:	Martijn D.B. van de Garde
ErasmusMC Department:	Gastroenterology and Hepatology
PhD period:	02-2013 t/m 02-2017
Promotor:	Prof. Dr. Robert A. de Man
Copromotor(s):	Dr. Thomas Vanwolleghem & Dr. Andre Boonstra

PhD Training:

Seminars
Weekly lab seminar 2013-2017 (4 ECTS)
Weekly viral hepatitis seminar 2013-2017 (4 ECTS)
Biweekly journal club 2013-2017 (2 ECTS)

Courses and workshop
- Bio Business Summer school, 2016 (1.5 ECTS)
- InDesign Workshop, 2015 (0.15 ECTS)
- Photoshop and Illustrator CS 6 Workshop, ErasmusMC, 2014 (0.3 ECTS)
- Research Integrity, ErasmusMC, 2014 (0.3 ECTS)
- Article 9 course, ErasmusMC, 2013 (3 ECTS)
- Infectious disease, AMC, 2012 (1.3 ECTS)

(inter)national conferences

Year	*Conference, Presentation, Location, ECTS*
2016	NVVI/BSI joint meeting, Poster, Liverpool, England (1.5 ECTS)
2016	Dutch liver retreat, Oral, Spier, The Netherlands (0.6 ECTS)
2016	European association for the study of the liver (EASL),Poster, Barcelona, Spain (1,5 ECTS)
2016	Dutch society for gastroenterology en hepatology (NVGE), Poster, Veldhoven, The Netherlands (0,6 ECTS)
2016	20th Molecular Medicine Day, Poster, Rotterdam, The Netherlands (0,3 ECTS)
2016	Belgian week of Gastroenterology, Oral, Brussel, Belgium (0,3 ECTS)
2015	Virgo Consortium Scientific meeting, Invited speaker, Scheveningen, The Netherlands (0,3 ECTS)
2015	19th Molecular Medicine Day, Poster+Pitch, Rotterdam, The Netherlands (0,3 ECTS)
2015	Dutch Annual Virology Symposium, None, Amsterdam, The Netherlands (0,3 ECTS)
2014	Dutch society for immunology, Poster, Kaatsheuvel, The Netherlands (0,9 ECTS)
2014	International meeting on molecular biology of hepatitis B viruses, Poster, Los Angeles, USA (1,5 ECTS)
2014	Dutch society for gastroenterology en hepatology (NVGE), Oral, Veldhoven, The Netherlands (0,6 ECTS)
2014	18th Molecular Medicine Day, Poster, Rotterdam, The Neterlands (0,3 ECTS)
2013	Dutch liver retreat, Oral, Spier, The Netherlands (0,6 ECTS)
2013	HCV animal models and vaccine development, Poster, Tallinn, Estonia (0,6 ECTS)
2012	Dutch society for immunology, Poster, Noordwijkerhout, The Netherlands (0,6 ECTS)

Teaching activities
Supervising
- Anusha Shankar, Master student Infection and Immunity, research internship 03-2016 (2 ECTS)
- Anne van Schoonhoven, Bachelor student Biomedical Sciences, research internship 02-2016 (2 ECTS)
- Juan Rodríguez-Coira, Master student Infection and Immunity, research internship 01-2015 (2 ECTS)

Lecturer for master infection and immunity winter course 2016
- Lecture: Animal models in viral hepatitis research

Grants
Travel grant, ErasmusMC, Trustfonds 2016
Travel grant, ErasmusMC, Trustfonds 2014

List of Publications

1. van de Garde MD, van Schoonhoven A, de Man RA, Boonstra A, Vanwolleghem T, Pas SD. 2017. The hepatitis E Virus genotype three genome adapts to in vitro conditions, but shows limited mutagenesis in immunocompromised hosts. Manuscript in preparation

2. van de Garde MD, Pas SD, van Oord GW, Gama L, Choi Y, de Man RA, Boonstra A, Vanwolleghem T. 2017. Interferon-alpha treatment rapidly clears hepatitis E virus infection in humanized mice. Sci Rep 7:8267

3. van de Garde MD, Pas SD, van der Net G, de Man RA, Osterhaus AD, Haagmans BL, Boonstra A, Vanwolleghem T. 2016. Hepatitis E Virus (HEV) Genotype 3 Infection of Human Liver Chimeric Mice as a Model for Chronic HEV Infection. J Virol 90:4394-4401.

4. van de Garde MD, Movita D, van der Heide M, Herschke F, De Jonghe S, Gama L, Boonstra A, Vanwolleghem T. 2016. Liver Monocytes and Kupffer Cells Remain Transcriptionally Distinct during Chronic Viral Infection. PLoS One 11:e0166094.

5. Chang GW, Hsiao CC, Peng YM, Vieira Braga FA, Kragten NA, Remmerswaal EB, **van de Garde MD**, Straussberg R, Konig GM, Kostenis E, Knauper V, Meyaard L, van Lier RA, van Gisbergen KP, Lin HH, Hamann J. 2016. The Adhesion G Protein-Coupled Receptor GPR56/ADGRG1 Is an Inhibitory Receptor on Human NK Cells. Cell Rep 15:1757-1770.

6. Movita D, **van de Garde MD**, Biesta P, Kreefft K, Haagmans B, Zuniga E, Herschke F, De Jonghe S, Janssen HL, Gama L, Boonstra A, Vanwolleghem T. 2015. Inflammatory monocytes recruited to the liver within 24 hours after virus-induced inflammation resemble Kupffer cells but are functionally distinct. J Virol 89:4809-4817.

7. van de Garde MD, Martinez FO, Melgert BN, Hylkema MN, Jonkers RE, Hamann J. 2014. Chronic exposure to glucocorticoids shapes gene expression and modulates innate and adaptive activation pathways in macrophages with distinct changes in leukocyte attraction. J Immunol 192:1196-1208.

8. Melief J, Schuurman KG, **van de Garde MD**, Smolders J, van Eijk M, Hamann J, Huitinga I. 2013. Microglia in normal appearing white matter of multiple sclerosis are alerted but immunosuppressed. Glia 61:1848-1861.

9. Melief J, Koning N, Schuurman KG, **van de Garde MD**, Smolders J, Hoek RM, Van Eijk M, Hamann J, Huitinga I. 2012. Phenotyping primary human microglia: tight regulation of LPS responsiveness. Glia 60:1506-1517.

10. Pegtel DM, **van de Garde MD**, Middeldorp JM. 2011. Viral miRNAs exploiting the endosomal-exosomal pathway for intercellular cross-talk and immune evasion. Biochim Biophys Acta 1809:715-721.

11. Peng YM, **van de Garde MD**, Cheng KF, Baars PA, Remmerswaal EB, van Lier RA, Mackay CR, Lin HH, Hamann J. 2011. Specific expression of GPR56 by human cytotoxic lymphocytes. J Leukoc Biol 90:735-740.

12. de Vries M, Deijs M, Canuti M, van Schaik BD, Faria NR, **van de Garde MD**, Jachimowski LC, Jebbink MF, Jakobs M, Luyf AC, Coenjaerts FE, Claas EC, Molenkamp R, Koekkoek SM, Lammens C, Leus F, Goossens H, Ieven M, Baas F, van der Hoek L. 2011. A sensitive assay for virus discovery in respiratory clinical samples. PLoS One 6:e16118.

Abbreviations

A549	Adenocarcinoma human alveolar basal epithelial cells
ALF	Acute liver failure
BSA	Bovine Albumin Fraction V
cccDNA	Covalently closed circular DNA
Cl	Clone
CPE	Cytopathogenic effect
Ct	Cycle threshold
DAB	33'-diaminobenzidine
DAPI	46-diamidino-2-phenylindole
DMEM	Dulbecco's modified Eagles Medium
ELISA	Enzyme-linked immunosorbent assay
EMEM	Minimal essential Medium Eagle
FBS	Fetal bovine serum
FCS	Fetal calf serum
Gt	Genotype
HBcAg	Hepatitis B core antigen
HBeAg	Hepatitis B early antigen
HBsAg	Hepatitis B surface antigen
HBV	Hepatitis B virus
HBX	Hepatitis B X protein
HCV	Hepatitis C virus
HD	Hepatocyte donor
HDV	Hepatitis D virus
HEV	Hepatitis E virus
HIV	Human Immunodeficiency Virus
i.p	Intraperitoneal.
i.v	Intravenous
IFN	Interferon
IL	Interleukin
IM	Inflammatory monocytes
iNOS	Inducible nitric oxide synthase
IRF	Interferon regulatory factor
ISG	Interferon stimulated gene
IU	International units
KC	Kupffer cell
LCMV	Lymphocytic choriomeningitis virus
LPS	Lipopolysaccharides
MARCO	Macrophage receptor with collagenous structure
MDA5	Melanoma Differentiation-Associated protein 5
MDSC	Myeloid derived suppressor cells
MHC	Major Histocompatibility complex
NCR	None coding region
NK	Natural killer
NOG	HSVtk-NOD/Shi-scid IL2Rgnull
OAS	Oligoadenylate synthetase
ORF	Open Reading Frame
P	Passage
p.i.	Post infection
PAMP	Pathogen-associated molecular pattern
PBS	Phosphate buffered saline
PCR	Polymerase chain reaction
pegIFNα	Pegylated interferon-alpha
pen/strep	Penicillin/streptomycin
PFU	Plaque forming units
PMA	Phorbol 12-myristate 13-acetate
PRR	Pathogen recognition receptor
RBV	Ribavirin
RIG-I	Retinoic acid-inducible gene I
RNA	Ribonucleic acid
ROS	Reactive oxygen species
SEM	Standard error of the mean
SOT	Solid Organ Transplant
SVR	Sustained virologic response
TGF	Transforming growth factor
TLR	Toll like receptor
TNF	Tumor necrosis factor
uPA	urokinase-type plasminogen activator
VLP	Virus like particle

References

1. W. M. Lee, Hepatitis B virus infection. The New England journal of medicine 337, 1733-1745 (1997).
2. S. L. Chen, T. R. Morgan, The natural history of hepatitis C virus (HCV) infection. International journal of medical sciences 3, 47-52 (2006).
3. N. Kamar et al., Factors associated with chronic hepatitis in patients with hepatitis E virus infection who have received solid organ transplants. Gastroenterology 140, 1481-1489 (2011).
4. S. D. Pas et al., Hepatitis E virus infection among solid organ transplant recipients, the Netherlands. Emerging infectious diseases 18, 869-872 (2012).
5. C. M. Nijskens et al., Hepatitis E virus genotype 3 infection in a tertiary referral center in the Netherlands: Clinical relevance and impact on patient morbidity. Journal of clinical virology : the official publication of the Pan American Society for Clinical Virology 74, 82-87 (2016).
6. R. Jardi et al., HIV, HEV and cirrhosis: evidence of a possible link from eastern Spain. HIV medicine 13, 379-383 (2012).
7. M. Kaba et al., Hepatitis E virus infection in patients infected with the human immunodeficiency virus. J Med Virol 83, 1704-1716 (2011).
8. A. Tamura et al., Persistent infection of hepatitis E virus transmitted by blood transfusion in a patient with T-cell lymphoma. Hepatology research : the official journal of the Japan Society of Hepatology 37, 113-120 (2007).
9. P. le Coutre et al., Reactivation of hepatitis E infection in a patient with acute lymphoblastic leukaemia after allogeneic stem cell transplantation. Gut 58, 699-702 (2009).
10. U. Halac et al., Cirrhosis due to chronic hepatitis E infection in a child post-bone marrow transplant. The Journal of pediatrics 160, 871-874 e871 (2012).
11. N. Kamar et al., Hepatitis E virus and chronic hepatitis in organ-transplant recipients. The New England journal of medicine 358, 811-817 (2008).
12. D. Ganem, A. M. Prince, Hepatitis B virus infection--natural history and clinical consequences. The New England journal of medicine 350, 1118-1129 (2004).
13. G. M. Lauer, B. D. Walker, Hepatitis C virus infection. The New England journal of medicine 345, 41-52 (2001).
14. S. Ohnishi, J. H. Kang, H. Maekubo, K. Takahashi, S. Mishiro, A case report: two patients with fulminant hepatitis E in Hokkaido, Japan. Hepatology research : the official journal of the Japan Society of Hepatology 25, 213-218 (2003).
15. C. L. Crossan et al., Hepatitis E virus in patients with acute severe liver injury. World journal of hepatology 6, 426-434 (2014).
16. Y. Wei, C. Neuveut, P. Tiollais, M. A. Buendia, Molecular biology of the hepatitis B virus and role of the X gene. Pathologie-biologie 58, 267-272 (2010).
17. M. Ohno et al., Novel therapeutic approaches for hepatitis B virus covalently closed circular DNA. World journal of gastroenterology 21, 7084-7088 (2015).
18. H. Yan et al., Sodium taurocholate cotransporting polypeptide is a functional receptor for human hepatitis B and D virus. eLife 1, e00049 (2012).
19. M. Nassal, HBV cccDNA: viral persistence reservoir and key obstacle for a cure of chronic hepatitis B. Gut 64, 1972-1984 (2015).
20. C. Seeger, W. S. Mason, Hepatitis B virus biology. Microbiology and molecular biology reviews : MMBR 64, 51-68 (2000).
21. F. Penin, J. Dubuisson, F. A. Rey, D. Moradpour, J. M. Pawlotsky, Structural biology of hepatitis C virus. Hepatology 39, 5-19 (2004).
22. D. Moradpour, F. Penin, C. M. Rice, Replication of hepatitis C virus. Nature reviews. Microbiology 5, 453-463 (2007).
23. K. E. Reed, C. M. Rice, Overview of hepatitis C virus genome structure, polyprotein processing, and protein properties. Current topics in microbiology and immunology 242, 55-84 (2000).
24. H. Barth et al., Cellular binding of hepatitis C virus envelope glycoprotein E2 requires cell surface heparan sulfate. The Journal of biological chemistry 278, 41003-41012 (2003).
25. D. Moradpour et al., Insertion of green fluorescent protein into nonstructural protein 5A allows direct visualization of functional hepatitis C virus replication complexes. Journal of virology 78, 7400-7409 (2004).
26. H. Koot, B. M. Hogema, M. Koot, M. Molier, H. L. Zaaijer, Frequent hepatitis E in the Netherlands without traveling or immunosuppression. Journal of clinical virology : the official publication of the Pan American Society for Clinical Virology 62, 38-40 (2015).
27. J. M. Mansuy et al., Seroprevalence in blood donors reveals widespread, multi-source exposure to hepatitis E virus, southern France, October 2011. Euro surveillance : bulletin Europeen sur les maladies transmissibles = European communicable disease bulletin 20, 27-34 (2015).
28. P. E. Hewitt et al., Hepatitis E virus in blood components: a prevalence and transmission study in southeast England. Lancet 384, 1766-1773 (2014).
29. D. B. Smith et al., Consensus proposals for classification of the family Hepeviridae. The Journal of general virology 95, 2223-2232 (2014).
30. Q. Ding et al., Hepatitis E virus ORF3 is a functional ion channel required for release of infectious particles. Proceedings of the National Academy of Sciences of the United States of America 114, 1147-1152 (2017).
31. M. Kalia, V. Chandra, S. A. Rahman, D. Sehgal, S. Jameel, Heparan sulfate proteoglycans are required for cellular binding of the hepatitis E virus ORF2 capsid protein and for viral infection. Journal of virology 83, 12714-12724 (2009).
32. R. P. Holla, I. Ahmad, Z. Ahmad, S. Jameel, Molecular virology of hepatitis E virus. Semin Liver Dis 33, 3-14 (2013).
33. M. K. Parvez, Molecular characterization of hepatitis E virus ORF1 gene supports a papain-like cysteine protease (PCP)-domain activity. Virus research 178, 553-556 (2013).
34. D. Cao, X. J. Meng, Molecular biology and replication of hepatitis E virus. Emerging microbes & infections 1, e17 (2012).
35. A. Boonstra, L. J. van der Laan, T. Vanwolleghem, H. L. Janssen, Experimental models for hepatitis C viral infection. Hepatology 50, 1646-1655 (2009).
36. Y. Debing, D. Moradpour, J. Neyts, J. Gouttenoire, Update on Hepatitis E Virology:Implications for Clinical Practice. Journal of hepatology, (2016).
37. C. Trepo, H. L. Chan, A. Lok, Hepatitis B virus infection. Lancet 384, 2053-2063 (2014).
38. N. A. Terrault et al., AASLD guidelines for treatment of chronic hepatitis B. Hepatology 63, 261-283 (2016).
39. P. Revill, S. Locarnini, Antiviral strategies to eliminate hepatitis B virus covalently closed circular DNA (cccDNA). Current opinion in pharmacology 30, 144-150 (2016).
40. J. Lucifora et al., Specific and nonhepatotoxic degradation of nuclear hepatitis B virus cccDNA. Science 343, 1221-1228 (2014).
41. S. D. Crockett, E. B. Keeffe, Natural history and treatment of hepatitis B virus and hepatitis C virus coinfection. Annals of clinical microbiology and antimicrobials 4, 13 (2005).
42. M. P. Manns et al., Peginterferon alfa-2b plus ribavirin compared with interferon alfa-2b plus ribavirin for initial treatment of chronic hepatitis C: a randomised trial. Lancet 358, 958-965 (2001).
43. L. Chen et al., Hepatic gene expression discriminates responders and nonresponders in treatment of chronic hepatitis C viral infection. Gastroenterology 128, 1437-1444 (2005).
44. I. McGilvray et al., Hepatic cell-type specific gene expression better predicts HCV treatment outcome than IL28B genotype. Gastroenterology 142, 1122-1131 e1121 (2012).
45. E. J. Gane et al., Efficacy of the Combination of Sofosbuvir, Velpatasvir, and the NS3/4A Protease Inhibitor GS-9857 in Treatment-Naive or Previously Treated Patients With Hepatitis C Virus Genotype 1 or 3 Infections. Gastroenterology 151, 448-456 e441 (2016).
46. G. T. Everson et al., Sofosbuvir With Velpatasvir in Treatment-Naive Noncirrhotic Patients With Genotype 1 to 6 Hepatitis C Virus Infection: A Randomized Trial. Annals of internal medicine 163, 818-826 (2015).
47. A. M. Peters van Ton, T. J. Gevers, J. P. Drenth, Antiviral therapy in chronic hepatitis E: a systematic review. Journal of viral hepatitis 22, 965-973 (2015).
48. L. Alric, D. Bonnet, G. Laurent, N. Kamar, J. Izopet, Chronic hepatitis E virus infection: successful virologic response to pegylated interferon-alpha therapy. Annals of internal medicine 153, 135-136 (2010).
49. C. Guha, S. Mohan, N. Roy-Chowdhury, J. Roy-Chowdhury, Cell culture and animal models of viral hepatitis. Part I: hepatitis B. Lab animal 33, 37-46 (2004).
50. E. Billerbeck, Y. de Jong, M. Dorner, C. de la Fuente, A. Ploss, Animal models for hepatitis C. Current topics in microbiology and immunology 369, 49-86 (2013).
51. J. A. Rhim, E. P. Sandgren, J. L. Degen, R. D. Palmiter, R. L. Brinster, Replacement of diseased mouse liver by hepatic cell transplantation. Science 263, 1149-1152 (1994).
52. P. Meuleman et al., Morphological and biochemical characterization of a human liver in a uPA-SCID mouse chimera. Hepatology 41, 847-856 (2005).
53. H. Suemizu et al., Establishment of a humanized model of liver using NOD/Shi-scid IL2Rgnull mice. Biochemical and biophysical research communications 377, 248-252 (2008).
54. M. Hasegawa et al., The reconstituted 'humanized liver' in TK-NOG mice is mature and functional. Biochemical and biophysical research communications 405, 405-410 (2011).
55. K. D. Bissig et al., Human liver chimeric mice provide a model for hepatitis B and C virus infection and treatment. The Journal of clinical investigation 120, 924-930 (2010).
56. D. F. Mercer et al., Hepatitis C virus replication in mice with chimeric human livers. Nat Med 7, 927-933 (2001).
57. K. Kosaka et al., A novel TK-NOG based humanized mouse model for the study of HBV and HCV infections. Biochemical and biophysical research communications 441, 230-235 (2013).
58. M. Dandri et al., Repopulation of mouse liver with human hepatocytes and

in vivo infection with hepatitis B virus. Hepatology 33, 981-988 (2001).
59. M. Lutgehetmann et al., Humanized chimeric uPA mouse model for the study of hepatitis B and D virus interactions and preclinical drug evaluation. Hepatology 55, 685-694 (2012).
60. E. Ohara et al., Elimination of hepatitis C virus by short term NS3-4A and NS5B inhibitor combination therapy in human hepatocyte chimeric mice. Journal of hepatology 54, 872-878 (2011).
61. T. Vanwolleghem et al., Ultra-rapid cardiotoxicity of the hepatitis C virus protease inhibitor BILN 2061 in the urokinase-type plasminogen activator mouse. Gastroenterology 133, 1144-1155 (2007).
62. N. M. Kneteman et al., HCV796: A selective nonstructural protein 5B polymerase inhibitor with potent anti-hepatitis C virus activity in vitro, in mice with chimeric human livers, and in humans infected with hepatitis C virus. Hepatology 49, 745-752 (2009).
63. M. Ohira et al., Adoptive immunotherapy with liver allograft-derived lymphocytes induces anti-HCV activity after liver transplantation in humans and humanized mice. The Journal of clinical investigation 119, 3226-3235 (2009).
64. R. M. Zinkernagel, P. C. Doherty, Immunological surveillance against altered self components by sensitised T lymphocytes in lymphocytic choriomeningitis. Nature 251, 547-548 (1974).
65. R. M. Zinkernagel, P. C. Doherty, Restriction of in vitro T cell-mediated cytotoxicity in lymphocytic choriomeningitis within a syngeneic or semiallogeneic system. Nature 248, 701-702 (1974).
66. P. C. Doherty, R. M. Zinkernagel, H-2 compatibility is required for T-cell-mediated lysis of target cells infected with lymphocytic choriomeningitis virus. J Exp Med 141, 502-507 (1975).
67. D. Masson, J. Tschopp, Isolation of a lytic, pore-forming protein (perforin) from cytolytic T-lymphocytes. The Journal of biological chemistry 260, 9069-9072 (1985).
68. D. Kagi et al., Cytotoxicity mediated by T cells and natural killer cells is greatly impaired in perforin-deficient mice. Nature 369, 31-37 (1994).
69. L. L. Lau, B. D. Jamieson, T. Somasundaram, R. Ahmed, Cytotoxic T-cell memory without antigen. Nature 369, 648-652 (1994).
70. K. Murali-Krishna et al., Counting antigen-specific CD8 T cells: a reevaluation of bystander activation during viral infection. Immunity 8, 177-187 (1998).
71. C. A. Mims, S. Wainwright, The immunodepressive action of lymphocytic choriomeningitis virus in mice. J Immunol 101, 717-724 (1968).
72. M. B. McChesney, M. B. Oldstone, Viruses perturb lymphocyte functions: selected principles characterizing virus-induced immunosuppression. Annual review of immunology 5, 279-304 (1987).
73. D. Moskophidis, F. Lechner, H. Pircher, R. M. Zinkernagel, Virus persistence in acutely infected immunocompetent mice by exhaustion of antiviral cytotoxic effector T cells. Nature 362, 758-761 (1993).
74. E. J. Wherry et al., Molecular signature of CD8+ T cell exhaustion during chronic viral infection. Immunity 27, 670-684 (2007).
75. R. M. Welsh, Jr., Cytotoxic cells induced during lymphocytic choriomeningitis virus infection of mice. I. Characterization of natural killer cell induction. J Exp Med 148, 163-181 (1978).
76. M. Salvato, P. Borrow, E. Shimomaye, M. B. Oldstone, Molecular basis of viral persistence: a single amino acid change in the glycoprotein of lymphocytic choriomeningitis virus is associated with suppression of the antiviral cytotoxic T-lymphocyte response and establishment of persistence. Journal of virology 65, 1863-1869 (1991).
77. M. Matloubian, S. R. Kolhekar, T. Somasundaram, R. Ahmed, Molecular determinants of macrophage tropism and viral persistence: importance of single amino acid changes in the polymerase and glycoprotein of lymphocytic choriomeningitis virus. Journal of virology 67, 7340-7349 (1993).
78. A. Tishon, H. Lewicki, G. Rall, M. Von Herrath, M. B. Oldstone, An essential role for type 1 interferon-gamma in terminating persistent viral infection. Virology 212, 244-250 (1995).
79. W. P. Fung-Leung, T. M. Kundig, R. M. Zinkernagel, T. W. Mak, Immune response against lymphocytic choriomeningitis virus infection in mice without CD8 expression. J Exp Med 174, 1425-1429 (1991).
80. R. Ahmed, A. Salmi, L. D. Butler, J. M. Chiller, M. B. Oldstone, Selection of genetic variants of lymphocytic choriomeningitis virus in spleens of persistently infected mice. Role in suppression of cytotoxic T lymphocyte response and viral persistence. J Exp Med 160, 521-540 (1984).
81. P. Borrow, C. F. Evans, M. B. Oldstone, Virus-induced immunosuppression: immune system-mediated destruction of virus-infected dendritic cells results in generalized immune suppression. Journal of virology 69, 1059-1070 (1995).
82. R. M. Zinkernagel et al., T cell-mediated hepatitis in mice infected with lymphocytic choriomeningitis virus. Liver cell destruction by H-2 class I-restricted virus-specific cytotoxic T cells as a physiological correlate of the 51Cr-release assay? J Exp Med 164, 1075-1092 (1986).
83. J. Lohler, J. Gossmann, T. Kratzberg, F. Lehmann-Grube, Murine hepatitis caused by lymphocytic choriomeningitis virus. I. The hepatic lesions. Lab Invest 70, 263-278 (1994).
84. A. Bhattacharya et al., Superoxide Dismutase 1 Protects Hepatocytes from Type I Interferon-Driven Oxidative Damage. Immunity 43, 974-986 (2015).
85. C. A. Janeway, Jr., R. Medzhitov, Innate immune recognition. Annual review of immunology 20, 197-216 (2002).
86. R. S. Mahla, M. C. Reddy, D. V. Prasad, H. Kumar, Sweeten PAMPs: Role of Sugar Complexed PAMPs in Innate Immunity and Vaccine Biology. Frontiers in immunology 4, 248 (2013).
87. E. Meylan, J. Tschopp, M. Karin, Intracellular pattern recognition receptors in the host response. Nature 442, 39-44 (2006).
88. K. A. Walters et al., Host-specific response to HCV infection in the chimeric SCID-beige/Alb-uPA mouse model: role of the innate antiviral immune response. PLoS pathogens 2, e59 (2006).
89. K. Giersch et al., Hepatitis Delta co-infection in humanized mice leads to pronounced induction of innate immune responses in comparison to HBV mono-infection. Journal of hepatology 63, 346-353 (2015).
90. A. G. Bowie, L. Unterholzner, Viral evasion and subversion of pattern-recognition receptor signalling. Nat Rev Immunol 8, 911-922 (2008).
91. M. H. Heim, R. Thimme, Innate and adaptive immune responses in HCV infections. Journal of hepatology 61, S14-25 (2014).
92. R. Thimme et al., Determinants of viral clearance and persistence during acute hepatitis C virus infection. J Exp Med 194, 1395-1406 (2001).
93. C. L. Day et al., Broad specificity of virus-specific CD4+ T-helper-cell responses in resolved hepatitis C virus infection. Journal of virology 76, 12584-12595 (2002).
94. G. M. Lauer et al., Comprehensive analysis of CD8(+)-T-cell responses against hepatitis C virus reveals multiple unpredicted specificities. Journal of virology 76, 6104-6113 (2002).
95. B. Rehermann, M. Nascimbeni, Immunology of hepatitis B virus and hepatitis C virus infection. Nat Rev Immunol 5, 215-229 (2005).
96. M. A. Claassen, H. L. Janssen, A. Boonstra, Role of T cell immunity in hepatitis C virus infections. Curr Opin Virol 3, 461-467 (2013).
97. S. N. Waggoner, M. Cornberg, L. K. Selin, R. M. Welsh, Natural killer cells act as rheostats modulating antiviral T cells. Nature 481, 394-398 (2011).
98. F. Ginhoux, S. Jung, Monocytes and macrophages: developmental pathways and tissue homeostasis. Nat Rev Immunol 14, 392-404 (2014).
99. A. Boltjes, D. Movita, A. Boonstra, A. M. Woltman, The role of Kupffer cells in hepatitis B and hepatitis C virus infections. Journal of hepatology 61, 660-671 (2014).
100. C. N. Jenne, P. Kubes, Immune surveillance by the liver. Nat Immunol 14, 996-1006 (2013).
101. F. Heymann et al., Liver inflammation abrogates immunological tolerance induced by Kupffer cells. Hepatology 62, 279-291 (2015).
102. P. A. Lang et al., Tissue macrophages suppress viral replication and prevent severe immunopathology in an interferon-I-dependent manner in mice. Hepatology 52, 25-32 (2010).
103. C. Shi, E. G. Pamer, Monocyte recruitment during infection and inflammation. Nat Rev Immunol 11, 762-774 (2011).
104. T. Bosschaerts et al., Tip-DC development during parasitic infection is regulated by IL-10 and requires CCL2/CCR2, IFN-gamma and MyD88 signaling. PLoS pathogens 6, e1001045 (2010).
105. N. V. Serbina, T. P. Salazar-Mather, C. A. Biron, W. A. Kuziel, E. G. Pamer, TNF/iNOS-producing dendritic cells mediate innate immune defense against bacterial infection. Immunity 19, 59-70 (2003).
106. A. Rivollier, J. He, A. Kole, V. Valatas, B. L. Kelsall, Inflammation switches the differentiation program of Ly6Chi monocytes from antiinflammatory macrophages to inflammatory dendritic cells in the colon. J Exp Med 209, 139-155 (2012).
107. K. Ersland, M. Wuthrich, B. S. Klein, Dynamic interplay among monocyte-derived, dermal, and resident lymph node dendritic cells during the generation of vaccine immunity to fungi. Cell Host Microbe 7, 474-487 (2010).
108. C. Cheong et al., Microbial stimulation fully differentiates monocytes to DC-SIGN/CD209(+) dendritic cells for immune T cell areas. Cell 143, 416-429 (2010).
109. E. Zigmond et al., Ly6C hi monocytes in the inflamed colon give rise to proinflammatory effector cells and migratory antigen-presenting cells. Immunity 37, 1076-1090 (2012).
110. J. Farache et al., Luminal bacteria recruit CD103+ dendritic cells into the intestinal epithelium to sample bacterial antigens for presentation. Immunity 38, 581-595 (2013).
111. E. Kurmaeva et al., Immunosuppressive monocytes: possible homeostatic mechanism to restrain chronic intestinal inflammation. J Leukoc Biol, (2014).
112. K. Chayama et al., Animal model for study of human hepatitis viruses. J

Gastroenterol Hepatol 26, 13-18 (2011).
113. X. Zhou, S. Ramachandran, M. Mann, D. L. Popkin, Role of lymphocytic choriomeningitis virus (LCMV) in understanding viral immunology: past, present and future. Viruses 4, 2650-2669 (2012).
114. E. I. Zuniga, L. Y. Liou, L. Mack, M. Mendoza, M. B. Oldstone, Persistent virus infection inhibits type I interferon production by plasmacytoid dendritic cells to facilitate opportunistic infections. Cell Host Microbe 4, 374-386 (2008).
115. L. N. Lee, S. Burke, M. Montoya, P. Borrow, Multiple mechanisms contribute to impairment of type 1 interferon production during chronic lymphocytic choriomeningitis virus infection of mice. J Immunol 182, 7178-7189 (2009).
116. T. Kurihara, G. Warr, J. Loy, R. Bravo, Defects in macrophage recruitment and host defense in mice lacking the CCR2 chemokine receptor. J Exp Med 186, 1757-1762 (1997).
117. M. Skold, S. M. Behar, Tuberculosis triggers a tissue-dependent program of differentiation and acquisition of effector functions by circulating monocytes. J Immunol 181, 6349-6360 (2008).
118. I. R. Dunay et al., Gr1(+) inflammatory monocytes are required for mucosal resistance to the pathogen Toxoplasma gondii. Immunity 29, 306-317 (2008).
119. T. C. Dawson, M. A. Beck, W. A. Kuziel, F. Henderson, N. Maeda, Contrasting effects of CCR5 and CCR2 deficiency in the pulmonary inflammatory response to influenza A virus. Am J Pathol 156, 1951-1959 (2000).
120. J. R. Aldridge, Jr. et al., TNF/iNOS-producing dendritic cells are the necessary evil of lethal influenza virus infection. Proceedings of the National Academy of Sciences of the United States of America 106, 5306-5311 (2009).
121. M. P. Holt, L. Cheng, C. Ju, Identification and characterization of infiltrating macrophages in acetaminophen-induced liver injury. J Leukoc Biol 84, 1410-1421 (2008).
122. K. R. Karlmark et al., Hepatic recruitment of the inflammatory Gr1+ monocyte subset upon liver injury promotes hepatic fibrosis. Hepatology 50, 261-274 (2009).
123. N. Nakamoto et al., CCR9+ macrophages are required for acute liver inflammation in mouse models of hepatitis. Gastroenterology 142, 366-376 (2012).
124. E. Helk et al., TNFalpha-mediated liver destruction by Kupffer cells and Ly6Chi monocytes during Entamoeba histolytica infection. PLoS pathogens 9, e1003096 (2013).
125. D. Movita et al., Kupffer cells express a unique combination of phenotypic and functional characteristics compared with splenic and peritoneal macrophages. J Leukoc Biol 92, 723-733 (2012).
126. M. Kinoshita et al., Characterization of two F4/80-positive Kupffer cell subsets by their function and phenotype in mice. Journal of hepatology 53, 903-910 (2010).
127. J. N. Russell, J. E. Clements, L. Gama, Quantitation of gene expression in formaldehyde-fixed and fluorescence-activated sorted cells. PLoS One 8, e73849 (2013).
128. S. Basta, R. Stoessel, M. Basler, M. van den Broek, M. Groettrup, Cross-presentation of the long-lived lymphocytic choriomeningitis virus nucleoprotein does not require neosynthesis and is enhanced via heat shock proteins. J Immunol 175, 796-805 (2005).
129. M. Rayamajhi, J. Humann, K. Penheiter, K. Andreasen, L. L. Lenz, Induction of IFN-alphabeta enables Listeria monocytogenes to suppress macrophage activation by IFN-gamma. J Exp Med 207, 327-337 (2010).
130. B. S. Liu, H. L. Janssen, A. Boonstra, IL-29 and IFNalpha differ in their ability to modulate IL-12 production by TLR-activated human macrophages and exhibit differential regulation of the IFNgamma receptor expression. Blood 117, 2385-2395 (2011).
131. K. Revill et al., Genome-Wide Methylation Analysis and Epigenetic Unmasking Identify Tumor Suppressor Genes in Hepatocellular Carcinoma. Gastroenterology 145, 1424-+ (2013).
132. R. A. Ezekowitz, J. Austyn, P. D. Stahl, S. Gordon, Surface properties of bacillus Calmette-Guerin-activated mouse macrophages. Reduced expression of mannose-specific endocytosis, Fc receptors, and antigen F4/80 accompanies induction of Ia. J Exp Med 154, 60-76 (1981).
133. R. A. Ezekowitz, S. Gordon, Down-regulation of mannosyl receptor-mediated endocytosis and antigen F4/80 in bacillus Calmette-Guerin-activated mouse macrophages. Role of T lymphocytes and lymphokines. J Exp Med 155, 1623-1637 (1982).
134. E. Liaskou et al., Monocyte subsets in human liver disease show distinct phenotypic and functional characteristics. Hepatology 57, 385-398 (2013).
135. L. R. Huang et al., Intrahepatic myeloid-cell aggregates enable local proliferation of CD8(+) T cells and successful immunotherapy against chronic viral liver infection. Nat Immunol 14, 574-583 (2013).
136. A. Arzumanyan, H. M. Reis, M. A. Feitelson, Pathogenic mechanisms in HBV- and HCV-associated hepatocellular carcinoma. Nat Rev Cancer 13, 123-135 (2013).
137. D. Movita et al., Inflammatory monocytes recruited to the liver within 24 hours after virus-induced inflammation resemble Kupffer cells but are functionally distinct. Journal of virology 89, 4809-4817 (2015).
138. C. Auffray et al., Monitoring of blood vessels and tissues by a population of monocytes with patrolling behavior. Science 317, 666-670 (2007).
139. F. Geissmann, S. Jung, D. R. Littman, Blood monocytes consist of two principal subsets with distinct migratory properties. Immunity 19, 71-82 (2003).
140. A. Boltjes et al., Monocytes from chronic HBV patients react in vitro to HBsAg and TLR by producing cytokines irrespective of stage of disease. PloS one 9, e97006 (2014).
141. C. Bleriot et al., Liver-resident macrophage necroptosis orchestrates type 1 microbicidal inflammation and type-2-mediated tissue repair during bacterial infection. Immunity 42, 145-158 (2015).
142. B. A. Norris et al., Chronic but not acute virus infection induces sustained expansion of myeloid suppressor cell numbers that inhibit viral-specific T cell immunity. Immunity 38, 309-321 (2013).
143. A. Boltjes et al., Kupffer cells interact with hepatitis B surface antigen in vivo and in vitro, leading to proinflammatory cytokine production and natural killer cell function. J Infect Dis 211, 1268-1278 (2015).
144. E. J. Wherry, J. N. Blattman, K. Murali-Krishna, R. van der Most, R. Ahmed, Viral persistence alters CD8 T-cell immunodominance and tissue distribution and results in distinct stages of functional impairment. Journal of virology 77, 4911-4927 (2003).
145. D. L. Barber et al., Restoring function in exhausted CD8 T cells during chronic viral infection. Nature 439, 682-687 (2006).
146. Y. Xia et al., Interferon-gamma and Tumor Necrosis Factor-alpha Produced by T Cells Reduce the HBV Persistence Form, cccDNA, Without Cytolysis. Gastroenterology 150, 194-205 (2016).
147. P. P. Reis et al., mRNA transcript quantification in archival samples using multiplexed, color-coded probes. BMC Biotechnol 11, 46 (2011).
148. C. Kendziorski, R. A. Irizarry, K. S. Chen, J. D. Haag, M. N. Gould, On the utility of pooling biological samples in microarray experiments. Proceedings of the National Academy of Sciences of the United States of America 102, 4252-4257 (2005).
149. A. Sica, A. Mantovani, Macrophage plasticity and polarization: in vivo veritas. The Journal of clinical investigation 122, 787-795 (2012).
150. N. Noel et al., Elevated IP10 levels are associated with immune activation and low CD4(+) T-cell counts in HIV controller patients. AIDS 28, 467-476 (2014).
151. C. E. Harvey et al., Expression of the chemokine IP-10 (CXCL10) by hepatocytes in chronic hepatitis C virus infection correlates with histological severity and lobular inflammation. J Leukoc Biol 74, 360-369 (2003).
152. E. Thomas et al., HCV infection induces a unique hepatic innate immune response associated with robust production of type III interferons. Gastroenterology 142, 978-988 (2012).
153. L. Chen et al., Cell-type specific gene expression signature in liver underlies response to interferon therapy in chronic hepatitis C infection. Gastroenterology 138, 1123-1133 e1121-1123 (2010).
154. M. Hosel et al., Not interferon, but interleukin-6 controls early gene expression in hepatitis B virus infection. Hepatology 50, 1773-1782 (2009).
155. J. F. Wu et al., Serum levels of interleukin-10 and interleukin-12 predict early, spontaneous hepatitis B virus e antigen seroconversion. Gastroenterology 138, 165-172 e161-163 (2010).
156. D. Peppa et al., Blockade of immunosuppressive cytokines restores NK cell antiviral function in chronic hepatitis B virus infection. PLoS pathogens 6, e1001227 (2010).
157. C. L. Scott et al., Bone marrow-derived monocytes give rise to self-renewing and fully differentiated Kupffer cells. Nat Commun 7, 10321 (2016).
158. R. Aggarwal, S. Jameel, Hepatitis E. Hepatology 54, 2218-2226 (2011).
159. L. J. Krain, K. E. Nelson, A. B. Labrique, Host immune status and response to hepatitis E virus infection. Clin Microbiol Rev 27, 139-165 (2014).
160. L. Koning et al., Clinical implications of chronic hepatitis E virus infection in heart transplant recipients. J Heart Lung Transplant 32, 78-85 (2013).
161. B. M. Hogema, M. Molier, E. Slot, H. L. Zaaijer, Past and present of hepatitis E in the Netherlands. Transfusion 54, 3092-3096 (2014).
162. J. J. Wenzel et al., Decline in hepatitis E virus antibody prevalence in southeastern Germany, 1996-2011. Hepatology 60, 1180-1186 (2014).
163. H. L. Zaaijer, No artifact, hepatitis E is emerging. Hepatology, doi: 10.1002/hep.27611 (2014).
164. S. A. Rutjes et al., Sources of Hepatitis E Virus Genotype 3 in the Netherlands. Emerging infectious diseases 15, 381-387 (2009).
165. T. Vanwolleghem et al., Factors determining successful engraftment of hepatocytes and susceptibility to hepatitis B and C virus infection in uPA-SCID mice. J Hepatol 53, 468-476 (2010).
166. T. Vanwolleghem et al., Polyclonal immunoglobulins from a chronic hepatitis C virus patient protect human liver-chimeric mice from infection with

a homologous hepatitis C virus strain. Hepatology 47, 1846-1855 (2008).
167. B. D. Lindenbach et al., Cell culture-grown hepatitis C virus is infectious in vivo and can be recultured in vitro. Proceedings of the National Academy of Sciences of the United States of America 103, 3805-3809 (2006).
168. H. Suemizu et al., Establishment of a humanized model of liver using NOD/Shi-scid IL2Rg(null) mice. Biochem Bioph Res Co 377, 248-252 (2008).
169. T. Tanaka, M. Takahashi, E. Kusano, H. Okamoto, Development and evaluation of an efficient cell-culture system for Hepatitis E virus. The Journal of general virology 88, 903-911 (2007).
170. J. Versluis et al., Hepatitis E virus: an underestimated opportunistic pathogen in recipients of allogeneic hematopoietic stem cell transplantation. Blood 122, 1079-1086 (2013).
171. S. Nagashima et al., The membrane on the surface of hepatitis E virus particles is derived from the intracellular membrane and contains trans-Golgi network protein 2. Arch Virol 159, 979-991 (2014).
172. M. Takahashi et al., Monoclonal antibodies raised against the ORF3 protein of hepatitis E virus (HEV) can capture HEV particles in culture supernatant and serum but not those in feces. Arch Virol 153, 1703-1713 (2008).
173. H. Okamoto, Culture systems for hepatitis E virus. Journal of gastroenterology 48, 147-158 (2013).
174. R. Johne et al., An ORF1-rearranged hepatitis E virus derived from a chronically infected patient efficiently replicates in cell culture. Journal of viral hepatitis 21, 447-456 (2014).
175. H. T. Nguyen et al., A naturally occurring human/hepatitis E recombinant virus predominates in serum but not in faeces of a chronic hepatitis E patient and has a growth advantage in cell culture. The Journal of general virology 93, 526-530 (2012).
176. P. Shukla et al., Adaptation of a genotype 3 hepatitis E virus to efficient growth in cell culture depends on an inserted human gene segment acquired by recombination. Journal of virology 86, 5697-5707 (2012).
177. P. Shukla et al., Cross-species infections of cultured cells by hepatitis E virus and discovery of an infectious virus-host recombinant. Proceedings of the National Academy of Sciences of the United States of America 108, 2438-2443 (2011).
178. K. Matsubayashi et al., A case of transfusion-transmitted hepatitis E caused by blood from a donor infected with hepatitis E virus via zoonotic food-borne route. Transfusion 48, 1368-1375 (2008).
179. K. Matsubayashi et al., Transfusion-transmitted hepatitis E caused by apparently indigenous hepatitis E virus strain in Hokkaido, Japan. Transfusion 44, 934-940 (2004).
180. J. M. Pawlotsky, Hepatitis E screening for blood donations: an urgent need? Lancet 384, 1729-1730 (2014).
181. D. Sitki-Green, M. Covington, N. Raab-Traub, Compartmentalization and transmission of multiple epstein-barr virus strains in asymptomatic carriers. Journal of virology 77, 1840-1847 (2003).
182. S. Ramirez et al., Hepatitis C virus compartmentalization and infection recurrence after liver transplantation. American journal of transplantation : official journal of the American Society of Transplantation and the American Society of Transplant Surgeons 9, 1591-1601 (2009).
183. S. Philpott et al., Human immunodeficiency virus type 1 genomic RNA sequences in the female genital tract and blood: compartmentalization and intrapatient recombination. Journal of virology 79, 353-363 (2005).
184. J. K. Wong et al., In vivo compartmentalization of human immunodeficiency virus: evidence from the examination of pol sequences from autopsy tissues. Journal of virology 71, 2059-2071 (1997).
185. G. Rozera et al., Quasispecies tropism and compartmentalization in gut and peripheral blood during early and chronic phases of HIV-1 infection: possible correlation with immune activation markers. Clinical microbiology and infection : the official publication of the European Society of Clinical Microbiology and Infectious Diseases 20, O157-166 (2014).
186. D. Harouaka et al., Diminished viral replication and compartmentalization of hepatitis C virus in hepatocellular carcinoma tissue. Proceedings of the National Academy of Sciences of the United States of America 113, 1375-1380 (2016).
187. S. Pischke et al., Hepatitis E virus: Infection beyond the liver? Journal of hepatology 66, 1082-1095 (2017).
188. S. Lhomme et al., Mutation in the Hepatitis E Virus Polymerase and Outcome of Ribavirin Therapy. Antimicrobial agents and chemotherapy 60, 1608-1614 (2015).
189. J. Inoue et al., Nucleotide substitutions of hepatitis E virus genomes associated with fulminant hepatitis and disease severity. The Tohoku journal of experimental medicine 218, 279-284 (2009).
190. K. Takahashi et al., Virulent strain of hepatitis E virus genotype 3, Japan. Emerging infectious diseases 15, 704-709 (2009).
191. Y. Debing et al., Hepatitis E virus mutations associated with ribavirin treatment failure result in altered viral fitness and ribavirin sensitivity. Journal of hepatology 65, 499-508 (2016).
192. M. D. van de Garde et al., Hepatitis E Virus (HEV) Genotype 3 Infection of Human Liver Chimeric Mice as a Model for Chronic HEV Infection. Journal of virology 90, 4394-4401 (2016).
193. L. Zhai, X. Dai, J. Meng, Hepatitis E virus genotyping based on full-length genome and partial genomic regions. Virus research 120, 57-69 (2006).
194. M. Munoz-Chimeno et al., Full coding hepatitis E virus genotype 3 genome amplification method. Journal of virological methods 230, 18-23 (2016).
195. J. Risso-Ballester, J. M. Cuevas, R. Sanjuan, Genome-Wide Estimation of the Spontaneous Mutation Rate of Human Adenovirus 5 by High-Fidelity Deep Sequencing. PLoS pathogens 12, e1006013 (2016).
196. J. Fonager et al., Identification of minority resistance mutations in the HIV-1 integrase coding region using next generation sequencing. Journal of clinical virology : the official publication of the Pan American Society for Clinical Virology 73, 95-100 (2015).
197. H. R. Dalton, J. Seghatchian, Hepatitis E virus: Emerging from the shadows in developed countries. Transfusion and apheresis science : official journal of the World Apheresis Association : official journal of the European Society for Haemapheresis, (2016).
198. M. S. Khuroo, S. Kamili, Aetiology, clinical course and outcome of sporadic acute viral hepatitis in pregnancy. Journal of viral hepatitis 10, 61-69 (2003).
199. L. J. Krain, K. E. Nelson, A. B. Labrique, Host immune status and response to hepatitis E virus infection. Clinical microbiology reviews 27, 139-165 (2014).
200. N. Kamar et al., Ribavirin for chronic hepatitis E virus infection in transplant recipients. The New England journal of medicine 370, 1111-1120 (2014).
201. A. Berto et al., Replication of hepatitis E virus in three-dimensional cell culture. Journal of virological methods 187, 327-332 (2013).
202. H. T. Nguyen, P. Shukla, U. Torian, K. Faulk, S. U. Emerson, Hepatitis E virus genotype 1 infection of swine kidney cells in vitro is inhibited at multiple levels. Journal of virology 88, 868-877 (2014).
203. V. P. Nair et al., Endoplasmic Reticulum Stress Induced Synthesis of a Novel Viral Factor Mediates Efficient Replication of Genotype-1 Hepatitis E Virus. PLoS pathogens 12, e1005521 (2016).
204. P. B. Devhare, S. Desai, K. S. Lole, Innate immune responses in human hepatocyte-derived cell lines alter genotype 1 hepatitis E virus replication efficiencies. Scientific reports 6, 26827 (2016).
205. D. Todt et al., Antiviral Activities of Different Interferon Types and Subtypes against Hepatitis E Virus Replication. Antimicrobial agents and chemotherapy 60, 2132-2139 (2016).
206. X. Zhou et al., Disparity of basal and therapeutically activated interferon signalling in constraining hepatitis E virus infection. Journal of viral hepatitis 23, 294-304 (2016).
207. C. Dong et al., Suppression of interferon-alpha signaling by hepatitis E virus. Hepatology 55, 1324-1332 (2012).
208. P. Keskinen et al., Impaired antiviral response in human hepatoma cells. Virology 263, 364-375 (1999).
209. M. van der Valk, H. L. Zaaijer, A. P. Kater, J. Schinkel, Sofosbuvir shows antiviral activity in a patient with chronic hepatitis E virus infection. Journal of hepatology, (2016).
210. M. C. Donnelly et al., Sofosbuvir and Daclatasvir Anti-Viral Therapy Fails to Clear HEV Viremia and Restore Reactive T Cells in a HEV/HCV Co-Infected Liver Transplant Recipient. Gastroenterology, (2016).
211. W. Wang et al., Distinct Antiviral Potency of Sofosbuvir Against Hepatitis C and E Viruses. Gastroenterology 151, 1251-1253 (2016).
212. V. L. Dao Thi et al., Sofosbuvir Inhibits Hepatitis E Virus Replication In Vitro and Results in an Additive Effect When Combined With Ribavirin. Gastroenterology 150, 82-85 e84 (2016).
213. I. M. Sayed et al., Study of hepatitis E virus infection of genotype 1 and 3 in mice with humanised liver. Gut, (2016).
214. L. Allweiss et al., Human liver chimeric mice as a new model of chronic hepatitis E virus infection and preclinical drug evaluation. Journal of hepatology 64, 1033-1040 (2016).
215. T. Vanwolleghem et al., Factors determining successful engraftment of hepatocytes and susceptibility to hepatitis B and C virus infection in uPA-SCID mice. Journal of hepatology 53, 468-476 (2010).
216. S. A. Tsarev et al., Characterization of a prototype strain of hepatitis E virus. Proceedings of the National Academy of Sciences of the United States of America 89, 559-563 (1992).
217. S. D. Pas, E. Fries, R. A. De Man, A. D. Osterhaus, H. G. Niesters, Development of a quantitative real-time detection assay for hepatitis B virus DNA and comparison with two commercial assays. J Clin Microbiol 38, 2897-2901 (2000).
218. S. D. Pas, H. G. Niesters, Detection of HBV DNA using real time analysis. Journal of clinical virology : the official publication of the Pan American Society

for Clinical Virology 25, 93-94 (2002).
219. M. D. van de Garde et al., Liver Monocytes and Kupffer Cells Remain Transcriptionally Distinct during Chronic Viral Infection. PloS one 11, e0166094 (2016).
220. J. J. Feld et al., Hepatic gene expression during treatment with peginterferon and ribavirin: Identifying molecular pathways for treatment response. Hepatology 46, 1548-1563 (2007).
221. L. Allweiss et al., Immune cell responses are not required to induce substantial hepatitis B virus antigen decline during pegylated interferon-alpha administration. Journal of hepatology 60, 500-507 (2014).
222. N. M. Kneteman et al., Anti-HCV therapies in chimeric scid-Alb/uPA mice parallel outcomes in human clinical application. Hepatology 43, 1346-1353 (2006).
223. T. Watanabe et al., Hepatitis C virus kinetics by administration of pegylated interferon-alpha in human and chimeric mice carrying human hepatocytes with variants of the IL28B gene. Gut 62, 1340-1346 (2013).
224. S. P. Fletcher et al., Intrahepatic Transcriptional Signature Associated with Response to Interferon-alpha Treatment in the Woodchuck Model of Chronic Hepatitis B. PLoS pathogens 11, e1005103 (2015).
225. U. Protzer, M. K. Maini, P. A. Knolle, Living in the liver: hepatic infections. Nature reviews. Immunology 12, 201-213 (2012).
226. Y. Nan et al., Hepatitis E virus inhibits type I interferon induction by ORF1 products. Journal of virology 88, 11924-11932 (2014).
227. C. Tateno et al., Morphological and microarray analyses of human hepatocytes from xenogeneic host livers. Laboratory investigation; a journal of technical methods and pathology 93, 54-71 (2013).
228. K. G. Tournoy, S. Depraetere, P. Meuleman, G. Leroux-Roels, R. A. Pauwels, Murine IL-2 receptor beta chain blockade improves human leukocyte engraftment in SCID mice. European journal of immunology 28, 3221-3230 (1998).
229. C. Yu et al., Pathogenesis of hepatitis E virus and hepatitis C virus in chimpanzees: similarities and differences. Journal of virology 84, 11264-11278 (2010).
230. D. T. Evans, R. Serra-Moreno, R. K. Singh, J. C. Guatelli, BST-2/tetherin: a new component of the innate immune response to enveloped viruses. Trends in microbiology 18, 388-396 (2010).
231. P. V. Suneetha et al., Hepatitis E virus (HEV)-specific T-cell responses are associated with control of HEV infection. Hepatology 55, 695-708 (2012).
232. A. Brown et al., Characterization of the Specificity, Functionality, and Durability of Host T-Cell Responses Against the Full-Length Hepatitis E Virus. Hepatology 64, 1934-1950 (2016).
233. M. Spaan et al., CD4+ CXCR5+ T cells in chronic HCV infection produce less IL-21, yet are efficient at supporting B cell responses. Journal of hepatology 62, 303-310 (2015).
234. M. Spaan, G. W. van Oord, H. L. Janssen, R. J. de Knegt, A. Boonstra, Longitudinal analysis of peripheral and intrahepatic NK cells in chronic HCV patients during antiviral therapy. Antiviral research 123, 86-92 (2015).
235. E. T. Tjwa et al., Similar frequencies, phenotype and activation status of intrahepatic NK cells in chronic HBV patients after long-term treatment with tenofovir disoproxil fumarate (TDF). Antiviral research 132, 70-75 (2016).
236. V. Stoneman et al., Monocyte/macrophage suppression in CD11b diphtheria toxin receptor transgenic mice differentially affects atherogenesis and established plaques. Circulation research 100, 884-893 (2007).
237. E. N. Bogdandi et al., Effects of low-dose radiation on the immune system of mice after total-body irradiation. Radiation research 174, 480-489 (2010).
238. C. Sunderkotter et al., Subpopulations of mouse blood monocytes differ in maturation stage and inflammatory response. J Immunol 172, 4410-4417 (2004).
239. M. Guilliams et al., Dendritic cells, monocytes and macrophages: a unified nomenclature based on ontogeny. Nat Rev Immunol 14, 571-578 (2014).
240. T. Vanwolleghem, A. Boonstra, Focus on the liver: Host-virus interactions in HBV. Journal of hepatology 66, 884-885 (2017).
241. M. Gale, Jr., E. M. Foy, Evasion of intracellular host defence by hepatitis C virus. Nature 436, 939-945 (2005).
242. C. B. Bigger et al., Intrahepatic gene expression during chronic hepatitis C virus infection in chimpanzees. Journal of virology 78, 13779-13792 (2004).
243. S. B. Prabhu et al., Study of cellular immune response against Hepatitis E virus (HEV). Journal of viral hepatitis 18, 587-594 (2011).
244. S. A. Tsarev et al., Successful passive and active immunization of cynomolgus monkeys against hepatitis E. Proceedings of the National Academy of Sciences of the United States of America 91, 10198-10202 (1994).
245. H. Strick-Marchand et al., A novel mouse model for stable engraftment of a human immune system and human hepatocytes. PloS one 10, e0119820 (2015).
246. H. L. Zaaijer, No artifact, hepatitis E is emerging. Hepatology 62, 654 (2015).
247. M. Takahashi et al., Hepatitis E Virus (HEV) strains in serum samples can replicate efficiently in cultured cells despite the coexistence of HEV antibodies: characterization of HEV virions in blood circulation. J Clin Microbiol 48, 1112-1125 (2010).
248. N. Kamar et al., Influence of immunosuppressive therapy on the natural history of genotype 3 hepatitis-E virus infection after organ transplantation. Transplantation 89, 353-360 (2010).
249. Y. Debing et al., A mutation in the hepatitis E virus RNA polymerase promotes its replication and associates with ribavirin treatment failure in organ transplant recipients. Gastroenterology 147, 1008-1011 e1007; quiz e1015-1006 (2014).
250. D. Todt et al., In vivo evidence for ribavirin-induced mutagenesis of the hepatitis E virus genome. Gut 65, 1733-1743 (2016).
251. R. P. Donnelly, S. V. Kotenko, Interferon-lambda: a new addition to an old family. Journal of interferon & cytokine research : the official journal of the International Society for Interferon and Cytokine Research 30, 555-564 (2010).
252. R. A. Bam et al., TLR7 Agonist GS-9620 Is a Potent Inhibitor of Acute HIV-1 Infection in Human Peripheral Blood Mononuclear Cells. Antimicrobial agents and chemotherapy 61, (2017).
253. A. Tsai et al., Toll-Like Receptor 7 Agonist GS-9620 Induces HIV Expression and HIV-Specific Immunity in Cells from HIV-Infected Individuals on Suppressive Antiretroviral Therapy. Journal of virology 91, (2017).
254. C. I. Real et al., Nucleic acid-based polymers effective against hepatitis B Virus infection in patients don't harbor immunostimulatory properties in primary isolated liver cells. Scientific reports 7, 43838 (2017).
255. M. D. van de Garde et al., Interferon-alpha treatment rapidly clears Hepatitis E virus infection in humanized mice. Scientific reports 7, 8267 (2017)

15-MI13572-07
14-MI12481-06
15-MI13567-05
16-MI16125-01
16-MI10848-04
14-MI17593-03
13-MI21063-01
13-MI13964-04
15-MI13567-04
15-MI23360-03
13-MI21142-01
14-MI12481-01
13-MI24342-03
16-MI10767-01
15-MI22943-04
15-MI21090-04
14-MI12480-08
15-MI13570-08
13-MI24339-05
13-MI14043-07
14-MI18903-02
15-MI15514-05
16-MI11009-04
15-MI20905-04
14-MI18664-01
16-MI11040-03
16-MI11009-01
15-MI15512-04
13-MI24342-04
14-MI12480-07
13-MI14041-09
16-MI13672-06
13-MI24473-04
13-MI16243-07
16-MI24419-02
15-MI13570-02
15-MI21069-02
16-MI10767-05
15-MI22858-06
15-MI15515-06
15-MI20545-02
16-MI14139-05
13-MI13854-04
14-MI12529-04
15-MI13645-02
16-MI10759-06
13-MI20955-01
14-MI21528-06
16-MI10759-01
15-MI15518-03
16-MI16230-0
14-MI18669-02
15-MI15518-02
14-MI21528-08
13-MI24340-02
14-MI12474-08
14-MI21519-04
15-MI15512-05
13-MI24424-09
13-MI23436-03
13-MI24421-10
13-MI21669-03
14-MI12474-05
15-MI10861-06
13-MI13964-05
15-MI23098-04
15-MI20905-02
15-MI13572-04
14-MI18798-05
13-MI14041-04
14-MI24079-02
13-MI20955-02
13-MI24340-06
13-MI13854-03
14-MI17688-01
13-MI14045-03
13-MI20993-02
14-MI21672-07
13-MI21064-09
13-MI21055-04
13-MI14045-07
15-MI19922-04
13-MI24424-01
13-MI22931-05
15-MI22943-05
14-MI18664-05
15-MI23436-05
15-MI22859-01
16-MI11040-04
15-MI10863-03
13-MI24424-07
15-MI22943-03
15-MI22943-06
14-MI12480-04
16-MI10936-01
15-MI19911-01
13-MI24339-0
16-MI13181-02
13-MI21053-04
15-MI18616
15-MI22943-0
14-MI21654-03
16-MI1703
13-MI21064-04
16-MI16230-01